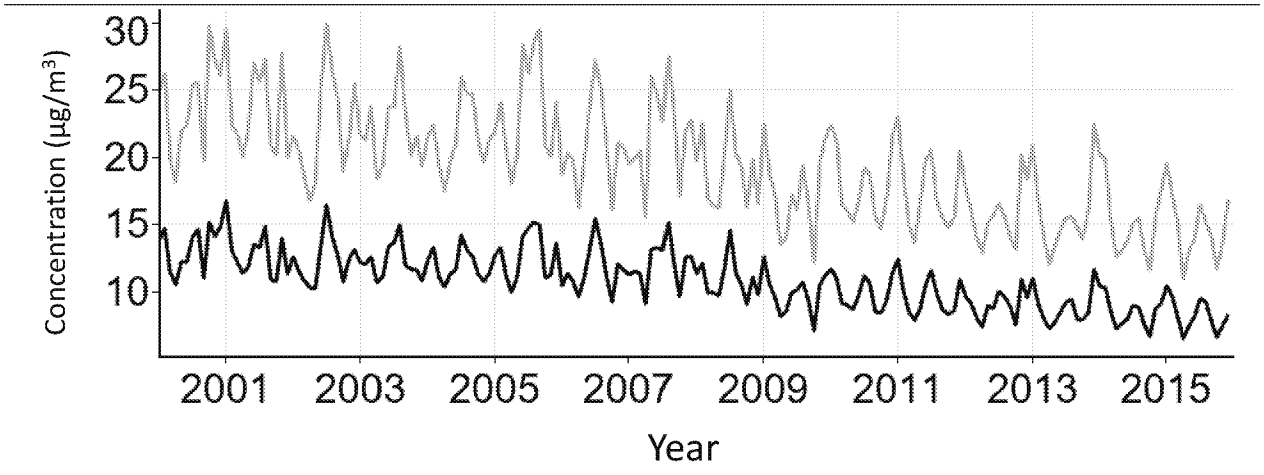

Black = mean, gray = 90th percentile.
Source Permission pending: Chan et al. (2018).

Figure 2-22 Long-term trend in national monthly and annual average $PM_{2.5}$ concentrations (µg/m³) from 2000–2015.

2.5.2.1.2 PM_{10}

Over the longer term PM_{10} has decreased steadily in several urban areas over the past several decades (U.S. EPA, 2004). Figure 2-23 shows a map of concentration trends in 98th percentile PM_{10} concentrations between 2003–2005 and 2013–2015 and Figure 2-24 shows a time series of national PM_{10} concentrations from 2005–2014. Most sites in the Eastern U.S. show decreasing concentrations over this period, consistent with the data of Table 2-5. However, there are locations in California, the Southwest, the Rocky Mountains, and the Great Plains that exhibit substantial increases in 98th percentile PM_{10} concentrations. The observed decreases in PM_{10} concentrations in many locations are consistent with similar observations for annual average $PM_{2.5}$ concentrations (see Section 2.3.4), reflecting that $PM_{2.5}$ has accounted for the majority of PM_{10} in the Eastern U.S. and a large fraction of PM_{10} throughout the U.S. over the period of decline. However, Figure 2-24 shows no evidence of a nationwide trend of decreasing PM_{10} concentrations in a time series of PM_{10} concentrations from network monitoring sites throughout the U.S.

ED_002220_00002287-00211

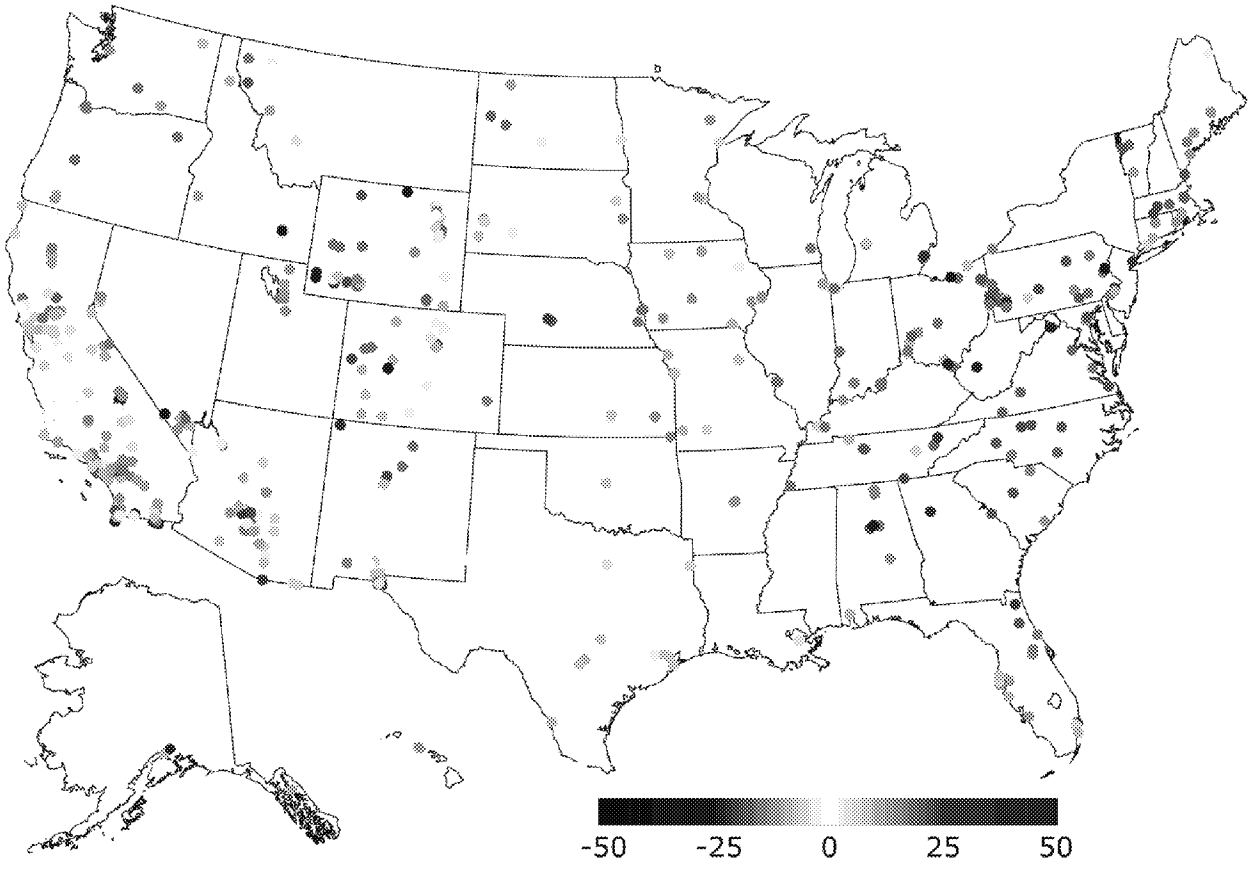

Blue indicates a decrease and red indicates an increase. Percentage increase or decrease is indicated by color intensity of the circle.

Source Permission pending: U.S. EPA 2016 analysis of Air Quality System network data 2003−2005 and 2013−2015.

Figure 2-23 Increase or decrease in 98th percentile 24-hour PM_{10} concentrations between 2003−2005 and 2013−2015.

ED_002220_00002287-00212

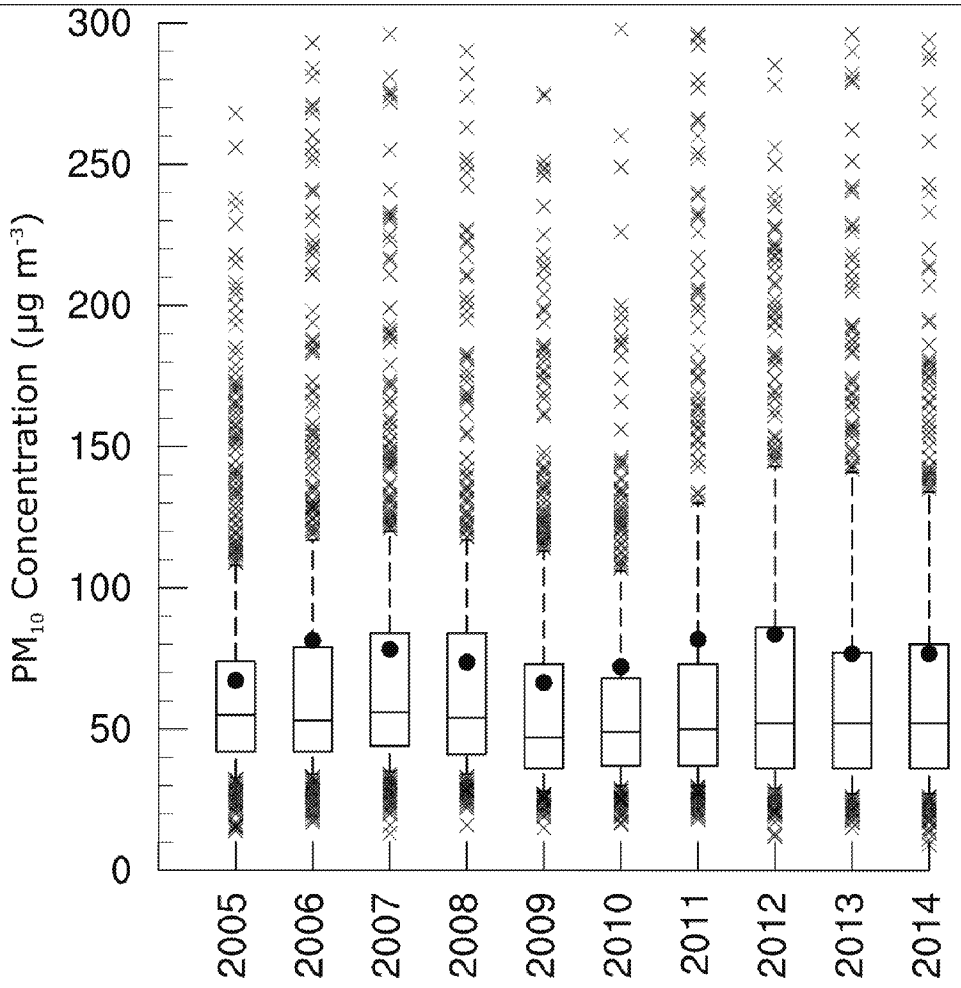

Source Permission pending: U.S. EPA 2016 analysis of Air Quality System network data 2003–2005 and 2013–2015.

Figure 2-24 PM_{10} 2nd highest concentration trends from 2005–2014.

2.5.2.1.3 $PM_{10-2.5}$

Long-term concentration trends for urban $PM_{10-2.5}$ are difficult to determine from network data because $PM_{10-2.5}$ monitoring was too recently implemented. However, some NCore stations began $PM_{10-2.5}$ measurements in the mid-2000's and IMPROVE measurements of $PM_{10-2.5}$ have been operating even longer, and although IMPROVE sites are mostly rural, some are collocated with CSN sites. These could be analyzed for long-term trends. In a Los Angeles field study $PM_{10-2.5}$ decreased by 0.39 µg/m^3 from 19 to 15 µg/m^3 for the period 1999 to 2009 compared to 0.92 µg/m^3 for $PM_{2.5}$ over the same period (Cheung et al., 2012b).

ED_002220_00002287-00213

2.5.2.1.4 Ultrafine Particles

Information on UFP concentrations is very limited, confined to very few network monitors that only recently became operational. Data from field studies have been published periodically, but are generally insufficient to assess long-term trends of UFP in any location. One exception is 8 years of UFP data from Rochester, NY, the particle number characteristics of which were summarized in Section 2.5.1.1.5 (Wang et al., 2011). On average over the 8 years that UFP data were collected in Rochester, total particle number concentrations were greater before 2006 than after 2006. This trend was most evident for particles between 0.01 and 0.1 μm. The difference was described as probably due to several changes in local sources due to the 2007 Heavy Duty Highway Rule, a reduction in local industrial activity, and the closure of a nearby coal-fired power plant (Wang et al., 2011).

2.5.2.1.5 Chemical Components

Figure 2-25 and Figure 2-26 show changes in the distribution of bulk $PM_{2.5}$ components, between the 3-year period from 2003–2005 and the 3-year period from 2013–2015. The most noticeable difference is the change in sulfate contribution, which dominates $PM_{2.5}$ mass in the East during the period 2003–2005, but by 2013–2015 it has declined enough that it is no longer the most abundant component in many Eastern locations.

In the 2009 PM ISA (U.S. EPA, 2009), sulfate is described as the most abundant component of $PM_{2.5}$ on a national average, with nitrate, particulate organic matter and sometimes crustal material also contributing substantially to $PM_{2.5}$ mass. The relative abundance of major $PM_{2.5}$ components has changed since the 2009 PM ISA (U.S. EPA, 2009), with lower contributions from sulfate and greater contributions of nitrate and particulate organic matter as a result of the steep decline in SO_2 emissions (see Section 2.3.2.1). The resulting decrease in sulfate concentrations closely follows the recent long-term decrease in $PM_{2.5}$ concentrations described in Section 2.5.2.1.1, and is magnified for monitoring sites in the Eastern half of the U.S., where sulfate has until recently been the most abundant $PM_{2.5}$ components, and where SO_2 emissions have declined the most.

ED_002220_00002287-00214

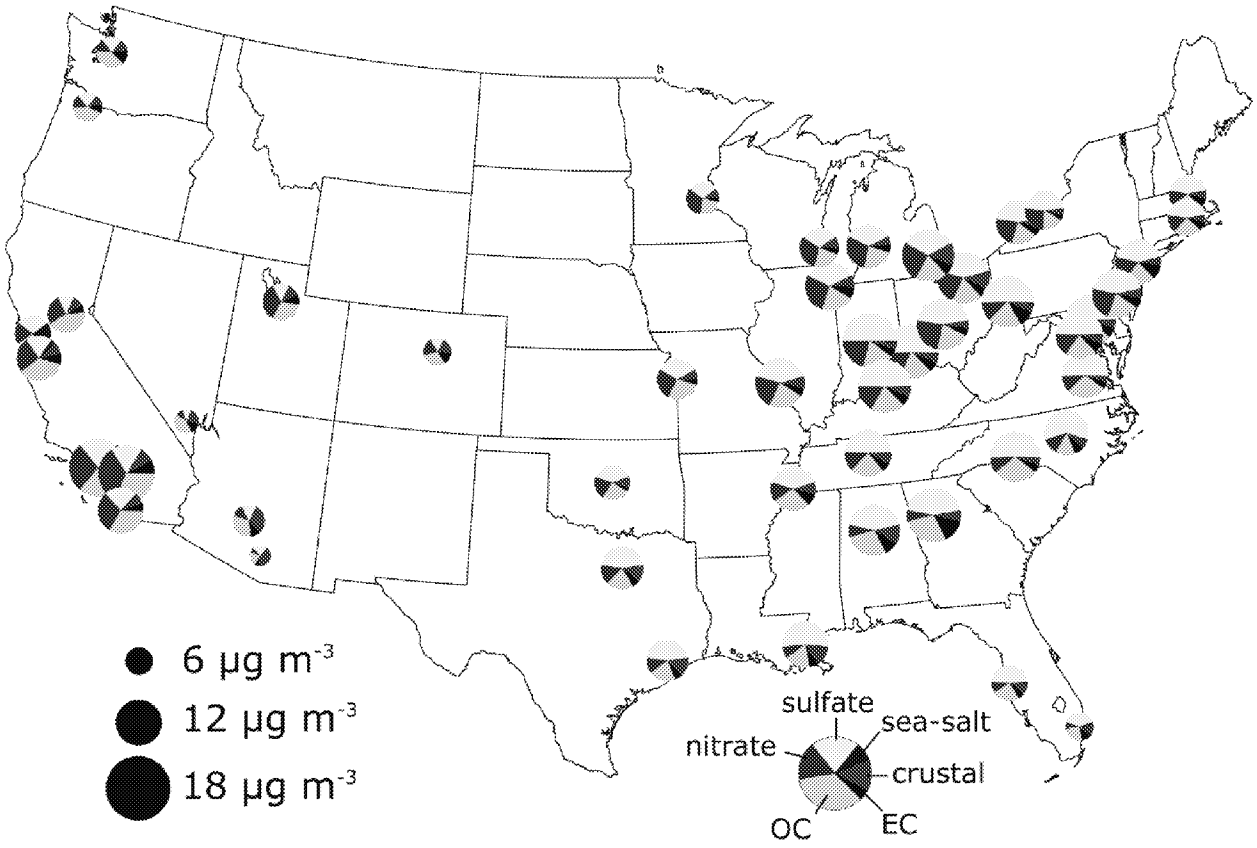

Source Permission pending: U.S. EPA 2016 analysis of Air Quality System network data 2003−2005.

Figure 2-25 Contributions of sulfate, nitrate, organic carbon (OC), elemental carbon (EC), crustal material, and sea salt to $PM_{2.5}$ at selected sites 2003−2005.

ED_002220_00002287-00215

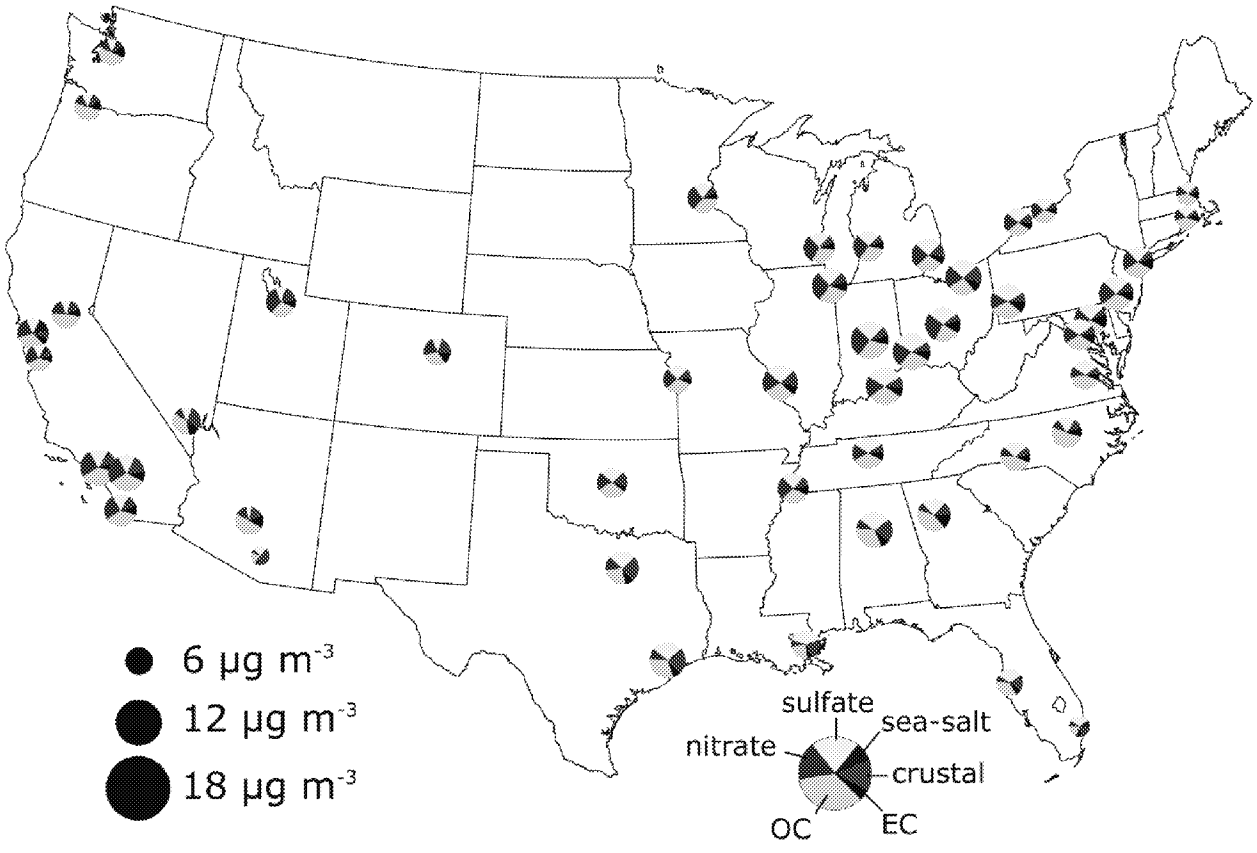

Source Permission pending: U.S. EPA 2016 analysis of Air Quality System network data 2013–2015.

Figure 2-26 Contributions of sulfate, nitrate, organic carbon (OC), elemental carbon (EC), crustal material, and sea salt to $PM_{2.5}$ at selected sites 2013–2015.

Figure 2-27 shows $PM_{2.5}$ sulfate, nitrate and OC concentrations from 2000–2015 based on IMPROVE and CSN network data. A steep decline in sulfate concentration is observed, but less change is evident for nitrate and OC concentrations. Like the summer $PM_{2.5}$ maximum (Figure 2-22), the summer sulfate peak also declines to become almost imperceptible toward the end of the period. Based on these observations, it appears that decreases in SO_2 emissions (Section 2.3) have contributed to a substantial decrease in atmospheric sulfate concentrations. The declining sulfate concentrations are also consistent with CMAQ predictions of the sulfate response to decreasing SO_2 emissions. Because sulfate has accounted for such a large fraction of $PM_{2.5}$ mass, the decreasing trend in sulfate concentration is also manifested in lower $PM_{2.5}$ concentrations (Section 2.5.2.1.1) and smaller $PM_{2.5}/PM_{10}$ ratios (Section 2.5.1.1.4). However, sulfate is not the only $PM_{2.5}$ species that exhibited decreasing concentrations over this period, as described below.

ED_002220_00002287-00216

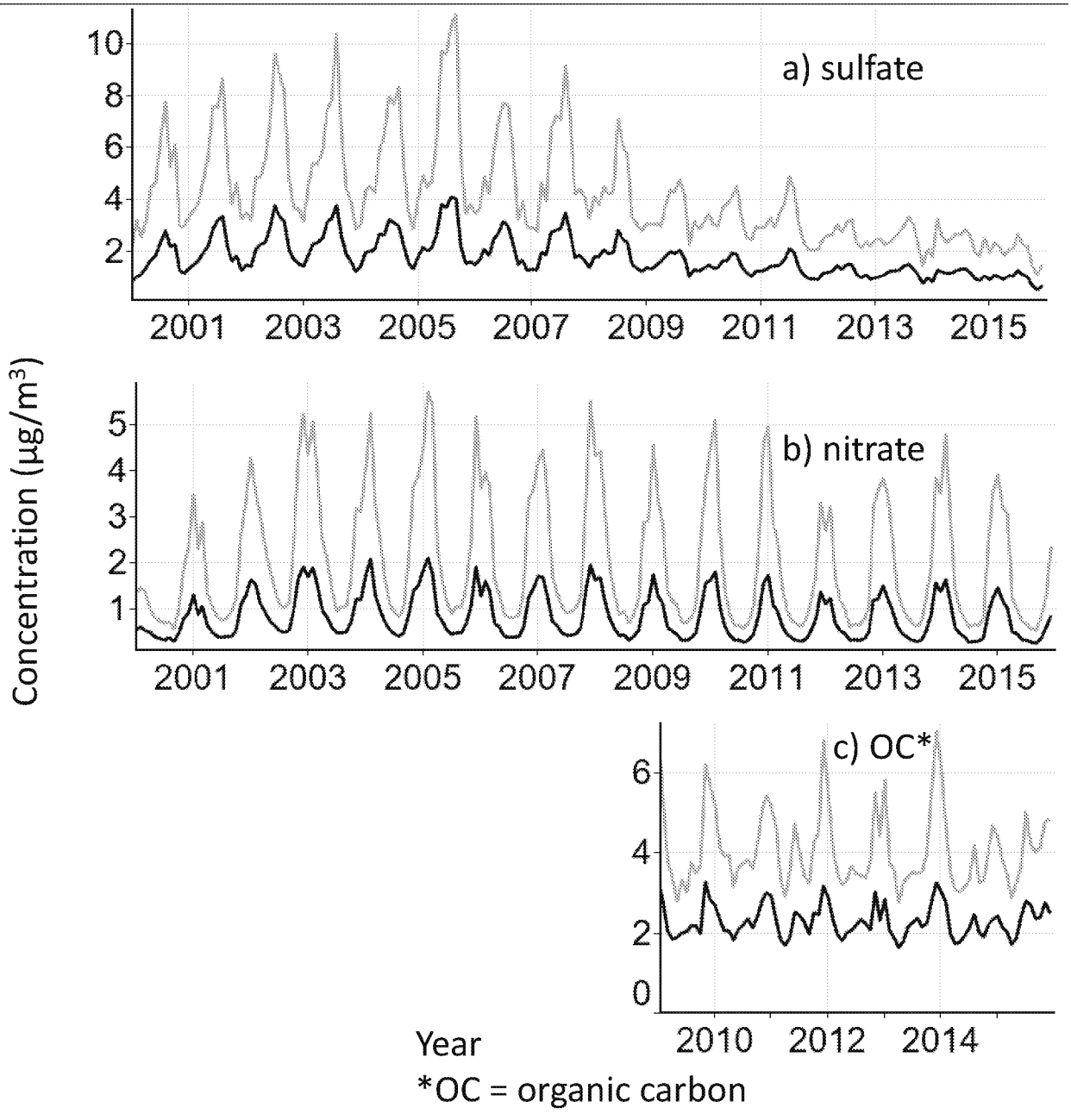

Black = mean, gray = 90th percentile.
Source Permission pending: Chan et al. (2018).

Figure 2-27 National monthly concentrations (µg/m^3) of (a) sulfate, (b) nitrate, and (c) organic carbon (OC) from 2000−2015.

ED_002220_00002287-00217

Long-term trends in $PM_{2.5}$ component concentrations from the CSN and IMPROVE networks were also recently described in a series of papers (Hand et al., 2013; Hand et al., 2012a; Hand et al., 2012b). In general sulfate has decreased fairly consistently at rural sites at a rate of −2.7% per year from 1992 to 2010 (Hand et al., 2012b). An even steeper decrease in sulfate concentrations has been observed in the most recent years, of −4.6% per year at rural sites from 2001 to 2010 and −6.2% per year at urban sites from 2002−2010 (Hand et al., 2012b). This is similar to the rate of decrease of SO_2 emissions from power plants, and decreases were greater and more linear in the East, where power plant emissions had the greatest contributions to sulfate concentration (Hand et al., 2012b). However, in the winter in the northern and central Great Plains sulfate and nitrate concentrations have increased at a rate of over 5% per year over the period 2000−2010, in spite of decreased nationwide emissions (Hand et al., 2012a), and sulfate increases in spring in some parts of the West were also observed (Hand et al., 2012b). These increases could not be explained by known changes in local or regional emissions (Hand et al., 2012b). In the SEARCH network downward trends in mean annual sulfate concentrations from 1999 to 2010 ranged from -3.7 ± 1.1 to -6.2 ± 1.1% per year. The sulfate reduction was linearly related but not proportional to SO_2 decrease of -7.9 ± 1.1% per year from 1999 to 2010. Over the same period mean organic matter concentration decreased by -3.3 ± 0.8 to 6.5 ± 0.3% per year and elemental carbon by -3.2 ± 1.4 to -7.8 ± 0.7% per year (Blanchard et al., 2013). Total carbon (OC + EC) generally decreased in both urban and rural areas, with the strongest trends in the West (Hand et al., 2013).

For species that are more strongly influenced by local urban sources, trends are manifested more locally, and largely controlled by changes in local source emissions. Al, Fe, and Si decreased in Los Angeles, suggesting successful control of fugitive dust emissions, but Cu declined little, probably indicating similar contributions from brake wear (Cheung et al., 2012b).

2.5.2.2 Seasonal Variations

2.5.2.2.1 $PM_{2.5}$

Observations described in Section 2.5.2.1.1 indicated that national average $PM_{2.5}$ concentrations and 98th percentile concentrations from 2013−2015 were both higher in winter than in summer (Table 2-4), and observations described in Section 2.5.2.1.1 indicated that monthly average $PM_{2.5}$ concentrations exhibited distinct summer and winter peaks superimposed on a steadily declining national average $PM_{2.5}$ (Figure 2-22). Averaged over all locations and years from 2001−2016, seasonal average $PM_{2.5}$ concentrations were approximately 12 $\mu g/m^3$ in summer and winter, but declined to approximately 9 $\mu g/m^3$ in the spring and fall (see Figure 2-28).

While monthly average $PM_{2.5}$ concentrations are higher in summer than in winter from 2002−2008, this pattern is reversed from 2009−2015, when monthly average $PM_{2.5}$ concentrations become higher in winter than in summer (see Section 2.5.2.1.1, Figure 2-22). This is a major departure

ED_002220_00002287-00218

from previous concentration trends. Observations that the highest seasonal average concentrations occurred in summer in the Eastern U.S. and in winter in the Western U.S. with a few exceptions was already clearly established from 1999–2001 data from the newly operational $PM_{2.5}$ network (U.S. EPA, 2004). These early $PM_{2.5}$ network results were in turn consistent with previous studies carried out prior to its implementation, and were confirmed in the 2009 PM ISA (U.S. EPA, 2009). The observed reduction in summer $PM_{2.5}$ concentrations in the East to the extent that summer is no longer the season with the highest national average $PM_{2.5}$ concentrations is a major development, and is a predictable consequence of successful reduction of SO_2 emissions.

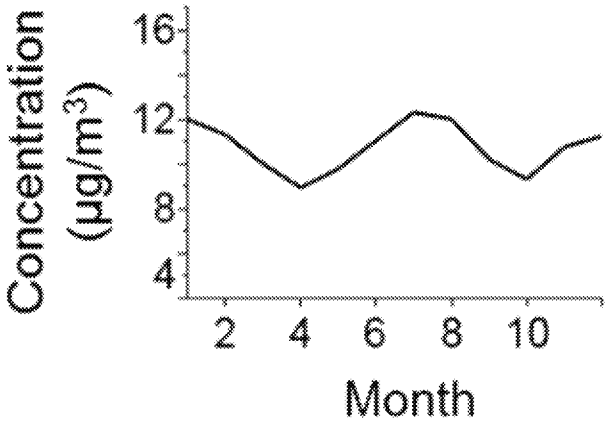

Source Permission pending: Chan et al. (2018).

Figure 2-28 National average $PM_{2.5}$ concentration by month 2000–2015.

2.5.2.2.2 $PM_{10-2.5}$

Relatively little had been published on the seasonal variability in $PM_{10-2.5}$ concentrations at the time of the 2009 PM ISA (U.S. EPA, 2009). Figure 2-29 shows three U.S. regions used for comparison of $PM_{10-2.5}$: the U.S. East of the Mississippi and the Northern and Southern portions of the U.S. West of the Mississippi. The regions were divided in this way because previous discussions based on limited data had suggested that PM_{10} was mostly $PM_{2.5}$ in the eastern U.S. and mostly $PM_{10-2.5}$ in the western U.S. (U.S. EPA, 2009, 2004), and these two regions were compared to investigate whether there were also seasonal differences between East and West. However, because results indicated that geographic differences within the western U.S. were greater than observed East-West differences, the western U.S. was further divided into northern and southern portions.

Figure 2-30 shows average concentrations on each day for 4 years from 2011–2014 by region based on data from the IMPROVE network, after dividing the U.S. into these three regions. All regions

ED_002220_00002287-00219

display clear seasonal variations, with the lowest concentrations occurring around January and the highest occurring in the summer months. The highest $PM_{10-2.5}$ concentrations are observed in the Southwest/Central region. Concentrations in this region are much higher than concentrations in the East and a seasonal pattern of high summer and low winter concentrations is apparent. By contrast, average concentrations in the Northwest region stretching all the way from the Pacific to the Dakotas were more similar to those in the East, but with a more pronounced seasonal pattern than either the East or the Southwest. These observations indicate that geographic patterns of $PM_{10-2.5}$ concentrations are more complicated than a simple East-West split, but that there are large areas of the Western U.S. where average $PM_{10-2.5}$ concentrations are similar to the Eastern U.S.

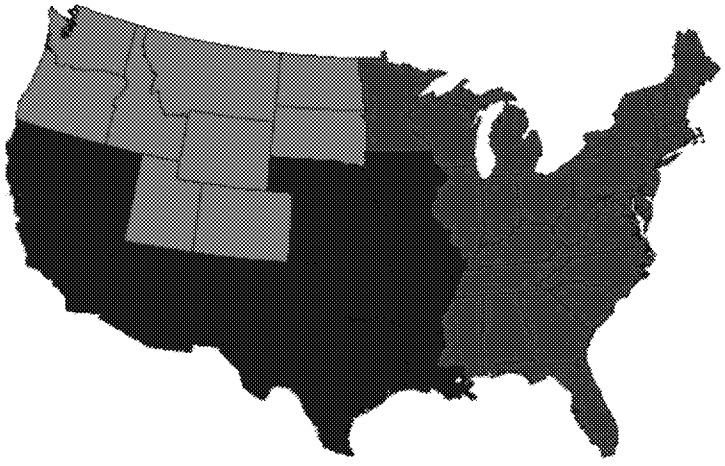

Source Permission pending: U.S. EPA analysis of Air Quality System network data 2011−2015.

Figure 2-29 Regions used for coarse PM comparison.

ED_002220_00002287-00220

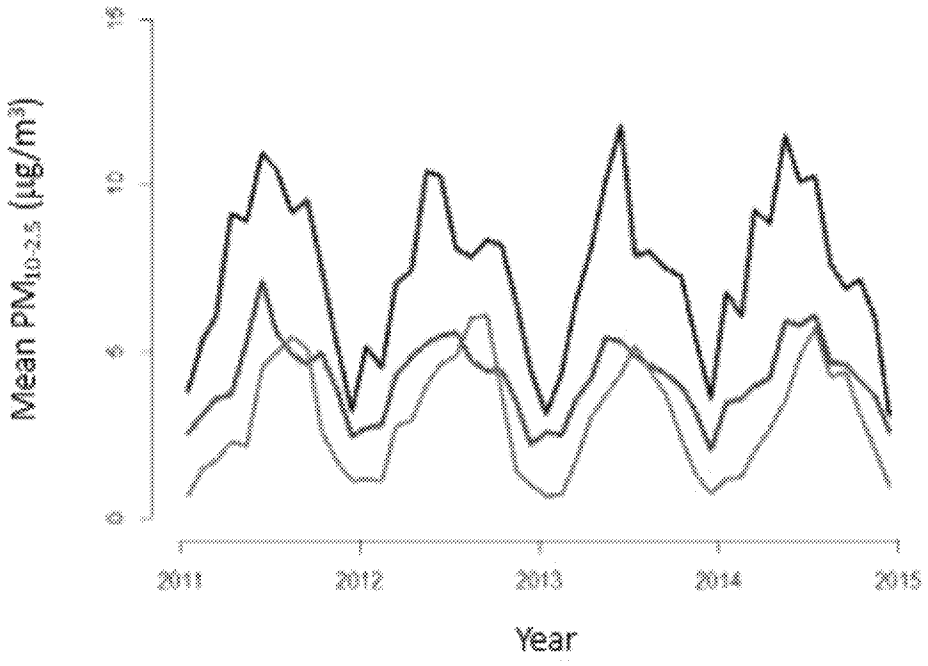

Colors of the lines correspond to the colors of the regions in Figure 2-29, i.e., red is East, green is Northwest, and blue is Southwest/Central.

Source Permission pending: U.S. EPA 2016 analysis of Air Quality System network data 2011−2015.

Figure 2-30 Average daily $PM_{10-2.5}$ concentrations over the 4-year period 2011−2014 collected by the Interagency Monitoring of Protected Visual Environments (IMPROVE) network.

The seasonal differences described in Section 2.5.1.1.3 of highest $PM_{10-2.5}$ concentrations in Spring and Fall and lowest concentration in winter (see Table 2-6) are consistent with other recent observations. In Colorado the highest $PM_{10-2.5}$ concentrations were observed in the Spring and Fall (Clements et al., 2014b). The monsoon period in this region is characterized by high wind events that increase $PM_{10-2.5}$ concentrations due to local wind driven soil, especially at rural sites with agricultural activity (Clements et al., 2014b). In Los Angeles $PM_{10-2.5}$ concentrations were 2−4 times higher in summer than in winter (Pakbin et al., 2010). However, organic coarse PM in Southern California was higher in winter than summer, and mostly was due to soil or biota, especially in "semirural" areas like Riverside and Lancaster (Cheung et al., 2012b).

ED_002220_00002287-00221

2.5.2.2.3 Ultrafine Particles

Relatively little has been published about seasonal or hourly differences in UFP concentrations except for localized studies in a few locations suggesting higher concentrations in winter than summer and an inverse relationship between UFP number and temperature (U.S. EPA, 2009). High afternoon concentrations during warmer months were attributed to NPF and high winter and evening UFP concentrations were attributed to lower mixing heights (U.S. EPA, 2009). More recent results indicate urban episodes of high UFP concentrations occur more often in winter than in summer (NYDEC, 2016).

2.5.2.2.4 PM Components

PM composition varies considerably with season. Figure 2-31 shows these changes. Seasonal concentration patterns are for the most part similar to those reported in the 2009 PM ISA (U.S. EPA, 2009) and conclusions from recent analyses of network data (Hand et al., 2013; Hand et al., 2012c) are consistent with patterns that can be observed in Figure 2-31. Sulfate and OC together accounted for the majority of $PM_{2.5}$ mass in many metropolitan areas in the summer, while higher nitrate concentrations were observed in the winter (U.S. EPA, 2009). Urban and rural seasonal variations of ammonium sulfate were similar, and both urban and rural concentrations were substantially higher in the East (Hand et al., 2012c). High winter nitrate concentrations were common in both urban and rural areas, but higher in urban areas (Hand et al., 2012c). Fine soil concentrations, highest in the Southwest, also had similar seasonal patterns for urban and rural sites (Hand et al., 2012c).

The higher OC contributions in fall and winter in the West compared to lower OC concentrations in winter in the Southeast reported in the 2009 PM ISA (U.S. EPA, 2009) are evident in Figure 2-31. EC mass concentration exhibited smaller seasonal variability than OC, particularly in the eastern half of the U.S. Carbonaceous aerosols varied more with season in the West than in the East for both urban and rural sites, although the seasonal patterns were different between Western urban and rural sites (Hand et al., 2013). PBAP often contributes more to PM mass in spring and summer than in fall and winter (U.S. EPA, 2009).

The metals Cu, Fe, Se, Pb, V, and Ni showed less seasonal variability than the sulfate, nitrate, and OC as reported in the 2009 PM ISA (U.S. EPA, 2009). More recently, in Los Angeles, trace element concentrations were higher in drier months of September and October, compared to December and January (Na and Cocker, 2009).

ED_002220_00002287-00222

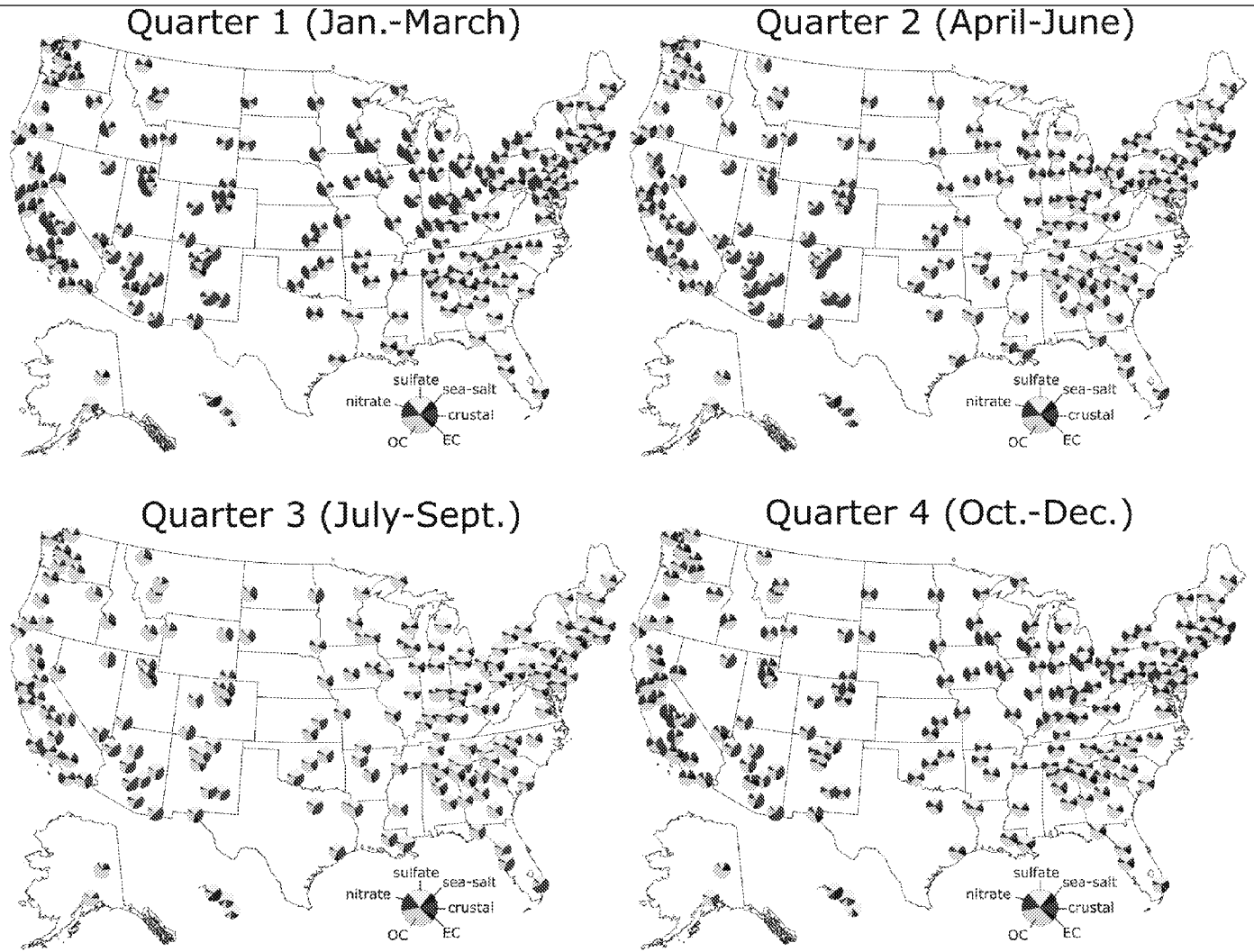

Source Permission pending: U.S. EPA 2016 analysis of Air Quality System network data 2013–2015.

Figure 2-31 Ambient $PM_{2.5}$ seasonal composition 2013–2015.

ED_002220_00002287-00223

2.5.2.3 Hourly and Weekday-Weekend Variability

As described in the 2009 PM ISA (U.S. EPA, 2009), hourly $PM_{2.5}$ and PM_{10} measurements are conducted at several hundred network monitoring sites. A two-peaked diel pattern was observed in diverse urban locations and attributed to rush-hour traffic for the morning peak and a combination of rush hour traffic, decreasing atmospheric dilution, and nucleation for the afternoon/evening peak (U.S. EPA, 2009). In most cities, a morning $PM_{2.5}$ peak was present starting at approximately 6:00 a.m., corresponding with the start of the morning rush hour just before the break-up of the planetary boundary layer. Figure 2-32 shows diurnal patterns for multiple cities using more recent data showing rush hour peaks in the morning and evening in most cases, which is consistent with the daily variability in $PM_{2.5}$ concentrations observed in the 2009 PM ISA (U.S. EPA, 2009).

Diurnal variations in $PM_{10-2.5}$ concentrations have also been investigated. In Los Angeles in the summer the highest concentrations of $PM_{10-2.5}$ were observed in midday and afternoon when winds were the strongest. Traffic was responsible for significant resuspension especially during winter nights when mixing heights were lowest at near-freeway sites in urban areas of Southern California (Cheung et al., 2012b).

As described in Section 2.5.1.1.5 (Figure 2-18), for UFP a diel maximum was observed on average during evening hours in diverse geographic locations. An inverse relationship between UFP number and temperature has also been observed, and high afternoon concentrations during warmer months were attributed to photochemical formation and high winter and evening UFP concentrations were attributed to lower mixing heights (U.S. EPA, 2009). Relatively little had been published about hourly differences in UFP concentrations at the time of the 2009 PM ISA except for localized studies in a few locations indicating a diel maximum during evening hours (U.S. EPA, 2009).

ED_002220_00002287-00224

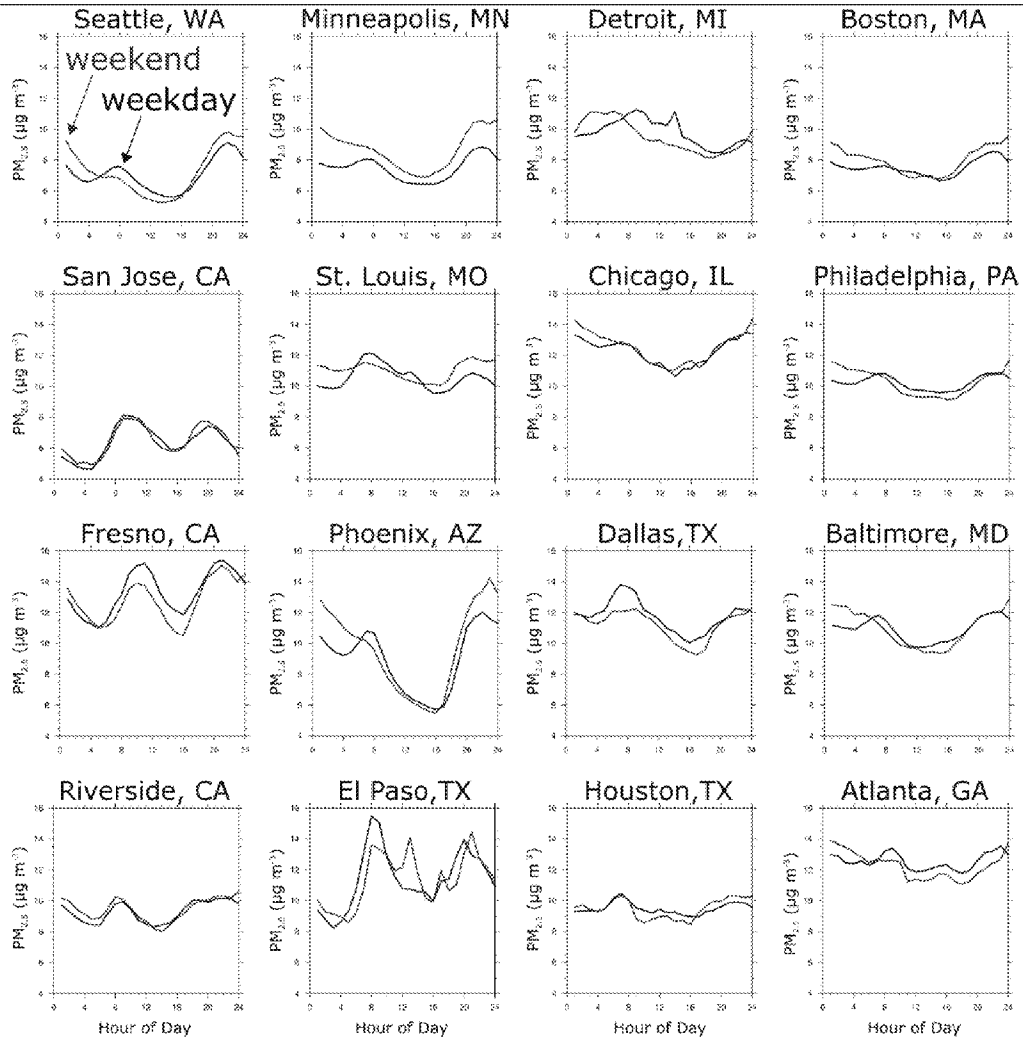

Source Permission pending: U.S. EPA 2016 analysis of Air Quality System network data 2012–2015.

Figure 2-32 Diurnal variation of $PM_{2.5}$ concentrations in urban areas

2.5.3 Common Patterns of Particulate Matter Characteristics in the U.S.

In this section the information on sources, particle size distribution and composition from recent research results and monitoring data are combined to describe common patterns of PM characteristics observed in the U.S. across different regional and seasonal conditions. Historically, $PM_{2.5}$ has been highest in the summer and has been largely accounted for by sulfate over a large area that encompasses most of the Eastern U.S., extending into the Great Plains. Figure 2-33 shows how sulfate concentrations have changed in major urban areas of the Eastern U.S. between 2003–2005 and 2013–2015 based on CSN monitors. At all of the locations shown in Figure 2-33 sulfate was the most abundant component measured for the period 2003–2005, accounting for close to half of the overall average $PM_{2.5}$ mass. In contrast, during the period 2013–2015 sulfate accounted for only about a quarter or a third of $PM_{2.5}$ mass.

ED_002220_00002287-00225

For example, the sulfate fraction dropped from 49 to 31% in Washington DC, 51 to 34% in Pittsburgh, 42 to 24% in New York, 43 to 26% in Philadelphia, 44 to 27% in Boston, and 52 to 33% in Cincinnati. In all but five of these locations, mostly in Ohio or the Ohio Valley (Cleveland, Cincinnati, and Dayton, OH, Louisville, KY, Dallas, TX), OC has replaced sulfate as the most abundant component, although OC and sulfate concentrations are very similar in most locations, as shown in Figure 2-31.

In the Eastern half of the U.S., the steep decline in sulfate concentrations has led to major changes in PM composition, seasonal concentration patterns, and size characteristics since publication of the 2009 PM ISA (U.S. EPA, 2009). PM_{10} concentrations in the Eastern U.S. and Midwest previously peaked in summer and was mostly composed of $PM_{2.5}$, with sulfate as the largest single component. More recently, summer concentrations are similar to other seasons, the $PM_{10-2.5}$ and $PM_{2.5}$ fractions are often comparable, and OC is frequently the most abundant single component.

Some finer scale trends within the Eastern U.S. are evident. While OC is becoming the component with the highest concentration throughout the Eastern U.S., in the Southeast annual average OC concentrations are somewhat higher than in the Northeast or Midwest, reaching their highest monitoring concentrations in a large area encompassing most of Alabama, Georgia, and South Carolina (Hand et al., 2011). The origin of summer OC in the Southeast has been intensively studied and is largely SOA due to oxidation of biogenic precursors (Marais et al., 2017; Rattanavaraha et al., 2016; Lewandowski et al., 2013), and urban areas of the Southeast like Atlanta have considerably more biogenic VOC precursors than urban areas of the Northeastern U.S. like New York City (Weber et al., 2007). Integrated modeling and measurement results (Kim et al., 2015), modeling predictions (Marais et al., 2017; Ying et al., 2015), and product concentration measurements (Lewandowski et al., 2013) are also consistent with higher OC concentrations and biogenic SOA at Southeastern sites than in the Northeast or Midwest. OC concentrations in the Southeast are decreasing (Marais et al., 2017).

Another area in the Eastern half of the U.S. stretching from Minnesota and Iowa through Wisconsin, Michigan, Indiana, and Ohio comprises as a region susceptible to high winter nitrate episodes resulting from high emissions of ammonia from animal agriculture combining with atmospheric nitric acid, that lead to mean winter ammonium nitrate concentrations exceeding 4 $\mu g/m^3$ (Pitchford et al., 2009). This region can be distinguished in Figure 2-31 for 2012–2014 by winter nitrate contributions of more than 40% to seasonal average $PM_{2.5}$ mass in Chicago, IL, Minneapolis, MN, Milwaukee, WI, Detroit and Grand Rapids, MI, Indianapolis, IN, Cincinnati and Dayton, OH, Davenport and Des Moines, IA, Omaha, NE, Kansas City, MO and at several other sites in the upper Midwest.

ED_002220_00002287-00226

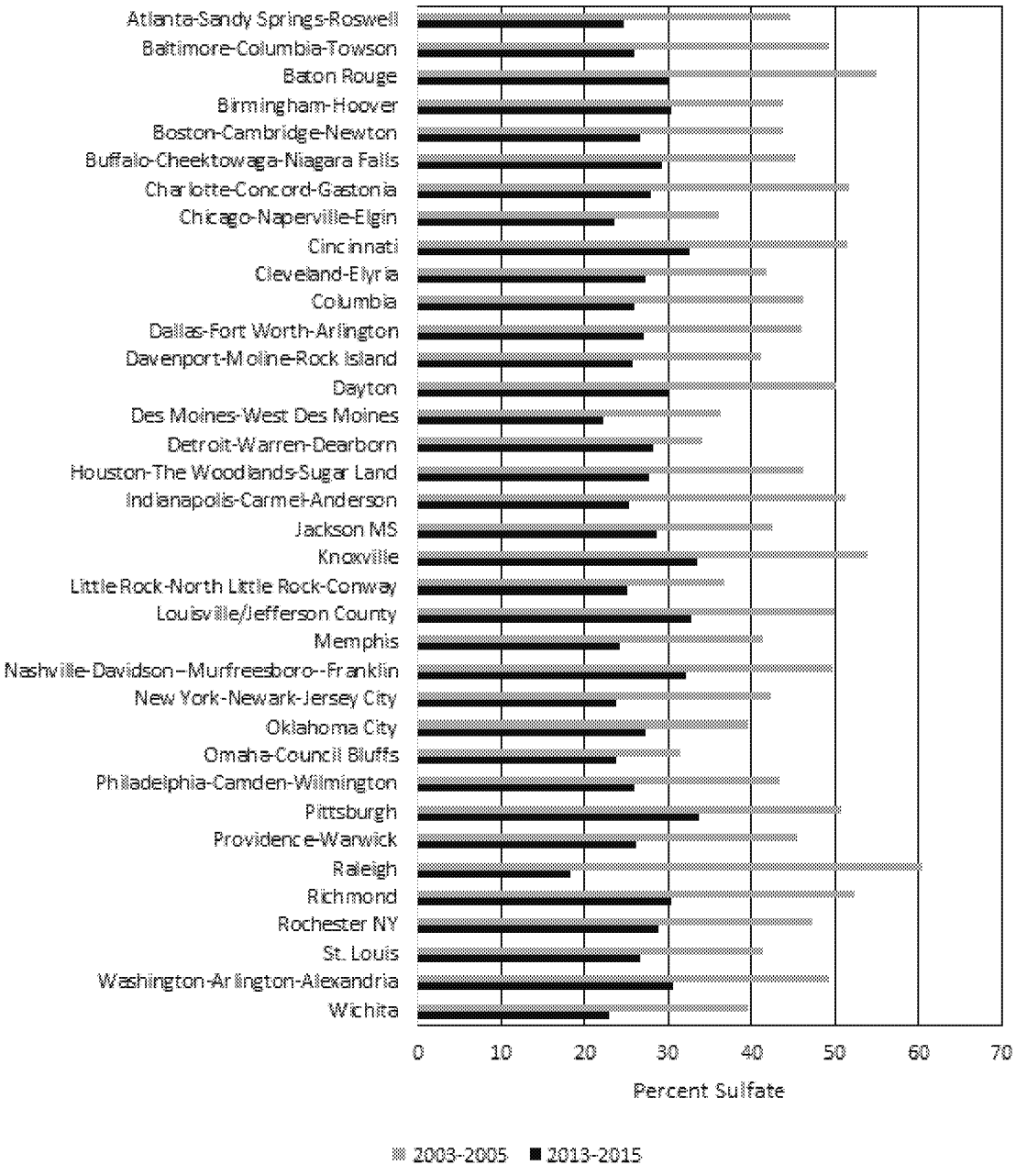

Source Permission pending: U.S. EPA 2016 analysis of Air Quality System network data 2003−2005 and 2013−2015.

Figure 2-33 Sulfate as percentage of $PM_{2.5}$ in eastern urban areas 2003−2005 and 2013−2015.

ED_002220_00002287-00227

While substantial differences in PM size distribution, composition, and other characteristics have been reported between the Eastern and Western U.S. (U.S. EPA, 2009), the diversity of PM characteristics across the West makes it more difficult to identify a set of fundamental PM characteristics that applies to the entire region. In interior urban areas, including Salt Lake City, UT, Reno, NV, Boise, ID, Missoula, MT, and Spokane, WA, $PM_{2.5}$ levels are higher under stable conditions on days with snow cover. In Salt Lake City, UT, Reno, NV, and Missoula, MT, most of the highest concentrations were observed on days with high nitrate concentrations enhanced by colder temperatures and higher relative humidity that occur with snow cover (Green et al., 2015). After multiday periods with stable conditions created by snow cover, $PM_{2.5}$ can build up rapidly in layers or in cold air pools. In one case in Salt Lake City $PM_{2.5}$ concentrations increased by 6 to 10 $\mu g/m^3$ per day over a period of several days (Whiteman et al., 2014; Silcox et al., 2011). This area is also subject to episodically high $PM_{10-2.5}$ concentrations from dust suspension.

Closer to the coast, high PM episodes cannot be explained by snow cover and extreme cold, yet some of the highest $PM_{2.5}$ concentrations in Figure 2-13 and Figure 2-14 are in California and concentrations are also highest in winter. In many California locations, a specific combination of conditions appears to be responsible for the highest PM concentrations. High winter $PM_{2.5}$ concentrations were studied intensively over 12 winters and the existence of several simultaneous conditions for at least 2 days duration were required for concentrations to exceed 35 $\mu g/m^3$, including a ridge of high pressure aloft, persistent easterly flow extending up vertically, orographically channeled winds resulting from stability, and enhanced nocturnal cooling under clear sky conditions (Beaver et al., 2010). Ammonium nitrate and organic PM from diverse combustion sources are the main contributors to $PM_{2.5}$ under winter conditions in California (Young et al., 2016; Zhang et al., 2016; Schiferl et al., 2014). Some of the highest 98th percentile concentrations were reported in California and other monitoring sites in the Western U.S. in Section 2.5.1.1.1 (Figure 2-14).

A common characteristic of PM in both California and the dryer areas of the Western U.S. that contrasts with the Eastern U.S. is the higher fraction of PM_{10} accounted for by $PM_{10-2.5}$, with $PM_{10-2.5}$ accounting for most PM_{10} mass in the West, but $PM_{2.5}$ accounting for most PM_{10} mass in the East (see Table 2-7). Populated areas of the Northwest (Western Oregon and Washington) make an exception to this trend. Table 2-7 shows that in both Seattle, WA and Portland, OR, $PM_{2.5}$ accounts for more than 50% of the PM_{10} mass and concentrations are higher in winter than in summer. Wood smoke is a major source of $PM_{2.5}$ in Portland, OR and Seattle, WA (Kotchenruther, 2016; U.S. EPA, 2009), as well as in smaller urban areas in this region.

$PM_{2.5}$ concentrations averaged over the 11-year period from 1998–2008 over the entire contiguous U.S. were reported to be 2.6 $\mu g/m^3$ higher on days under stagnant conditions than for non-stagnant days (Tai et al., 2010). When all U.S. data over a multiyear period are considered, temperature is positively correlated with $PM_{2.5}$ (Tai et al., 2012a; Tai et al., 2012b), especially in the Eastern U.S. (Tai et al., 2012a). Much of $PM_{2.5}$ variability could be explained by cold frontal passages in the East, maritime

ED_002220_00002287-00228

inflow in the West, and cyclone frequency in the Midwest (Tai et al., 2012b). Other meteorological conditions that have been reported to enhance PM concentrations include sea breezes (Georgoulias et al., 2009) and drought (Wang et al., 2015).

2.5.4 Background Particulate Matter

The definition of background PM can vary depending upon context, but it generally refers to PM that is formed by sources or processes that cannot be influenced by actions within the jurisdiction of concern. Consistent with other recent NAAQS reviews (U.S. EPA, 2014); U.S. EPA, 2015, 4679035}, there are two specific definitions of background PM of interest: natural background and U.S. background. Natural background is the narrowest definition of background, and it is defined as the PM that would exist in the absence of any manmade emissions of PM or PM precursors. U.S. background PM is defined as any PM formed from sources or processes other than U.S. manmade emissions. Approaches to estimating background PM have evolved over the years. Different approaches for estimating background concentrations in the western and eastern U.S. were taken in the 2004 PM AQCD (U.S. EPA, 2004). Data from IMPROVE monitoring sites in the western U.S. thought to be among the least influenced by regional pollution sources exhibited annual mean concentrations of ~3 $\mu g/m^3$. However, even the most remote monitors within the U.S. can be periodically affected by U.S. anthropogenic emissions, and concentrations observed at the most remote sites in the Eastern U.S. were considerably higher than in the western U.S. In the 2009 ISA (U.S. EPA, 2009), estimates of background concentrations were calculated by CMAQ and classified by region and quarter. All quarterly and annual estimates were less than 2 $\mu g/m^3$, with many <1 $\mu g/m^3$. However, episodic contributions from dust storms or wildfires can be much higher. Further details are given by (U.S. EPA, 2009).

As illustrated by this example, background PM concentrations can be best characterized with chemical transport modeling simulations via source apportionment modeling or estimating what the residual PM concentrations would be were the U.S. anthropogenic emissions entirely removed (i.e., "zero-out" modeling). Unfortunately, there has not been a similar national scale effort to update background $PM_{2.5}$ concentration estimates since the 2009 PM ISA. However, there has been considerable research focused on better understanding the sources and processes that influence background contribution to $PM_{2.5}$ in the U.S.

Background contributions to PM can come from a variety of sources. Natural sources include wind erosion of natural surfaces, volcanic production of SO_4^{2-}; primary biological aerosol particles (PBAP); wildfires producing EC, OC, and inorganic and organic PM precursors; and SOA produced by oxidation of biogenic hydrocarbons such as isoprene and terpenes (U.S. EPA, 2009). However, human intervention can be involved in the formation of SOA. For example, the production of SOA from the oxidation products of isoprene and other biogenic VOC's can be enhanced by the presence of SO_2, NO_X, and other anthropogenic pollutants, accounting for as much 50% of SOA from biogenic VOC's

ED_002220_00002287-00229

(Section 2.3.2.3). Other sources of background PM are anthropogenic, principally emissions from outside the U.S. which can be transported into the U.S. The importance of different contributors to background PM varies across the contiguous U.S. (CONUS) by region and season as a function of the complex mechanisms of transport, dispersion, deposition, and re-entrainment.

Background PM can also be viewed as coming from two conceptually separate components: a somewhat consistent "baseline" component and an episodic component. The baseline component consists of contributions that are generally well characterized by a reasonably consistent distribution of daily values each year, although there is variability by region and season. The episodic component consists of infrequent, sporadic contributions from high-concentration events occurring over shorter periods of time (e.g., hours to several days) both within North America (e.g., volcanic eruptions, large forest fires, dust storms) and outside North America (e.g., transport from dust storms occurring in deserts in North Africa and China). These episodic natural events, as well as events like the uncontrolled biomass burning in Central America, are essentially uncontrollable and do not necessarily occur in all years. Section 2.5.4.1 and Section 2.5.4.2 below discuss natural background and intercontinental transport contributions to background PM in the U.S.

2.5.4.1 Natural Background

On average, natural sources including soil dust and sea salt have been estimated to account for approximately 10% of U.S. urban $PM_{2.5}$ (Karagulian et al., 2015). Dust storms are common occurrences in arid regions of the U.S. and the rest of the world. An extreme example is the haboob. During one of these affecting Phoenix in July of 2011, peak hourly average PM_{10} concentrations were >5,000 $\mu g/m^3$ with area wide average hourly concentrations ranging from a few hundred to a few thousand $\mu g/m^3$ (Vukovic et al., 2014). Dust can also make up a substantial fraction of total $PM_{2.5}$ in the Southwestern U.S. This is illustrated in Figure 2-19 (Section 2.5.1.1.6), which shows that at many locations in the Southwestern U.S., crustal material from soil accounts for close to half of the annual average $PM_{2.5}$ mass. Although similar network data do not exist for $PM_{10-2.5}$, the soil contribution to $PM_{10-2.5}$ mass in these locations is likely to be even higher. Dust also accounts for much of the PM that originates from outside the U.S. (Section 2.5.4.2).

Wildfires are a variable contributor to particulate matter emissions. Satellite-based fire detections are combined with ground-based estimates of area burned, fuel availability, and emission factors to quantify PM and precursor emissions at high spatial and temporal resolution (Strand et al., 2012). The gas-phase species emitted from fires can affect oxidation and formation of semivolatile compounds that can condense into the particle phase (Baker et al., 2016). Invasive species, historical fire management practices, frequency of drought, and extreme heat have brought longer fire seasons (Jolly et al., 2015) and more large fires (Dennison et al., 2014). In addition to emissions from forest fires in the U.S., emissions from forest fires in other countries can be transported to the U.S., and transport from Canada, Mexico,

ED_002220_00002287-00230

Central America, and Siberia have been documented (U.S. EPA, 2009). According to the U.S. EPA's National Emission Inventory, wildfire smoke contributes between 10 and 20% of primary PM emissions per year (Section 2.3.1), however these emissions are concentrated at the burn area and mostly during the wildfire season, rather than evenly distributed through the year (Sturtz et al., 2014).

Primary biological aerosol particles (PBAP) such as bacteria and pollen can also contribute substantially to $PM_{10-2.5}$ mass in some locations. These are discussed in more detail in Section 2.3.3.

2.5.4.2 Intercontinental Transport

Intercontinental transport contributes 0.05 to 0.15 $\mu g/m^3$ to annual average $PM_{2.5}$ concentrations in the U.S. (Kolb et al., 2010). Large continuous data sets are available to examine the intensity and frequency of intercontinental PM transport events. Ground-based lidar networks and mountain top measurements in Europe, North America, and Asia have been used to establish that intercontinental transport of PM from dust, forest fires, and anthropogenic sources impact local $PM_{2.5}$ and PM_{10} concentrations. Satellites also provide estimates of the amount of PM transported, as well as the altitude at which the transport occurs. Transport at midlatitudes is dominated by westerly winds, which transport East Asian emissions across the North Pacific Ocean to North America. Transport occurs at greater speeds and over longer distances in winter than in summer because the westerly winds are stronger, and greater precipitation in winter in the Western U.S. brings more of the transported PM to the surface. Numerous studies have now documented long-range transport of desert dust from East Asian deserts. Both the frequency of transport events and the overall contribution to PM in the U.S. are reported to be increasing (Kolb et al., 2010; TFHTAP, 2006). By one estimate, 18 Tg/year PM exits Asia between 30 to 60 degrees N latitude, with 4.4 Tg/yr arriving in North America (Yu et al., 2008).

Episodic concentrations as high as 20 $\mu g/m^3$ of PM associated with transport to the U.S. from Asia have been estimated (Jaffe et al., 2005), and $PM_{2.5}$ from Asia has been shown to account for a large fraction total $PM_{2.5}$ in polluted urban air (Jaffe et al., 2003). Over longer time periods, long range transport can make a substantial contribution to local PM concentrations in remote areas like the Arctic. However, in regions with local sources, observed trends in PM are usually more closely related to local emission trends than to long-range transport, and at monitoring sites throughout the U.S. intercontinental influences are small (Henze et al., 2009).

On average, Asian dust contributes typically <~1 $\mu g/m^3$ to $PM_{2.5}$ at remote sites in western states (Creamean et al., 2014). However, transport of Asian dust shows both strong seasonal and interannual variability. Dust emissions are at a maximum in spring, associated with strong winds following cold fronts as the Siberian High extends southward and before there is sufficient vegetation to stabilize the surface. Based on inverse modeling of Asian dust over the period 2005–2012, Yumimoto and Takemura (2015) suggested that dust emissions, transport and deposition are largest during the La Niña phase of the El Niño-Southern Oscillation cycle. They also found that dust emissions were closely related to a strong

ED_002220_00002287-00231

meridional pressure gradient and a strong winter monsoon. Husar et al. (2001) report that the average PM_{10} concentration at 25 reporting stations throughout the northwestern U.S. reached 65 μg/m^3 during an episode of Asian dust transport during the last week of April 1998, compared to an average of 10−25 μg/m^3 during the rest of April and May. This was accompanied by visual reports of milky-white discoloration of the normally blue sky in nonurban areas along the West Coast. Satellite data have been especially useful for tracking the trans-Pacific transport of Asian dust. Uno et al. (2011) documented the occurrence of multiple large plumes of Asian dust in April of 2010 that had passed over most of the continental U.S. based on space-borne lidar (the Cloud-Aerosol Lidar with orthogonal Polarization) on board the CALIPSO satellite. Three-dimensional, global-scale CTMs have also been used to estimate intercontinental transport of PM pollution (TFHTAP, 2007) and trans-Pacific transport of mineral dust from Asian deserts (Fairlie et al., 2007).

Transport of dust from the Sahara Desert and the Sahel in North Africa (Prospero, 1999a, b), (Chiapello et al., 2005), (Mckendry et al., 2007) can affect the eastern U.S., while transport of dust from the Gobi and Taklimikan deserts in Asia (Vancuren and Cahill, 2002), (Yu et al., 2008) can exert effects in the western U.S. The ability of African dust to substantively affect PM levels in the U.S. was extensively reviewed in the 2004 PM AQCD (U.S. EPA, 2004) and in the 2009 PM ISA (U.S. EPA, 2009). A multidecade record of African dust reaching Miami indicates that the highest loadings are found in July (Prospero, 1999a, b) with concentrations ranging from ~10 to ~100 μg/m^3. Sample collection began in 1974, before network PM_{10} and $PM_{2.5}$ samplers were developed, and no size cut was specified (Prospero, 1999b). Yu et al. (2015) found that the transport of North African dust across the Atlantic Ocean is strongly negatively correlated with precipitation in the Sahel during preceding year. Dust from Africa has shown a decreasing trend of ~ 10% per decade from 1982 to 2008, based on measurements of aerosol optical depth and surface concentrations in Barbados by Ridley et al. (2014), who also suggest that this decrease is due to a corresponding decrease in surface winds over source regions.

ED_002220_00002287-00232

In addition to desert dust, a portion of the PM reaching the U.S. through intercontinental transport is from combustion and industrial sources, and formation of sulfate from SO_2 during transport of air masses to the U.S. from Asia is also well documented. In the Spring in the Northwestern U.S., transport from Asia accounted for 0.16 ± 0.08 $\mu g/m^3$ $PM_{2.5}$ sulfate (Heald et al., 2006). Sulfate of Asian origin can account for a large fraction of sulfate in the upper troposphere in western North America, and an increasing fraction of sulfate measured off the northwest coast of the U.S. is of Asian origin. Measurements from an event over the Pacific Ocean were consistent with nearly pure sulfuric acid. Transboundary transport within North America can also be important. Model results suggest that SO_2 emissions in Mexico influence sulfate formation in the U.S. (Henze et al., 2009). Leibensperger et al. (2011) estimated that trans-Pacific transport of SO_2 and NO_X results in a combined increase in background PM[40] in the western U.S. of a few tenths of a $\mu g/m^3$.

2.6 Summary

New observations indicate that some fundamental characteristics of atmospheric PM in the U.S. are changing. These range from source emissions and atmospheric formation processes to size distributions, particle composition, and spatial and temporal concentration trends. The most noticeable change in PM or precursor source emissions is the large reduction in SO_2 emissions, mainly from decreased EGU coal combustion. In addition, advances in engine and emissions control technologies have led to continued decreases in automobile emissions. The major urban stationary sources of PM are still industrial processes, construction and road dust, residential wood burning and other fuel combustion, and cooking. The major primary mobile sources are still diesel and gasoline powered highway vehicles as well as off-road vehicles and engines like locomotives, ships, aircraft, and construction and agricultural equipment. $PM_{2.5}$ particles from combustion sources are usually emitted as UFP and grow into larger particles after emission. Secondary $PM_{2.5}$ still accounts for a substantial fraction of the $PM_{2.5}$ mass from both natural and anthropogenic sources (U.S. EPA, 2009). Major $PM_{10-2.5}$ sources are dust suspension, sea spray, and biological materials. Automobile traffic, other combustion sources, and new particle formation are major UFP sources.

Research on atmospheric chemistry has largely focused on better understanding OC sources and SOA formation pathways. Progress in understanding SOA precursors centered on model results of large fractions of SOA from aromatic and monoterpene precursors, observations of gas phase VOC oxidation products continuing to react to form PM, and the discovery of isoprene as a major SOA precursor. Progress related to understanding SOA formation processes was directed toward evidence of cloud processing as well as repeated cycles of volatilization and condensation of semivolatile reaction products as important processes for SOA evolution, investigation of misclassification of SOA as primary organic

[40] PM size was not specified, but secondary PM formed from NO_X and SO_2 is usually nearly all in the $PM_{2.5}$ size range.

ED_002220_00002287-00233

aerosol under typical sampling conditions, and observations of greater SOA yields at high NO_X concentrations. Progress in understanding SOA products involved identification of higher molecular weight particle phase oligomers and organic peroxides as an abundant class of reactive oxygen species (ROS) with high oxidizing potential in SOA, as well as observations of abundant organosulfates and organonitrates in SOA.

Major developments in PM monitoring and monitoring capabilities have taken place, and these have had an important impact on our understanding of PM characteristics. For example, before the availability of network data, the 2009 PM ISA was based on literature results and concluded that $PM_{10-2.5}$ concentrations were higher in the Western U.S. than in the Eastern U.S. (U.S. EPA, 2009). The NCore network was implemented in 2011 and now produces multipollutant concentration and data at 78 stations throughout the U.S. Through NCore, more reliable data on $PM_{10-2.5}$ concentrations are available than were possible before. The first years of NCore data reveal a more complicated concentration pattern than a simple East-West split, with the highest $PM_{10-2.5}$ concentrations observed in the Southwest from California to Texas, and in the Central U.S. from Texas and Louisiana as far north as Nebraska and Iowa. In contrast, there are large areas in the Northwest where average $PM_{10-2.5}$ concentrations and $PM_{2.5}/PM_{10}$ are similar to the Eastern U.S. Rapid advances are taking place in UFP measurement technology, but measurements are more method dependent and network monitoring is in its beginning stages. Network monitoring of $PM_{2.5}$ has expanded to include numerous near road monitoring sites.

Annual mean ambient $PM_{2.5}$ concentrations in the U.S. on average are 4–5 $\mu g/m^3$ lower than they were in the last decade, continuing a downward trend described in the 2009 PM ISA (U.S. EPA, 2009). $PM_{2.5}$ concentrations are highest in the San Joaquin Valley, the Los Angeles-South Coast Air Basin of California, and parts of Utah. In the Eastern U.S. there is a region of higher $PM_{2.5}$ concentrations with annual average concentrations greater than 10 $\mu g/m^3$ stretching from Eastern Iowa and Northern Illinois across Indiana, Ohio, and into to Eastern Pennsylvania. While monthly national average $PM_{2.5}$ concentrations were higher in summer than in winter from 2002–2008, this pattern is reversed from 2012–2015, when monthly average $PM_{2.5}$ concentrations become higher in winter than in summer. Summer $PM_{10-2.5}$ concentrations are generally higher than other seasons, but extreme $PM_{10-2.5}$ events appear to be more likely in the spring. PM_{10} reflects characteristic concentration patterns of both $PM_{10-2.5}$ and $PM_{2.5}$, with the highest concentrations in summer. The decrease in $PM_{2.5}$ concentrations has resulted in smaller $PM_{2.5}/PM_{10}$ ratios, and PM_{10} in the East and Northwest is in the range of 50–60% $PM_{2.5}$, while PM_{10} in the Western U.S. is generally less than 50% $PM_{2.5}$. On urban and neighborhood scales, both spatial and temporal variations are strongly influenced by motor vehicle emissions, with the highest $PM_{2.5}$ and UFP concentrations at rush hour, and the highest concentrations of $PM_{10-2.5}$, UFP, and many $PM_{2.5}$ components near roads with heavy traffic.

Recent changes in $PM_{2.5}$ long-term and seasonal concentration trends are consistent with observed changes in $PM_{2.5}$ composition compared to the 2009 PM ISA (U.S. EPA, 2009), the greatest of which is the reduction in sulfate concentrations, resulting in a smaller sulfate contribution to $PM_{2.5}$ mass

ED_002220_00002287-00234

in 2013−2015 than in the last decade, especially in the Eastern U.S. As a result, at many locations sulfate has been replaced as the greatest single contributor to $PM_{2.5}$ mass by organic matter. Sulfate and OC are the components with the highest contribution to total mass in most eastern locations and OC usually makes the greatest contribution to $PM_{2.5}$ mass in the west, although sulfate, nitrate, and crustal material can also be abundant. The highest nitrate concentrations are found in the west, particularly in California, but with some elevated concentrations in the upper Midwest. Ammonium concentrations follow both nitrate and sulfate spatial patterns because it is mostly present as ammonium sulfate and ammonium nitrate. Larger contributions of OC to $PM_{2.5}$ mass are observed in the Southeast and the West than in the Central and Northeastern U.S. A large fraction of organic PM can be water soluble. Crustal elements and biological material account for large fraction of $PM_{10-2.5}$ mass. There is still little information on the composition of UFP, but urban UFP is often rich in OC and EC.

Background PM originates from natural and international sources. Natural sources include windblown dust, wildfires, and sea salt. International contributions include intercontinental transport of dust, wildfire smoke, and pollution as well as transboundary transport of these contributors from Canada, Mexico. Background PM usually makes a relatively small contribution to urban annual average $PM_{2.5}$ concentrations. However, it is an important contributor to $PM_{2.5}$ concentrations in the southwestern U.S., and impacts $PM_{2.5}$ concentrations elsewhere on an episodic basis. Background contributions to $PM_{10-2.5}$ can be substantial, as it is generally dominated by dust and sea salt. Less is known about background contributions to UFP.

ED_002220_00002287-00235

2.7 References

Ahlm, L; Liu, S; Day, DA; Russell, LM; Weber, R; Gentner, DR; Goldstein, AH; Digangi, JP; Henry, SB; Keutsch, FN; Vandenboer, TC; Markovic, MZ; Murphy, JG; Ren, X; Scheller, S. (2012). Formation and growth of ultrafine particles from secondary sources in Bakersfield, California. J Geophys Res 117: n/a-n/a. http://dx.doi.org/10.1029/2011JD017144

Alexis, A; Garcia, A; Nystrom, M; Rosenkranz, K. (2001). The 2001 California almanac of emissions and air quality. Sacremento, CA: California Air Resources Board. http://www.arb.ca.gov/aqd/almanac/almanac01/almanac01.htm

Allen, GA; Oh, JAA; Koutrakis, P; Sioutas, C. (1999). Techniques for high-quality ambient coarse particle mass measurements. J Air Waste Manag Assoc 49: 133-141.

Almeida, J; Schobesberger, S; Kuerten, A; Ortega, IK; Kupiainen-Maatta, O; Praplan, AP; Adamov, A; Amorim, A; Bianchi, F; Breitenlechner, M; David, A; Dommen, J; Donahue, NM; Downard, A; Dunne, E; Duplissy, J; Ehrhart, S; Flagan, RC; Franchin, A; Guida, R; Hakala, J; Hansel, A; Heinritzi, M; Henschel, H; Jokinen, T; Junninen, H; Kajos, M; Kangasluoma, J; Keskinen, H; Kupc, A; Kurten, T; Kvashin, AN; Laaksonen, A, ri; Lehtipalo, K; Leiminger, M; Leppa, J; Loukonen, V; Makhmutov, V; Mathot, S; Mcgrath, MJ; Nieminen, T; Olenius, T; Onnela, A; Petaja, T; Riccobono, F; Riipinen, I; Rissanen, M; Rondo, L; Ruuskanen, T; Santos, FD; Sarnela, N; Schallhart, S; Schnitzhofer, R; Seinfeld, JH; Simon, M; Sipila, M; Stozhkov, Y; Stratmann, F; Tome, A; Troestl, J; Tsagkogeorgas, G; Vaattovaara, P; Viisanen, Y; Virtanen, A; Vrtala, A; Wagner, PE; Weingartner, E; Wex, H; Williamson, C; Wimmer, D; Ye, P; Yli-Juuti, T; Carslaw, KS; Kulmala, M; Curtius, J; Baltensperger, U, rs; Worsnop, DR; Vehkamaki, H; Kirkby, J. (2013). Molecular understanding of sulphuric acid-amine particle nucleation in the atmosphere. Nature 502: 359-+. http://dx.doi.org/10.1038/nature12663

Appel, KW; Napelenok, SL; Foley, KM; Pye, HOT; Hogrefe, C; Luecken, DJ; Bash, JO; Roselle, SJ; Pleim, JE; Foroutan, H; Hutzell, WT; Pouliot, GA; Sarwar, G; Fahey, KM; Gantt, B; Gilliam, RC; Heath, NK; Kang, D; Mathur, R; Schwede, DB; Spero, TL; Wong, DC; Young, JO. (2017). Description and evaluation of the Community Multiscale Air Quality (CMAQ) modeling system version 5.1. GMD 10: 1703-1732. http://dx.doi.org/10.5194/gmd-10-1703-2017

Arakaki, T; Anastasio, C; Kuroki, Y; Nakajima, H; Okada, K; Kotani, Y; Handa, D; Azechi, S; Kimura, T; Tsuhako, A; Miyagi, Y. (2013). A general scavenging rate constant for reaction of hydroxyl radical with organic carbon in atmospheric waters. Environ Sci Technol 47: 8196-8203. http://dx.doi.org/10.1021/es401927b

Asbach, C; Fissan, H; Stahlmecke, B; Kuhlbusch, TAJ; Pui, DYH. (2009). Conceptual limitations and extensions of lung-deposited Nanoparticle Surface Area Monitor (NSAM). J Nanopart Res 11: 101-109. http://dx.doi.org/10.1007/s11051-008-9479-8

Asmi, A; Wiedensohler, A; Laj, P; Fjaeraa, AM; Sellegri, K; Birmili, W; Weingartner, E; Baltensperger, U; Zdimal, V; Zikova, N; Putaud, JP; Marinoni, A; Tunved, P; Hansson, HC; Fiebig, M; Kivekas, N; Lihavainen, H; Asmi, E; Ulevicius, V; Aalto, PP; Swietlicki, E; Kristensson, A; Mihalopoulos, N; Kalivitis, N; Kalapov, I; Kiss, G; de Leeuw, G; Henzing, B; Harrison, RM; Beddows, D; O'Dowd, C; Jennings, SG; Flentje, H; Weinhold, K; Meinhardt, F; Ries, L; Kulmala, M. (2011). Number size distributions and seasonality of submicron particles in Europe 2008-2009. Atmos Chem Phys 11: 5505-5538. http://dx.doi.org/10.5194/acp-11-5505-2011

Baker, KR; Woody, MC; Tonnesen, GS; Hutzell, W; Pye, HOT; Beaver, MR; Pouliot, G; Pierce, T. (2016). Contribution of regional-scale fire events to ozone and PM2.5 air quality estimated by photochemical modeling approaches. Atmos Environ 140: 539-554. http://dx.doi.org/10.1016/j.atmosenv.2016.06.032

Banzhaf, S; Schaap, M; Kranenburg, R; Manders, AMM; Segers, AJ; Visschedijk, AJH; van Der Gon, HAC, D; Kuenen, JJP; van Meijgaard, E; van Ulft, LH; Cofala, J; Builtjes, PJH. (2015). Dynamic model evaluation for secondary inorganic aerosol and its precursors over Europe between 1990 and 2009. GMD 8: 1047-1070. http://dx.doi.org/10.5194/gmd-8-1047-2015

ED_002220_00002287-00236

Barberán, A; Ladau, J; Leff, JW; Pollard, KS; Menninger, HL; Dunn, RR; Fierer, N. (2015). Continental-scale distributions of dust-associated bacteria and fungi. Proc Natl Acad Sci USA 112: 5756-5761. http://dx.doi.org/10.1073/pnas.1420815112

Bash, JO; Baker, KR; Beaver, MR. (2016). Evaluation of improved land use and canopy representation in BEIS v3.61 with biogenic VOC measurements in California. GMD 9: 2191-2207. http://dx.doi.org/10.5194/gmd-9-2191-2016

Bash, JO; Cooter, EJ; Dennis, RL; Walker, JT; Pleim, JE. (2013). Evaluation of a regional air-quality model with bidirectional NH3 exchange coupled to an agroecosystem model. Biogeosciences 10: 1635-1645. http://dx.doi.org/10.5194/bg-10-1635-2013

Beaver, S; Palazoglu, A; Singh, A; Soong, ST; Tanrikulu, S. (2010). Identification of weather patterns impacting 24-hour average fine particulate matter levels. Atmos Environ 44: 1761-1771. http://dx.doi.org/10.1016/j.atmosenv.2010.02.001

Bereznicki, SD; Sobus, J; Vette, AF; Stiegel, MA; Williams, R. (2012). Assessing spatial and temporal variability of VOCs and PM-components in outdoor air during the Detroit Exposure and Aerosol Research Study (DEARS). Atmos Environ 61: 159-168. http://dx.doi.org/10.1016/j.atmosenv.2012.07.008

Berkemeier, T; Ammann, M; Mentel, TF; Pöschl, U; Shiraiwa, M. (2016). Organic nitrate contribution to new particle formation and growth in secondary organic aerosols from α-pinene ozonolysis. Environ Sci Technol 50: 6334-6342. http://dx.doi.org/10.1021/acs.est.6b00961

Berndt, T; Jokinen, T; Mauldin, R, III; Petaja, T; Herrmann, H; Junninen, H; Paasonen, P; Worsnop, DR; Sipila, M. (2012). Gas-phase ozonolysis of selected olefins: The yield of stabilized criegee intermediate and the reactivity toward SO2. J Phys Chem Lett 3: 2892-2896. http://dx.doi.org/10.1021/jz301158u

Blanchard, CL; Tanenbaum, S; Hidy, GM. (2013). Source attribution of air pollutant concentrations and trends in the southeastern aerosol research and characterization (SEARCH) network. Environ Sci Technol 47: 13536-13545. http://dx.doi.org/10.1021/es402876s

Blanchard, CL; Tanenbaum, S; Hidy, GM. (2014). Spatial and temporal variability of air pollution in Birmingham, Alabama. Atmos Environ 89: 382-391. http://dx.doi.org/10.1016/j.atmosenv.2014.01.006

Boogaard, H; Kos, GPA; Weijers, EP; Janssen, NAH; Fischer, PH; van der Zee, SC; de Hartog, JJ; Hoek, G. (2011). Contrast in air pollution components between major streets and background locations: Particulate matter mass, black carbon, elemental composition, nitrogen oxide and ultrafine particle number. Atmos Environ 45: 650-658. http://dx.doi.org/10.1016/j.atmosenv.2010.10.033

Borgie, M; Dagher, Z; Ledoux, F; Verdin, A; Cazier, F; Martin, P; Hachimi, A; Shirali, P; Greige-Gerges, H; Courcot, D. (2015). Comparison between ultrafine and fine particulate matter collected in Lebanon: Chemical characterization, in vitro cytotoxic effects and metabolizing enzymes gene expression in human bronchial epithelial cells. Environ Pollut 205: 250-260. http://dx.doi.org/10.1016/j.envpol.2015.05.027

Boys, BL; Martin, RV; van Donkelaar, A; MacDonell, RJ; Hsu, NC; Cooper, MJ; Yantosca, RM; Lu, Z; Streets, DG; Zhang, Q; Wang, SW. (2014). Fifteen-year global time series of satellite-derived fine particulate matter. Environ Sci Technol 48: 11109-11118. http://dx.doi.org/10.1021/es502113p

Bruggemann, E; Gerwig, H; Gnauk, T; Muller, K; Herrmann, H. (2009). Influence of seasons, air mass origin and day of the week on size-segregated chemical composition of aerosol particles at a kerbside. Atmos Environ 43: 2456-2463. http://dx.doi.org/10.1016/j.atmosenv.2009.01.054

Byun, D; Schere, KL. (2006). Review of the governing equations, computational algorithms, and other components of the models-3 community multiscale air quality (CMAQ) modeling system [Review]. Appl Mech Rev 59: 51-77. http://dx.doi.org/10.1115/1.2128636

Byun, DW; Ching, JKS. (1999). Science algorithms of the EPA models-3 community multiscale air quality (CMAQ) modeling system. (EPA/600-R-99-030). Washington, DC: U.S. Environmental Protection Agency. http://www.epa.gov/asmdnerl/CMAQ/CMAQscienceDoc.html

ED_002220_00002287-00237

Bzdek, BR; Horan, AJ; Pennington, MR; Depalma, JW; Zhao, J, un; Jen, CN; Hanson, DR; Smith, JN; Mcmurry, PH; Johnston, MV. (2013). Quantitative and time-resolved nanoparticle composition measurements during new particle formation. Faraday Discuss 165: 25-43. http://dx.doi.org/10.1039/c3fd00039g

Bzdek, BR; Lawler, MJ; Horan, AJ; Pennington, MR; Depalma, JW; Zhao, J, un; Smith, JN; Johnston, MV. (2014). Molecular constraints on particle growth during new particle formation. Geophys Res Lett 41: 6045-6054. http://dx.doi.org/10.1002/2014GL060160

Bzdek, BR; Pennington, MR; Johnston, MV. (2012). Single particle chemical analysis of ambient ultrafine aerosol: A review. J Aerosol Sci 52: 109-120. http://dx.doi.org/10.1016/j.jaerosci.2012.05.001

Cacciottolo, M; Wang, X; Driscoll, I; Woodward, N; Saffari, A; Reyes, J; Serre, ML; Vizuete, W; Sioutas, C; Morgan, TE; Gatz, M; Chui, HC; Shumaker, SA; Resnick, SM; Espeland, MA; Finch, CE; Chen, JC. (2017). Particulate air pollutants, APOE alleles and their contributions to cognitive impairment in older women and to amyloidogenesis in experimental models. Transl Psychiatry 7: e1022. http://dx.doi.org/10.1038/tp.2016.280

Cahill, TM. (2013). Annual cycle of size-resolved organic aerosol characterization in an urbanized desert environment. Atmos Environ 71: 226-233. http://dx.doi.org/10.1016/j.atmosenv.2013.02.004

Camp, DC. (1980). An intercomparison of results from samplers used in the determination of aerosol composition. Environ Int 4: 83-100.

Carlton, AG; Pinder, RW; Bhave, PV; Pouliot, GA. (2010). To what extent can biogenic SOA be controlled. Environ Sci Technol 44: 3376-3380. http://dx.doi.org/10.1021/es903506b

Carlton, AG; Wiedinmyer, C; Kroll, JH. (2009). A review of Secondary Organic Aerosol (SOA) formation from isoprene [Review]. Atmos Chem Phys 9: 4987-5005.

CFR 40 Part 58 Appendix E. CFR Appendix E to part 58Probe and monitoring path siting criteria for ambient air quality monitoring (40 CFR Part 58, Appendix 58, 2018), (Goverment Publishing Office2018). https://www.ecfr.gov/cgi-bin/retrieveECFR?n=40y6.0.1.1.6#ap40.6.58_161.e

Chan, AWH; Kautzman, KE; Chhabra, PS; Surratt, JD; Chan, MN; Crounse, JD; Kurten, A; Wennberg, PO; Flagan, RC; Seinfeld, JH. (2009). Secondary organic aerosol formation from photooxidation of naphthalene and alkylnaphthalenes: implications for oxidation of intermediate volatility organic compounds (IVOCs). Atmos Chem Phys 9: 3049-3060.

Chan, EAW; Gantt, B; McDow, S. (2018). The reduction of summer sulfate and switch from summertime to wintertime PM2.5 concentration maxima in the United States. Atmos Environ 175: 25-32. http://dx.doi.org/10.1016/j.atmosenv.2017.11.055

Chan, MN; Surratt, JD; Chan, AWH; Schilling, K; Offenberg, JH; Lewandowski, M; Edney, EO; Kleindienst, TE; Jaoui, M; Edgerton, ES; Tanner, RL; Shaw, SL; Zheng, M; Knipping, EM; Seinfeld, JH. (2011). Influence of aerosol acidity on the chemical composition of secondary organic aerosol from beta-caryophyllene. Atmos Chem Phys 11: 1735-1751. http://dx.doi.org/10.5194/acp-11-1735-2011

Chen, SC; Tsai, CJ; Chou, CCK; Roam, GD; Cheng, SS; Wang, YN. (2010). Ultrafine particles at three different sampling locations in Taiwan. Atmos Environ 44: 533-540. http://dx.doi.org/10.1016/j.atmosenv.2009.10.044

Cheng, H; Saffari, A; Sioutas, C; Forman, HJ; Morgan, TE; Finch, CE. (2016). Nano-scale particulate matter from urban traffic rapidly induces oxidative stress and inflammation in olfactory epithelium with concomitant effects on brain. Environ Health Perspect 124: 1537-1546. http://dx.doi.org/10.1289/EHP134

Cheng, Y; He, KB; Duan, FK; Zheng, M; Ma, YL; Tan, JH. (2009). Positive sampling artifact of carbonaceous aerosols and its influence on the thermal-optical split of OC/EC. Atmos Chem Phys 9: 7243-7256.

Cheng, Y; He, KB; Duan, FK; Zheng, M; Ma, YL; Tan, JH; Du, ZY. (2010). Improved measurement of carbonaceous aerosol: evaluation of the sampling artifacts and inter-comparison of the thermal-optical analysis methods. Atmos Chem Phys 10: 8533-8548. http://dx.doi.org/10.5194/acp-10-8533-2010

ED_002220_00002287-00238

Cheung, HC; Chou, CCK; Chen, MJ; Huang, WR; Huang, SH; Tsai, CY; Lee, CSL. (2016). Seasonal variations of ultra-fine and submicron aerosols in Taipei, Taiwan: implications for particle formation processes in a subtropical urban area. Atmos Chem Phys 16: 1317-1330. http://dx.doi.org/10.5194/acp-16-1317-2016

Cheung, K; Daher, N; Kam, W; Shafer, MM; Ning, Z; Schauer, JJ; Sioutas, C. (2011). Spatial and temporal variation of chemical composition and mass closure of ambient coarse particulate matter (PM10-2.5) in the Los Angeles area. Atmos Environ 45: 2651-2662. http://dx.doi.org/10.1016/j.atmosenv.2011.02.066

Cheung, K; Shafer, MM; Schauer, JJ; Sioutas, C. (2012a). Diurnal trends in oxidative potential of coarse particulate matter in the Los Angeles Basin and their relation to sources and chemical composition. Environ Sci Technol 46: 3779-3787. http://dx.doi.org/10.1021/es204211v

Cheung, K; Shafer, MM; Schauer, JJ; Sioutas, C. (2012b). Historical trends in the mass and chemical species concentrations of coarse particulate matter in the Los Angeles Basin and relation to sources and air quality regulations. J Air Waste Manag Assoc 62: 541-556. http://dx.doi.org/10.1080/10962247.2012.661382

Chiapello, I; Moulin, C; Prospero, JM. (2005). Understanding the long-term variability of African dust transport across the Atlantic as recorded in both Barbados surface concentrations and large-scale Total Ozone Mapping Spectrometer (TOMS) optical thickness. J Geophys Res 110: D18S10. http://dx.doi.org/10.1029/2004JD005132

Choi, S; Myung, CL; Park, S. (2014). Review on characterization of nano-particle emissions and PM morphology from internal combustion engines: Part 2. Int J Automot Tech 15: 219-227. http://dx.doi.org/10.1007/s12239-014-0023-9

Chow, JC; Watson, JG; Chen, LWA; Rice, J; Frank, NH. (2010a). Quantification of PM2.5 organic carbon sampling artifacts in US networks. Atmos Chem Phys 10: 5223-5239. http://dx.doi.org/10.5194/acp-10-5223-2010

Chow, JC; Watson, JG; Lowenthal, DH; Chen, LW; Motallebi, N. (2010b). Black and organic carbon emission inventories: review and application to California [Review]. J Air Waste Manag Assoc 60: 497-507. http://dx.doi.org/10.3155/1047-3289.60.4.497

Chudnovsky, A; Tang, C; Lyapustin, A; Wang, Y; Schwartz, J; Koutrakis, P. (2013a). A critical assessment of high-resolution aerosol optical depth retrievals for fine particulate matter predictions. Atmos Chem Phys 13: 10907-10917. http://dx.doi.org/10.5194/acp-13-10907-2013

Chudnovsky, AA; Kostinski, A; Lyapustin, A; Koutrakis, P. (2013b). Spatial scales of pollution from variable resolution satellite imaging. Environ Pollut 172: 131-138. http://dx.doi.org/10.1016/j.envpol.2012.08.016

Ciarelli, G; El Haddad, I; Bruns, E; Aksoyoglu, S; Moehler, O; Baltensperger, U, rs; Prevot, ASH. (2017). Constraining a hybrid volatility basis-set model for aging of wood-burning emissions using smog chamber experiments: a box-model study based on the VBS scheme of the CAMx model (v5.40). Geoscientific Model Development 10: 2303-2320. http://dx.doi.org/10.5194/gmd-10-2303-2017

Civerolo, K; Hogrefe, C; Zalewsky, E; Hao, W; Sistla, G; Lynn, B; Rosenzweig, C; Kinney, PL. (2010). Evaluation of an 18-year CMAQ simulation: Seasonal variations and long-term temporal changes in sulfate and nitrate. Atmos Environ 44: 3745-3752. http://dx.doi.org/10.1016/j.atmosenv.2010.06.056

Clements, AL; Fraser, MP; Upadhyay, N; Herckes, P; Sundblom, M; Lantz, J; Solomon, PA. (2013). Characterization of summertime coarse particulate matter in the Desert SouthwestArizona, USA. J Air Waste Manag Assoc 63: 764-772. http://dx.doi.org/10.1080/10962247.2013.787955

Clements, AL; Fraser, MP; Upadhyay, N; Herckes, P; Sundblom, M; Lantz, J; Solomon, PA. (2014a). Chemical characterization of coarse particulate matter in the Desert Southwest - Pinal County Arizona, USA. Atmos Pollut Res 5: 52-61. http://dx.doi.org/10.5094/APR.2014.007

Clements, N; Eav, J; Xie, M; Hannigan, MP; Miller, SL; Navidi, W; Peel, JL; Schauer, JJ; Shafer, MM; Milford, JB. (2014b). Concentrations and source insights for trace elements in fine and coarse particulate matter. Atmos Environ 89: 373-381. http://dx.doi.org/10.1016/j.atmosenv.2014.01.011

Clements, N; Piedrahita, R; Ortega, J; Peel, JL; Hannigan, M; Miller, SL; Milford, JB. (2012). Characterization and nonparametric regression of rural and urban coarse particulate matter mass concentrations in Northeastern Colorado. Aerosol Sci Technol 46: 108-123. http://dx.doi.org/10.1080/02786826.2011.607478

ED_002220_00002287-00239

Clougherty, JE; Kheirbek, I; Eisl, HM; Ross, Z; Pezeshki, G; Gorczynski, JE; Johnson, S; Markowitz, S; Kass, D; Matte, T. (2013). Intra-urban spatial variability in wintertime street-level concentrations of multiple combustion-related air pollutants: The New York City Community Air Survey (NYCCAS). J Expo Sci Environ Epidemiol 23: 232-240. http://dx.doi.org/10.1038/jes.2012.125

Cohan, DS; Chen, R. (2014). Modeled and observed fine particulate matter reductions from state attainment demonstrations. J Air Waste Manag Assoc 64: 995-1002. http://dx.doi.org/10.1080/10962247.2014.905509

Cook, RD; Lin, YH; Peng, Z; Boone, E; Chu, RK; Dukett, JE; Gunsch, MJ; Zhang, W; Tolic, N; Laskin, A; Pratt, KA. (2017). Biogenic, urban, and wildfire influences on the molecular composition of dissolved organic compounds in cloud water. Atmos Chem Phys 17: 15167-15180. http://dx.doi.org/10.5194/acp-17-15167-2017

Creamean, JM; Spackman, JR; Davis, SM; White, AB. (2014). Climatology of long-range transported Asian dust along the West Coast of the United States. J Geophys Res Atmos 119: 12171-12185. http://dx.doi.org/10.1002/2014JD021694

Crilley, LR; Jayaratne, ER; Ayoko, GA; Miljevic, B; Ristovski, Z; Morawska, L. (2014). Observations on the formation, growth and chemical composition of aerosols in an urban environment. Environ Sci Technol 48: 6588-6596. http://dx.doi.org/10.1021/es5019509

Crippa, P; Sullivan, RC; Thota, A; Pryor, SC. (2016). Evaluating the skill of high-resolution WRF-Chem simulations in describing drivers of aerosol direct climate forcing on the regional scale. Atmos Chem Phys 16: 397-416. http://dx.doi.org/10.5194/acp-16-397-2016

Daher, N; Hasheminassab, S; Shafer, MM; Schauer, JJ; Sioutas, C. (2013). Seasonal and spatial variability in chemical composition and mass closure of ambient ultrafine particles in the megacity of Los Angeles. Environ Sci Process Impacts 15: 283-295. http://dx.doi.org/10.1039/c2em30615h

Day, DA; Liu, S; Russell, LM; Ziemann, PJ. (2010). Organonitrate group concentrations in submicron particles with high nitrate and organic fractions in coastal southern California. Atmos Environ 44: 1970-1979. http://dx.doi.org/10.1016/j.atmosenv.2010.02.045

Demokritou, P; Kavouras, IG; Ferguson, ST; Koutrakis, P. (2002). Development of a high volume cascade impactor for toxicological and chemical characterization studies. Aerosol Sci Technol 36: 925-933. http://dx.doi.org/10.1080/02786820290092113

Dennison, PE; Brewer, SC; Arnold, JD; Moritz, M, axA. (2014). Large wildfire trends in the western United States, 1984-2011. Geophys Res Lett 41: 2928-2933. http://dx.doi.org/10.1002/2014GL059576

Despres, VR; Huffman, JA; Burrows, SM; Hoose, C; Safatov, AS; Buryak, G; Froehlich-Nowoisky, J; Elbert, W; Andreae, MO; Poeschl, U; Jaenicke, R. (2012). Primary biological aerosol particles in the atmosphere: a review. Tellus B Chem Phys Meteorol 64. http://dx.doi.org/10.3402/tellusb.v64i0.15598

Dhaniyala, S; Fierz, M; Keskinen, J; Marjamäki, M. (2011). Instruments based on electrical detection of aerosols. In P Kulkami; PA Baron; K Willeke (Eds.), Aerosol measurement: Principles, techniques, and applications (3rd ed., pp. 393-416). Hoboken, NJ: Wiley. http://dx.doi.org/10.1002/9781118001684.ch18

Docherty, KS; Wu, W; Lim, YB; Ziemann, PJ. (2005). Contributions of organic peroxides to secondary aerosol formed from reactions of monoterpenes with O3. Environ Sci Technol 39: 4049-4059. http://dx.doi.org/10.1021/es050228s

Donahue, NM; Ortega, IK; Chuang, W; Riipinen, I; Riccobono, F; Schobesberger, S; Dommen, J; Baltensperger, U; Kulmala, M; Worsnop, DR; Vehkamaki, H. (2013). How do organic vapors contribute to new-particle formation? Faraday Discuss 165: 91-104. http://dx.doi.org/10.1039/c3fd00046j

Duvall, RM; Norris, GA; Burke, JM; Olson, DA; Vedantham, R; Williams, R. (2012). Determining spatial variability in PM2.5 source impacts across Detroit, MI. Atmos Environ 47: 491-498. http://dx.doi.org/10.1016/j.atmosenv.2011.09.071

ED_002220_00002287-00240

Ehn, M; Thornton, JA; Kleist, E; Sipilä, M; Junninen, H; Pullinen, I; Springer, M; Rubach, F; Tillmann, R; Lee, B; Lopez-Hilfiker, F; Andres, S; Acir, IH; Rissanen, M; Jokinen, T; Schobesberger, S; Kangasluoma, J; Kontkanen, J; Nieminen, T; Kurtén, T; Nielsen, LB; Jørgensen, S; Kjaergaard, HG; Canagaratna, M; Maso, MD; Berndt, T; Petäjä, T; Wahner, A; Kerminen, VM; Kulmala, M; Worsnop, DR; Wildt, J; Mentel, TF. (2014). A large source of low-volatility secondary organic aerosol. Nature 506: 476-479. http://dx.doi.org/10.1038/nature13032

Engel-Cox, JA; Hollomon, CH; Coutant, BW; Hoff, RM. (2004). Qualitative and quantitative evaluation of MODIS satellite sensor data for regional and urban scale air quality. Atmos Environ 38: 2495-2509. http://dx.doi.org/10.1016/j.atmosenv.2004.01.039

Ervens, B; Turpin, BJ; Weber, RJ. (2011). Secondary organic aerosol formation in cloud droplets and aqueous particles (aqSOA): a review of laboratory, field and model studies. Atmos Chem Phys 11: 11069-11102. http://dx.doi.org/10.5194/acp-11-11069-2011

Evans, KA; Halterman, JS; Hopke, PK; Fagnano, M; Rich, DQ. (2014). Increased ultrafine particles and carbon monoxide concentrations are associated with asthma exacerbation among urban children. Environ Res 129: 11-19. http://dx.doi.org/10.1016/j.envres.2013.12.001

Fahey, KM; Carlton, AG; Pye, HOT; Baeka, J; Hutzell, WT; Stanier, CO; Baker, KR; Appel, KW; Jaoui, M; Offenberg, JH. (2017). A framework for expanding aqueous chemistry in the Community Multiscale Air Quality (CMAQ) model version 5.1. GMD 10: 1587-1605. http://dx.doi.org/10.5194/gmd-10-1587-2017

Fairlie, TD; Jacob, DJ; Park, RJ. (2007). The impact of transpacific transport of mineral dust in the United States. Atmos Environ 41: 1251-1266. http://dx.doi.org/10.1016/j.atmosenv.2006.09.048

Fisher, JA; Jacob, DJ; Travis, KR; Kim, PS; Marais, EA; Chan Miller, C; Yu, K; Zhu, L; Yantosca, RM; Sulprizio, MP; Mao, J; Wennberg, PO; Crounse, JD; Teng, AP; Nguyen, TB; St. Clair, JM; Cohen, RC; Romer, P; Nault, BA; Wooldridge, PJ; Jimenez, JL; Campuzano-Jost, P; Day, DA; Shepson, PB; Xiong, F; Blake, DR; Goldstein, AH; Misztal, PK; Hanisco, TF; Wolfe, GM; Ryerson, TB; Wisthaler, A; Mikoviny, T. (2016). Organic nitrate chemistry and its implications for nitrogen budgets in an isoprene- and monoterpene-rich atmosphere: Constraints from aircraft (SEAC4RS) and ground-based (SOAS) observations in the Southeast US. Atmos Chem Phys Discuss 16: 5969-5991. http://dx.doi.org/10.5194/acp-16-5969-2016

Flechard, CR; Massad, RS; Loubet, B; Personne, E; Simpson, D; Bash, JO; Cooter, EJ; Nemitz, E; Sutton, MA. (2013). Advances in understanding, models and parameterizations of biosphere-atmosphere ammonia exchange. Biogeosciences 10: 5183-5225. http://dx.doi.org/10.5194/bg-10-5183-2013

Fletcher, RA; Mulholland, GW; Winchester, MR; King, RL; Klinedinst, DB. (2009). Calibration of a condensation particle counter using a NIST traceable method. Aerosol Sci Technol 43: 425-441. http://dx.doi.org/10.1080/02786820802716735

Forkel, R; Balzarini, A; Baro, R; Bianconi, R; Curci, G; Jimenez-Guerrero, P; Hirtl, M; Honzak, L; Lorenz, C; Im, U; Perez, JL; Pirovano, G; San Jose, R; Tuccella, P; Werhahn, J; Zabkar, R. (2015). Analysis of the WRF-Chem contributions to AQMEII phase2 with respect to aerosol radiative feedbacks on meteorology and pollutant distributions. Atmos Environ 115: 630-645. http://dx.doi.org/10.1016/j.atmosenv.2014.10.056

Foroutan, H; Young, J; Napelenok, S; Ran, L; Appel, KW; Gilliam, RC; Pleim, JE. (2017). Development and evaluation of a physics-based windblown dust emission scheme implemented in the CMAQ modeling system. JAMES 9: 585-608. http://dx.doi.org/10.1002/2016MS000823

Friedlander, SK. (1977). Smoke, dust and haze: fundamentals of aerosol behavior.

Froehlich-Nowoisky, J; Kampf, CJ; Weber, B; Huffman, JA; Poehlker, C; Andreae, MO; Lang-Yona, N; Burrows, SM; Gunthe, SS; Elbert, W; Su, H; Hoor, P; Thines, E; Hoffmann, T; Despres, VR; Poeschl, U. (2016). Bioaerosols in the Earth system: Climate, health, and ecosystem interactions. Atmos Res 182: 346-376. http://dx.doi.org/10.1016/j.atmosres.2016.07.018

Fruin, S; Urman, R; Lurmann, F; Mcconnell, R, ob; Gauderman, J; Rappaport, E; Franklin, M; Gilliland, FD; Shafer, M; Gorski, P; Avol, E. (2014). Spatial variation in particulate matter components over a large urban area. Atmos Environ 83: 211-219. http://dx.doi.org/10.1016/j.atmosenv.2013.10.063

ED_002220_00002287-00241

Furuuchi, M; Eryu, K; Nagura, M; Hata, M; Kato, T; Tajima, N; Sekiguchi, K; Ehara, K; Seto, T; Otani, Y. (2010). Development and performance evaluation of air sampler with inertial filter for nanoparticle sampling. Aerosol Air Qual Res 10: 185-192. http://dx.doi.org/10.4209/aaqr.2009.11.0070

Fushimi, A; Kondo, Y; Kobayashi, S; Fujitani, Y; Saitoh, K; Takami, A; Tanabe, K. (2016). Chemical composition and source of fine and nanoparticles from recent direct injection gasoline passenger cars: Effects of fuel and ambient temperature. Atmos Environ 124: 77-84. http://dx.doi.org/10.1016/j.atmosenv.2015.11.017

Fushimi, A; Saitoh, K; Fujitani, Y; Hasegawa, S; Takahashi, K; Tanabe, K; Kobayashi, S. (2011). Organic-rich nanoparticles (diameter: 10-30 nm) in diesel exhaust: Fuel and oil contribution based on chemical composition. Atmos Environ 45: 6326-6336. http://dx.doi.org/10.1016/j.atmosenv.2011.08.053

Gaggeler, HW; Baltensperger, U; Emmenegger, M; Jost, DT; Schmidt-Ott, A; Haller, P; Hofmann, M. (1989). The epiphaniometer, a new device for continuous aerosol monitoring. J Aerosol Sci 20: 557-564.

Gan, CM; Pleim, J; Mathur, R; Hogrefe, C; Long, CN; Xing, J; Wong, D; Gilliam, R; Wei, C. (2015). Assessment of long-term WRF-CMAQ simulations for understanding direct aerosol effects on radiation "brightening" in the United States. Atmos Chem Phys 15: 12193-12209. http://dx.doi.org/10.5194/acp-15-12193-2015

Geiss, O; Bianchi, I; Barrero-Moreno, J. (2016). Lung-deposited surface area concentration measurements in selected occupational and non-occupational environments. J Aerosol Sci 96: 24-37. http://dx.doi.org/10.1016/j.jaerosci.2016.02.007

Georgoulias, AK; Papanastasiou, DK; Melas, D; Amiridis, V; Alexandri, G. (2009). Statistical analysis of boundary layer heights in a suburban environment. Meteorol Atmos Phys 104: 103-111. http://dx.doi.org/10.1007/s00703-009-0021-z

Ghio, AJ; Kim, C; Devlin, RB. (2000). Concentrated ambient air particles induce mild pulmonary inflammation in healthy human volunteers. Am J Respir Crit Care Med 162: 981-988.

Gidney, J; Twigg, M; Kittelson, D. (2010). Effect of organometallic fuel additives on nanoparticle emissions from a gasoline passenger car. Environ Sci Technol 44: 2562-2569. http://dx.doi.org/10.1021/es901868c

Giechaskiel, B; Maricq, M; Ntziachristos, L; Dardiotis, C; Wang, X; Axmann, H; Bergmann, A; Schindler, W. (2014). Review of motor vehicle particulate emissions sampling and measurement: From smoke and filter mass to particle number. J Aerosol Sci 67: 48-86. http://dx.doi.org/10.1016/j.jaerosci.2013.09.003

Gini, MI; Helmis, CG; Eleftheriadis, K. (2013). Cascade Epiphaniometer: An instrument for aerosol "Fuchs" surface area size distribution measurements. J Aerosol Sci 63: 87-102. http://dx.doi.org/10.1016/j.jaerosci.2013.05.001

Goldstein, AH; Koven, CD; Heald, CL; Fung, IY. (2009). Biogenic carbon and anthropogenic pollutants combine to form a cooling haze over the southeastern United States. Proc Natl Acad Sci USA 106: 8835-8840. http://dx.doi.org/10.1073/pnas.0904128106

Green, MC; Chow, JC; Watson, JG; Dick, K; Inouye, D. (2015). Effects of snow cover and atmospheric stability on winter PM2.5 concentrations in western U.S. valleys. J Appl Meteor Climatol 54: 1191-1201. http://dx.doi.org/10.1175/JAMC-D-14-0191.1

Grover, BD; Eatough, NL; Eatough, DJ; Chow, JC; Watson, JG; Ambs, JL; Meyer, MB; Hopke, PK; Al-Horr, R; Later, DW; Wilson, WE. (2006). Measurement of both nonvolatile and semi-volatile fractions of fine particulate matter in Fresno, CA. Aerosol Sci Technol 40: 811-826. http://dx.doi.org/10.1080/02786820600615071

Grythe, H; Strom, J; Krejci, R; Quinn, P; Stohl, A. (2014). A review of sea-spray aerosol source functions using a large global set of sea salt aerosol concentration measurements. Atmos Chem Phys 14: 1277-1297. http://dx.doi.org/10.5194/acp-14-1277-2014

Gupta, T; Demokritou, P; Koutrakis, P. (2004). Development and performance evaluation of a high-volume ultrafine particle concentrator for inhalation toxicological studies. Inhal Toxicol 16: 851-862. http://dx.doi.org/10.1080/08958370490506664

ED_002220_00002287-00242

Hakkinen, SAK; Manninen, HE; Yli-Juuti, T; Merikanto, J; Kajos, MK; Nieminen, T; D'Andrea, SD; Asmi, A; Pierce, J. R.; Kulmala, M; Riipinen, I. (2013). Semi-empirical parameterization of size-dependent atmospheric nanoparticle growth in continental environments. Atmos Chem Phys 13: 7665-7682. http://dx.doi.org/10.5194/acp-13-7665-2013

Hallquist, ÅM; Fridell, E; Westerlund, J; Hallquist, M. (2013). Onboard measurements of nanoparticles from a SCR-equipped marine diesel engine. Environ Sci Technol 47: 773-780. http://dx.doi.org/10.1021/es302712a

Hallquist, M; Wenger, JC; Baltensperger, U; Rudich, Y; Simpson, D; Claeys, M; Dommen, J; Donahue, NM; George, C; Goldstein, AH; Hamilton, JF; Herrmann, H; Hoffmann, T; Iinuma, Y; Jang, M; Jenkin, ME; Jimenez, JL; Kiendler-Scharr, A; Maenhaut, W; Mcfiggans, G; Mentel, T, hF; Monod, A; Prevot, ASH; Seinfeld, JH; Surratt, JD; Szmigielski, R; Wildt, J. (2009). The formation, properties and impact of secondary organic aerosol: current and emerging issues. Atmos Chem Phys 9: 5155-5236.

Hampel, R; Breitner, S; Schneider, A; Zareba, W; Kraus, U; Cyrys, J; Geruschkat, U; Belcredi, P; Müller, M; Wichmann, HE; Peters, A; Group, F. (2012). Acute air pollution effects on heart rate variability are modified by SNPs involved in cardiac rhythm in individuals with diabetes or impaired glucose tolerance. Environ Res 112: 177-185. http://dx.doi.org/10.1016/j.envres.2011.10.007

Han, Y; Iwamoto, Y; Nakayama, T; Kawamura, K; Mochida, M. (2014). Formation and evolution of biogenic secondary organic aerosol over a forest site in Japan. J Geophys Res Atmos 119: 259-273. http://dx.doi.org/10.1002/2013JD020390

Hand, JL; Copeland, SA; Day, DA; Dillner, AM; Indresand, H; Malm, WC; McDade, CE; Moore, CT, Jr; Pitchford, ML; Schichtel, BA; Watson, JG. (2011). Spatial and seasonal patterns and temporal variability of haze and its constituents in the United States, IMPROVE Report V. Fort Collins, CO: Colorado State University.

Hand, JL; Gebhart, KA; Schichtel, BA; Malm, WC. (2012a). Increasing trends in wintertime particulate sulfate and nitrate ion concentrations in the Great Plains of the United States (20002010). Atmos Environ 55: 107-110. http://dx.doi.org/10.1016/j.atmosenv.2012.03.050

Hand, JL; Schichtel, BA; Malm, WC; Pitchford, M. (2013). Widespread reductions in sulfate across the United States since the early 1990s. AIP Conference Proceedings 1527: 495-498. http://dx.doi.org/10.1063/1.4803313

Hand, JL; Schichtel, BA; Malm, WC; Pitchford, ML. (2012b). Particulate sulfate ion concentration and SO2 emission trends in the United States from the early 1990s through 2010. Atmos Chem Phys 12: 10353-10365. http://dx.doi.org/10.5194/acp-12-10353-2012

Hand, JL; Schichtel, BA; Pitchford, M; Malm, WC; Frank, NH. (2012c). Seasonal composition of remote and urban fine particulate matter in the United States. J Geophys Res Atmos 117. http://dx.doi.org/10.1029/2011JD017122

Hata, M; Linfa, B, ao; Otani, Y; Furuuchi, M. (2012). Performance Evaluation of an Andersen Cascade Impactor with an Additional Stage for Nanoparticle Sampling. Aerosol Air Qual Res 12: 1041-1048. http://dx.doi.org/10.4209/aaqr.2012.08.0204

He, X; Son, SY; James, K; Yermakov, M; Reponen, T; McKay, R; Grinshpun, SA. (2013). Exploring a novel ultrafine particle counter for utilization in respiratory protection studies. J Occup Environ Hyg 10: D52-D54. http://dx.doi.org/10.1080/15459624.2013.766555

Heald, CL; Jacob, DJ; Park, RJ; Alexander, B; Fairlie, TD; Yantosca, RM; Chu, DA. (2006). Transpacific transport of Asian anthropogenic aerosols and its impact on surface air quality in the United States. J Geophys Res Atmos 111. http://dx.doi.org/10.1029/2005JD006847

Heikkilä, J; Virtanen, A; Rönkkö, T; Keskinen, J; Aakko-Saksa, P; Murtonen, T. (2009). Nanoparticle emissions from a heavy-duty engine running on alternative diesel fuels. Environ Sci Technol 43: 9501-9506. http://dx.doi.org/10.1021/es9013807

Henze, DK; Seinfeld, JH; Shindell, DT. (2009). Inverse modeling and mapping US air quality influences of inorganic PM2.5 precursor emissions using the adjoint of GEOS-Chem. Atmos Chem Phys 9: 5877-5903.

ED_002220_00002287-00243

Herrmann, H; Hoffmann, D; Schaefer, T; Bräuer, P; Tilgner, A. (2010). Tropospheric aqueous-phase free-radical chemistry: radical sources, spectra, reaction kinetics and prediction tools. Chemphyschem 11: 3796-3822. http://dx.doi.org/10.1002/cphc.201000533

Hinds, WC. (1999). Aerosol technology: Properties, behavior, and measurement of airborne particles (2nd ed.). New York: John Wiley & Sons.

Hirsikko, A; Nieminen, T; Gagne, S; Lehtipalo, K; Manninen, HE; Ehn, M; Horrak, U; Kerminen, VM; Laakso, L; Mcmurry, PH; Mirme, A; Mirme, S; Petaja, T; Tammet, H; Vakkari, V; Vana, M; Kulmala, M. (2011). Atmospheric ions and nucleation: a review of observations. Atmos Chem Phys 11: 767-798. http://dx.doi.org/10.5194/acp-11-767-2011

Hoff, RM; Christopher, SA. (2009). Remote sensing of particulate pollution from space: Have we reached the Promised Land? [Review]. J Air Waste Manag Assoc 59: 645-675. http://dx.doi.org/10.3155/1047-3289.59.6.645

Hogrefe, C; Pouliot, G; Wong, D; Torian, A; Roselle, S; Pleim, J; Mathur, R. (2015). Annual application and evaluation of the online coupled WRF-CMAQ system over North America under AQMEII phase 2. Atmos Environ 115: 683-694. http://dx.doi.org/10.1016/j.atmosenv.2014.12.034

Holzinger, R; Kasper-Giebl, A; Staudinger, M; Schauer, G; Rockmann, T. (2010). Analysis of the chemical composition of organic aerosol at the Mt. Sonnblick observatory using a novel high mass resolution thermal-desorption proton-transfer-reaction mass-spectrometer (hr-TD-PTR-MS). Atmos Chem Phys 10: 10111-10128. http://dx.doi.org/10.5194/acp-10-10111-2010

Hoyle, CR; Boy, M; Donahue, NM; Fry, JL; Glasius, M; Guenther, A; Hallar, AG; Hartz, KH; Petters, MD; Petaja, T; Rosenoern, T; Sullivan, AP. (2011). A review of the anthropogenic influence on biogenic secondary organic aerosol. Atmos Chem Phys 11: 321-343. http://dx.doi.org/10.5194/acp-11-321-2011

Hu, Z. (2009). Spatial analysis of MODIS aerosol optical depth, PM2.5, and chronic coronary heart disease. Int J Health Geogr 8: 27. http://dx.doi.org/10.1186/1476-072X-8-27

Hudda, N; Cheung, K; Moore, KF; Sioutas, C. (2010). Inter-community variability in total particle number concentrations in the eastern Los Angeles air basin. Atmos Chem Phys 10: 11385-11399. http://dx.doi.org/10.5194/acp-10-11385-2010

Hughes, LS; Cass, GR; Gone, J; Ames, M; Olmez, I. (1998). Physical and chemical characterization of atmospheric ultrafine particles in the Los Angeles area. Environ Sci Technol 32: 1153-1161.

Husar, RB; Tratt, DM; Schichtel, BA; Falke, S. R.; Li, F; Jaffe, D; Gasso, S; Gill, T; Laulainen, NS; Lu, F; Reheis, MC; Chun, Y; Westphal, D; Holben, BN; Gueymard, C; McKendry, I; Kuring, N; Feldman, GC; Mcclain, C; Frouin, RJ; Merrill, J; Dubois, D; Vignola, F; Murayama, T; Nickovic, S; Wilson, WE; Sassen, K; Sugimoto, N; Malm, WC. (2001). Asian dust events of April 1998. J Geophys Res 106: 18,317-318,330.

Iida, K; Stolzenburg, MR; McMurry, PH; Smith, JN; Quant, FR; Oberreit, DR; Keady, PB; Eiguren-Fernandez, A; Lewis, GS; Kreisberg, NM; Hering, SV. (2008). An ultrafine, water-based condensation particle counter and its evaluation under field conditions. Aerosol Sci Technol 42: 862-871. http://dx.doi.org/10.1080/02786820802339579

Im, U; Bianconi, R; Solazzo, E; Kioutsioukis, I; Badia, A; Balzarini, A; Baro, R; Bellasio, R; Brunner, D; Chemel, C; Curci, G; Flemming, J; Forkel, R; Giordano, L, ea; Jimenez-Guerrero, P; Hirtl, M; Hodzic, A; Honzak, L; Jorba, O; Knote, C; Kuenen, JJP; Makar, PA; Manders-Groot, A; Neal, L; Perez, JL; Pirovano, G; Pouliot, G; San Jose, R; Savage, N; Schroder, W; Sokhi, RS; Syrakov, D; Torian, A; Tuccella, P; Werhahn, J; Wolke, R; Yahya, K; Zabkar, R; Zhang, Y; Zhang, J; Hogrefe, C; Galmarini, S. (2015a). Evaluation of operational on-line-coupled regional air quality models over Europe and North America in the context of AQMEII phase 2. Part I: Ozone. Atmos Environ 115: 404-420. http://dx.doi.org/10.1016/j.atmosenv.2014.09.042

ED_002220_00002287-00244

Im, U; Bianconi, R; Solazzo, E; Kioutsioukis, I; Badia, A; Balzarini, A; Baro, R; Bellasio, R; Brunner, D; Chemel, C; Curci, G; van Der Gon, HD; Flemming, J; Forkel, R; Giordano, L, ea; Jimenez-Guerrero, P; Hirtl, M; Hodzic, A; Honzak, L; Jorba, O; Knote, C; Makar, PA; Manders-Groot, A; Neal, L; Perez, JL; Pirovano, G; Pouliot, G; San Jose, R; Savage, N; Schroder, W; Sokhi, RS; Syrakov, D; Torian, A; Tuccella, P; Wang, K, ai; Werhahn, J; Wolke, R; Zabkar, R; Zhang, Y; Zhang, J; Hogrefe, C; Galmarini, S. (2015b). Evaluation of operational online-coupled regional air quality models over Europe and North America in the context of AQMEII phase 2. Part II: Particulate matter. Atmos Environ 115: 421-441. http://dx.doi.org/10.1016/j.atmosenv.2014.08.072

Iskandar, A; Andersen, ZJ; Bønnelykke, K; Ellermann, T; Andersen, KK; Bisgaard, H. (2012). Coarse and fine particles but not ultrafine particles in urban air trigger hospital admission for asthma in children. Thorax 67: 252-257. http://dx.doi.org/10.1136/thoraxjnl-2011-200324

Jaffe, D; Snow, J; Cooper, O. (2003). The 2001 Asian Dust Events: Transport and impact on surface aerosol concentrations in the U.S. Eos 84: 501-506. http://dx.doi.org/10.1029/2003EO460001

Jaffe, D; Tamura, S; Harris, J. (2005). Seasonal cycle and composition of background fine particles along the west coast of the US. Atmos Environ 39: 297-306. http://dx.doi.org/10.1016/j.atmonsenv.2004.09.016

Janhaell, S; Andreae, MO; Poeschl, U. (2010). Biomass burning aerosol emissions from vegetation fires: particle number and mass emission factors and size distributions. Atmos Chem Phys 10: 1427-1439.

Jiang, J; Chen, M; Kuang, C; Attoui, M; McMurry, PH. (2011). Electrical mobility spectrometer using a diethylene glycol condensation particle counter for measurement of aerosol size distributions down to 1 nm. Aerosol Sci Technol 45: 510-521. http://dx.doi.org/10.1080/02786826.2010.547538

Jiang, J; Kim, C; Wang, X; Stolzenburg, MR; Kaufman, SL; Qi, C; Sem, GJ; Sakurai, H; Hama, N; McMurry, PH. (2014). Aerosol charge fractions downstream of six bipolar chargers: Effects of ion source, source activity, and flowrate. Aerosol Sci Technol 48: 1207-1216. http://dx.doi.org/10.1080/02786826.2014.976333

Johnson, TV. (2009). Review of diesel emissions and control. International Journal of Engine Research 10: 275-285. http://dx.doi.org/10.1243/14680874JER04009

Jolly, WM; Cochrane, MA; Freeborn, PH; Holden, ZA; Brown, TJ; Williamson, GJ; Bowman, DMJ, S. (2015). Climate-induced variations in global wildfire danger from 1979 to 2013. Nat Commun 6. http://dx.doi.org/10.1038/ncomms8537

Jonsson, AM; Westerlund, J; Hallquist, M. (2011). Size-resolved particle emission factors for individual ships. Geophys Res Lett 38: L13809. http://dx.doi.org/10.1029/2011GL047672

Jung, H; Kittelson, DB. (2005). Characterization of aerosol surface instruments in transition regime. Aerosol Sci Technol 39: 902-911. http://dx.doi.org/10.1080/02786820500295701

Kaminski, H; Kuhlbusch, TAJ; Fissan, H; Ravi, L; Horn, HG; Han, H, eeS; Caldow, R, ob; Asbach, C. (2012). Mathematical Description of Experimentally Determined Charge Distributions of a Unipolar Diffusion Charger. Aerosol Sci Technol 46: 708-716. http://dx.doi.org/10.1080/02786826.2012.659360

Kangasluoma, J; Ahonen, L; Attoui, M; Vuollekoski, H; Kulmala, M; Petaja, T. (2015). Sub-3nm particle detection with Commercial TSI 3772 and Airmodus A20 fine condensation particle counters. Aerosol Sci Technol 49: 674-681. http://dx.doi.org/10.1080/02786826.2015.1058481

Karagulian, F; Belis, CA; Dora, CFC; Pruess-Ustuen, AM; Bonjour, S; Adair-Rohani, H; Amann, M. (2015). Contributions to cities' ambient particulate matter (PM): A systematic review of local source contributions at global level. Atmos Environ 120: 475-483. http://dx.doi.org/10.1016/j.atmosenv.2015.08.087

Karavalakis, G; Short, D; Hajbabaei, M; Vu, D; Villela, M; Russell, R; Durbin, T; Asa-Awuku, A. (2013). Criteria emissions, particle number emissions, size distributions, and black carbon measurements from PFI gasoline vehicles fuelled with different ethanol and butanol blends. (2013-01-1147). Warrendale, PA: SAE International. http://dx.doi.org/10.4271/2013-01-1147

Karjalainen, P; Ronkko, T; Pirjola, L; Heikkila, J; Happonen, M; Arnold, F; Rothe, D; Bielaczyc, P; Keskinen, J. (2014). Sulfur driven nucleation mode formation in diesel exhaust under transient driving conditions. Environ Sci Technol 48: 2336-2343. http://dx.doi.org/10.1021/es405009g

ED_002220_00002287-00245

Kavouras, IG; Nikolich, G; Etyemezian, V, ic; Dubois, DW; King, J; Shafer, D. (2012). In situ observations of soil minerals and organic matter in the early phases of prescribed fires. J Geophys Res Atmos 117. http://dx.doi.org/10.1029/2011JD017420

Kelly, JT; Baker, KR; Nowak, JB; Murphy, JG; Markovic, MZ; Vandenboer, TC; Ellis, RA; Neuman, JA; Weber, RJ; Roberts, JM; Veres, PR; de Gouw, JA; Beaver, MR; Newman, S; Misenis, C. (2014). Fine-scale simulation of ammonium and nitrate over the South Coast Air Basin and San Joaquin Valley of California during CalNex-2010. J Geophys Res Atmos 119: 3600-3614. http://dx.doi.org/10.1002/2013JD021290

Kelly, JT; Parworth, CL; Zhang, Q; Miller, DJ; Sun, K; Zondlo, MA; Baker, KR; Wisthaler, A; Nowak, JB; Pusede, SE; Cohen, RC; Weinheimer, AJ; Beyersdorf, AJ; Tonnesen, GS; Bash, JO; Valin, LC; Crawford, JH; Fried, A; Walega, JG. (2018). Modeling NH4NO3 over the San Joaquin Valley during the 2013 DISCOVERAQ Campaign. J Geophys Res Atmos 123: 4727-4745. http://dx.doi.org/10.1029/2018JD028290

Kerminen, VM; Petaja, T; Manninen, HE; Paasonen, P; Nieminen, T; Sipila, M; Junninen, H; Ehn, M; Gagne, S; Laakso, L; Riipinen, I; Vehkamaki, H; Kurten, T; Ortega, IK; Dal Maso, M; Brus, D; Hyvarinen, A; Lihavainen, H; Leppa, J; Lehtinen, KEJ; Mirme, A; Mirme, S; Horrak, U; Berndt, T; Stratmann, F; Birmili, W; Wiedensohler, A; Metzger, A; Dommen, J; Baltensperger, U; Kiendler-Scharr, A; Mentel, TF; Wildt, J; Winkler, PM; Wagner, PE; Petzold, A; Minikin, A; Plass-Duelmer, C; Poeschl, U; Laaksonen, A; Kulmala, M. (2010). Atmospheric nucleation: highlights of the EUCAARI project and future directions. Atmos Chem Phys 10: 10829-10848. http://dx.doi.org/10.5194/acp-10-10829-2010

Khalek, IA; Blanks, MG; Merritt, PM; Zielinska, B. (2015). Regulated and unregulated emissions from modern 2010 emissions-compliant heavy-duty on-highway diesel engines. J Air Waste Manag Assoc 65: 987-1001. http://dx.doi.org/10.1080/10962247.2015.1051606

Kim, PS; Jacob, DJ; Fisher, JA; Travis, K; Yu, K; Zhu, L; Yantosca, RM; Sulprizio, MP; Jimenez, JL; Campuzano-Jost, P; Froyd, KD; Liao, J; Hair, JW; Fenn, MA; Butler, CF; Wagner, NL; Gordon, TD; Welti, A; Wennberg, PO; Crounse, JD; St. Clair, JM; Teng, AP; Millet, DB; Schwarz, JP; Markovic, MZ; Perring, AE. (2015). Sources, seasonality, and trends of southeast US aerosol: An integrated analysis of surface, aircraft, and satellite observations with the GEOS-Chem chemical transport model. Atmos Chem Phys 15: 10411-10433. http://dx.doi.org/10.5194/acp-15-10411-2015

Kim, S; Jaques, PA; Chang, MC; Froines, JR; Sioutas, C. (2001). Versatile aerosol concentration enrichment system (VACES) for simultaneous in vivo and in vitro evaluation of toxic effects of ultrafine, fine and coarse ambient particles Part I: development and laboratory characterization. J Aerosol Sci 32: 1281-1297.

Kirkby, J; Curtius, J; Almeida, J; Dunne, E; Duplissy, J; Ehrhart, S; Franchin, A; Gagné, S; Ickes, L; Kürten, A; Kupc, A; Metzger, A; Riccobono, F; Rondo, L; Schobesberger, S; Tsagkogeorgas, G; Wimmer, D; Amorim, A; Bianchi, F; Breitenlechner, M; David, A; Dommen, J; Downard, A; Ehn, M; Flagan, RC; Haider, S; Hansel, A; Hauser, D; Jud, W; Junninen, H; Kreissl, F; Kvashin, A; Laaksonen, A; Lehtipalo, K; Lima, J; Lovejoy, ER; Makhmutov, V; Mathot, S; Mikkilä, J; Minginette, P; Mogo, S; Nieminen, T; Onnela, A; Pereira, P; Petäjä, T; Schnitzhofer, R; Seinfeld, JH; Sipilä, M; Stozhkov, Y; Stratmann, F; Tomé, A; Vanhanen, J; Viisanen, Y; Vrtala, A; Wagner, PE; Walther, H; Weingartner, E; Wex, H; Winkler, PM; Carslaw, KS; Worsnop, DR; Baltensperger, U; Kulmala, M. (2011). Role of sulphuric acid, ammonia and galactic cosmic rays in atmospheric aerosol nucleation. Nature 476: 429-433. http://dx.doi.org/10.1038/nature10343

Kittelson, D; Kraft, M. (2015). Particle formation and models in internal combustion engines. In D Crolla; D Foster; T Kobayashi; N Vaughen (Eds.), Encyclopedia of automotive engineering: Part 1: Engines-fundamentals (1st ed.). Hoboken, NJ: Wiley.

Kittelson, DB. (1998). Engines and nanoparticles: a review [Review]. J Aerosol Sci 29: 575-588. http://dx.doi.org/10.1016/S0021-8502(97)10037-4

Kittelson, DB; Watts, WF; Johnson, JP; Schauer, JJ; Lawson, DR. (2006). On-road and laboratory evaluation of combustion aerosolsPart 2: Summary of spark ignition engine results. J Aerosol Sci 37: 931-949. http://dx.doi.org/10.1016/j.jaerosci.2005.08.008

ED_002220_00002287-00246

Kleindienst, TE; Jaoui, M; Lewandowski, M; Offenberg, JH; Docherty, KS. (2012). The formation of SOA and chemical tracer compounds from the photooxidation of naphthalene and its methyl analogs in the presence and absence of nitrogen oxides. Atmos Chem Phys 12: 8711-8726. http://dx.doi.org/10.5194/acp-12-8711-2012

Kolb, CE; Bond, T; Carmichael, GR; Ebi, KL; Edwards, DP; Fuelberg, H; Gustin, M, aeS; Hao, J; Jacob, DJ; Jaffe, DA; Kreidenweis, S; Law, KS; Prather, MJ; Simonich, SLM; Thiemens, MH; Rowland, FS; Bierbaum, RM; Busalacchi, AJ, Jr; Carbone, R; Dabberdt, WF; Dow, K; Forbes, GS; Held, I; Lee, A; Pierrehumbert, RT; Prather, K; Smith, KR; Snow, JT; Vonder Haar, TH; Zeng, X. (2010). Global sources of local pollution: An assessment of long-range transport of key air pollutants to and from the United States summary. In Global Sources of Local Pollution: An Assessment of Long-Range Transport of Key Air Pollutants to and from the United States. Washington, DC: The National Academies Press.

Koo, B; Knipping, E; Yarwood, G. (2014). 1.5-Dimensional volatility basis set approach for modeling organic aerosol in CAMx and CMAQ. Atmos Environ 95: 158-164. http://dx.doi.org/10.1016/j.atmosenv.2014.06.031

Kotchenruther, RA. (2016). Source apportionment of PM2.5 at multiple Northwest US sites: Assessing regional winter wood smoke impacts from residential wood combustion. Atmos Environ 142: 210-219. http://dx.doi.org/10.1016/j.atmosenv.2016.07.048

Kourtchev, I; O'Connor, IP; Giorio, C; Fuller, SJ; Kristensen, K; Maenhaut, W; Wenger, JC; Sodeau, J. R.; Glasius, M; Kalberer, M. (2014). Effects of anthropogenic emissions on the molecular composition of urban organic aerosols: An ultrahigh resolution mass spectrometry study. Atmos Environ 89: 525-532. http://dx.doi.org/10.1016/j.atmosenv.2014.02.051

Krechmer, JE; Coggon, MM; Massoli, P; Nguyen, TB; Crounse, JD; Hu, W; Day, DA; Tyndall, GS; Henze, DK; Rivera-Rios, JC; Nowak, JB; Kimmel, JR; Mauldin, RL; Stark, H; Jayne, JT; Sipilä, M; Junninen, H; Clair, JM; Zhang, X; Feiner, PA; Zhang, L; Miller, DO; Brune, WH; Keutsch, FN; Wennberg, PO; Seinfeld, JH; Worsnop, DR; Jimenez, JL; Canagaratna, MR. (2015). Formation of low volatility organic compounds and secondary organic aerosol from isoprene hydroxyhydroperoxide low-NO oxidation. Environ Sci Technol 49: 10330-10339. http://dx.doi.org/10.1021/acs.est.5b02031

Krudysz, M; Moore, K; Geller, M; Sioutas, C; Froines, J. (2009). Intra-community spatial variability of particulate matter size distributions in Southern California/Los Angeles. Atmos Chem Phys 9: 1061-1075.

Ku, BK; Maynard, AD. (2005). Comparing aerosol surface-area measurements of monodisperse ultrafine silver agglomerates by mobility analysis, transmission electron microscopy and diffusion charging. J Aerosol Sci 36: 1108-1124.

Kuang, C; Chen, M; McMurry, PH; Wang, J. (2012a). Modification of laminar flow ultrafine condensation particle counters for the enhanced detection of 1 nm condensation nuclei. Aerosol Sci Technol 46: 309-315. http://dx.doi.org/10.1080/02786826.2011.626815

Kuang, C; Chen, M; Zhao, J; Smith, J; McMurry, PH; Wang, J. (2012b). Size and time-resolved growth rate measurements of 1 to 5 nm freshly formed atmospheric nuclei. Atmos Chem Phys 12: 3573-3589. http://dx.doi.org/10.5194/acp-12-3573-2012

Kudo, S; Sekiguchi, K; Kim, KH; Kinoshita, M; Moeller, D; Wang, Q; Yoshikado, H; Sakamoto, K. (2012). Differences of chemical species and their ratios between fine and ultrafine particles in the roadside environment. Atmos Environ 62: 172-179. http://dx.doi.org/10.1016/j.atmosenv.2012.08.039

Kulmala, M; Kerminen, VM. (2008). On the formation and growth of atmospheric nanoparticles. Atmos Res 90: 132-150. http://dx.doi.org/10.1016/j.atmosres.2008.01.005

Kulmala, M; Kontkanen, J; Junninen, H; Lehtipalo, K; Manninen, HE; Nieminen, T; Petaja, T; Sipila, M; Schobesberger, S; Rantala, P; Franchin, A; Jokinen, T; Jarvinen, E; Aijala, M; Kangasluoma, J; Hakala, J; Aalto, PP; Paasonen, P; Mikkila, J; Vanhanen, J; Aalto, J; Hakola, H; Makkonen, U; Ruuskanen, T; Mauldin, R, III; Duplissy, J; Vehkamaki, H; Back, J; Kortelainen, A, ki; Riipinen, I; Kurten, T; Johnston, MV; Smith, JN; Ehn, M; Mentel, TF; Lehtinen, KEJ; Laaksonen, A, ri; Kerminen, VM; Worsnop, DR. (2013). Direct Observations of Atmospheric Aerosol Nucleation. Science 339: 943-946. http://dx.doi.org/10.1126/science.1227385

ED_002220_00002287-00247

Kulmala, M; Petaja, T; Ehn, M; Thornton, J; Sipila, M; Worsnop, DR; Kerminen, VM. (2014). Chemistry of atmospheric nucleation: on the recent advances on precursor characterization and atmospheric cluster composition in connection with atmospheric new particle formation. Annu Rev Phys Chem 65: 21-37. http://dx.doi.org/10.1146/annurev-physchem-040412-110014

Kumar, P; Pirjola, L; Ketzel, M; Harrison, R. (2013). Nanoparticle emissions from 11 non-vehicle exhaust sources - A review. Atmos Environ 67: 252-277. http://dx.doi.org/10.1016/j.atmosenv.2012.11.011

Kumar, P; Robins, A; Vardoulakis, S; Britter, R. (2010). A review of the characteristics of nanoparticles in the urban atmosphere and the prospects for developing regulatory controls. Atmos Environ 44: 5035-5052. http://dx.doi.org/10.1016/j.atmosenv.2010.08.016

Kürten, A; Jokinen, T; Simon, M; Sipilä, M; Sarnela, N; Junninen, H; Adamov, A; Almeida, J; Amorim, A; Bianchi, F; Breitenlechner, M; Dommen, J; Donahue, NM; Duplissy, J; Ehrhart, S; Flagan, RC; Franchin, A; Hakala, J; Hansel, A; Heinritzi, M; Hutterli, M; Kangasluoma, J; Kirkby, J; Laaksonen, A; Lehtipalo, K; Leiminger, M; Makhmutov, V; Mathot, S; Onnela, A; Petäjä, T; Praplan, AP; Riccobono, F; Rissanen, MP; Rondo, L; Schobesberger, S; Seinfeld, JH; Steiner, G; Tomé, A; Tröstl, J; Winkler, PM; Williamson, C; Wimmer, D; Ye, P; Baltensperger, U; Carslaw, KS; Kulmala, M; Worsnop, DR; Curtius, J. (2014). Neutral molecular cluster formation of sulfuric acid-dimethylamine observed in real time under atmospheric conditions. Proc Natl Acad Sci USA 111: 15019-15024. http://dx.doi.org/10.1073/pnas.1404853111

Lack, DA; Corbett, JJ; Onasch, T; Lerner, B; Massoli, P; Quinn, PK; Bates, TS; Covert, DS; Coffman, D; Sierau, B; Herndon, S; Allan, J; Baynard, T; Lovejoy, E; Ravishankara, AR; Williams, E. (2009). Particulate emissions from commercial shipping: Chemical, physical, and optical properties. J Geophys Res 114: D00F04. http://dx.doi.org/10.1029/2008jd011300

Lagudu, URK; Raja, S; Hopke, PK; Chalupa, DC; Utell, MJ; Casuccio, G; Lersch, TL; West, RR. (2011). Heterogeneity of coarse particles in an urban area. Environ Sci Technol 45: 3288-3296. http://dx.doi.org/10.1021/es103831w

Langmann, B; Duncan, B; Textor, C; Trentmann, J; van Der Werf, GR. (2009). Vegetation fire emissions and their impact on air pollution and climate. Atmos Environ 43: 107-116. http://dx.doi.org/10.1016/j.atmosenv.2008.09.047

Lary, DJ; Faruque, FS; Malakar, N; Moore, A; Roscoe, B; Adams, ZL; Eggelston, Y. (2014). Estimating the global abundance of ground level presence of particulate matter (PM2.5). Geospat Health 8: S611-S630. http://dx.doi.org/10.4081/gh.2014.292

Lee, B; Mohr, C; Lopez-Hilfiker, FD; Lutz, A; Hallquist, M; Lee, L; Romer, P; Cohen, RC; Iyer, S; Kurten, T; Hu, W; Day, DA; Campuzano-Jost, P; Jimenez, JL; Xu, L, u; Ng, N; Guo, H; Weber, RJ; Wild, RJ; Brown, SS; Koss, A; de Gouw, J; Olson, K; Goldstein, AH; Seco, R; Kim, S; Mcavey, K; Shepson, PB; Starn, T, im; Baumann, K; Edgerton, ES; Liu, J; Shilling, JE; Miller, DO; Brune, W; Schobesberger, S; D'Ambro, EL; Thornton, JA. (2016). Highly functionalized organic nitrates in the southeast United States: Contribution to secondary organic aerosol and reactive nitrogen budgets. Proc Natl Acad Sci USA 113: 1516-1521. http://dx.doi.org/10.1073/pnas.1508108113

Lehtipalo, K; Leppa, J; Kontkanen, J; Kangasluoma, J; Franchin, A; Wimmner, D; Schobesberger, S; Junninen, H; Petaja, T; Sipila, M; Mikkila, J; Vanhanen, J; Worsnop, DR; Kulmala, M. (2014). Methods for determining particle size distribution and growth rates between 1 and 3 nm using the Particle Size Magnifier. Boreal Environ Res 19: 215-236.

Leibensperger, EM; Mickley, LJ; Jacob, DJ; Barrett, SRH. (2011). Intercontinental influence of NO(x) and CO emissions on particulate matter air quality. Atmos Environ 45: 3318-3324. http://dx.doi.org/10.1016/j.atmosenv.2011.02.023

Lewandowski, M; Piletic, IR; Kleindienst, TE; Offenberg, JH; Beaver, MR; Jaoui, M; Docherty, KS; Edney, EO. (2013). Secondary organic aerosol characterisation at field sites across the United States during the spring-summer period. Int J Environ Anal Chem 93: 1084-1103. http://dx.doi.org/10.1080/03067319.2013.803545

Li, R; Wiedinmyer, C; Hannigan, MP. (2013). Contrast and correlations between coarse and fine particulate matter in the United States. Sci Total Environ 456-457: 346-358. http://dx.doi.org/10.1016/j.scitotenv.2013.03.041

ED_002220_00002287-00248

Liggio, J; Li, SM; Vlasenko, A; Stroud, C; Makar, P. (2011). Depression of ammonia uptake to sulfuric acid aerosols by competing uptake of ambient organic gases. Environ Sci Technol 45: 2790-2796. http://dx.doi.org/10.1021/es103801g

Lim, YB, in; Kim, H; Kim, J, inY; Turpin, BJ. (2016). Photochemical organonitrate formation in wet aerosols. Atmos Chem Phys 16: 12631-12647. http://dx.doi.org/10.5194/acp-16-12631-2016

Liu, BYH; Kim, CS. (1977). Counting efficiency of condensation nuclei counters. Atmos Environ 11: 1097-1100.

Liu, H, ui; Wang, Z, hi; Long, Y, an; Xiang, S; Wang, J; Fatouraie, M. (2015). Comparative study on alcohol-gasoline and gasoline-alcohol Dual-Fuel Spark Ignition (DFSI) combustion for engine particle number (PN) reduction. Fuel 159: 250-258. http://dx.doi.org/10.1016/j.fuel.2015.06.059

Liu, J; Horowitz, LW; Fan, S; Carlton, AG; Levy, H. (2012). Global in-cloud production of secondary organic aerosols: Implementation of a detailed chemical mechanism in the GFDL atmospheric model AM3. J Geophys Res 117: D15303. http://dx.doi.org/10.1029/2012JD017838

Liu, L; Breitner, S; Schneider, A; Cyrys, J; Brueske, I; Franck, U; Schlink, U, we; Leitte, AM; Herbarth, O, lf; Wiedensohler, A; Wehner, B; Pan, X; Wichmann, HE; Peters, A. (2013). Size-fractioned particulate air pollution and cardiovascular emergency room visits in Beijing, China. Environ Res 121: 52-63. http://dx.doi.org/10.1016/j.envres.2012.10.009

Liu, L; Urch, B; Szyszkowicz, M; Speck, M; Leingartner, K; Shutt, R; Pelletier, G; Gold, DR; Scott, JA; Brook, JR; Thorne, PS; Silverman, FS. (2017). Influence of exposure to coarse, fine and ultrafine urban particulate matter and their biological constituents on neural biomarkers in a randomized controlled crossover study. Environ Int 101: 89-95. http://dx.doi.org/10.1016/j.envint.2017.01.010

Lukacs, H; Gelencser, A; Hoffer, A; Kiss, G; Horvath, K; Hartyani, Z. (2009). Quantitative assessment of organosulfates in size-segregated rural fine aerosol. Atmos Chem Phys 9: 231-238.

Maciejczyk, P; Zhong, M; Li, Q; Xiong, J; Nadziejko, C; Chen, LC. (2005). Effects of subchronic exposures to concentrated ambient particles (CAPs) in mice: II The design of a CAPs exposure system for biometric telemetry monitoring. Inhal Toxicol 17: 189-197. http://dx.doi.org/10.1080/08958370590912743

Malm, WC; Schichtel, BA; Pitchford, ML. (2011). Uncertainties in PM2.5 gravimetric and speciation measurements and what we can learn from them. J Air Waste Manag Assoc 61: 1131-1149. http://dx.doi.org/10.1080/10473289.2011.603998

Mamakos, A; Dardiotis, C; Martini, G. (2012). Assessment of particle number limits for petrol vehicles. (Report EUR 25592 EN). Luxembourg, Luxembourg: European Commission, Publications Office of the European Union. http://dx.doi.org/10.2788/66109

Manninen, HE; Nieminen, T; Asmi, E; Gagne, S; Hakkinen, S; Lehtipalo, K; Aalto, P; Vana, M; Mirme, A; Mirme, S; Horrak, U; Plass-Duelmer, C; Stange, G; Kiss, G; Hoffer, A; Toeroe, N; Moerman, M; Henzing, B; de Leeuw, G; Brinkenberg, M; Kouvarakis, GN; Bougiatioti, A; Mihalopoulos, N; O'Dowd, C; Ceburnis, D; Arneth, A; Svenningsson, B; Swietlicki, E; Tarozzi, L; Decesari, S; Facchini, MC; Birmili, W; Sonntag, A; Wiedensohler, A; Boulon, J; Sellegri, K; Laj, P; Gysel, M; Bukowiecki, N; Weingartner, E; Wehrle, G; Laaksonen, A; Hamed, A; Joutsensaari, J; Petaja, T; Kerminen, VM; Kulmala, M. (2010). EUCAARI ion spectrometer measurements at 12 European sites - analysis of new particle formation events. Atmos Chem Phys 10: 7907-7927. http://dx.doi.org/10.5194/acp-10-7907-2010

Marais, EA; Jacob, DJ; Turner, JR; Mickley, LJ. (2017). Evidence of 1991-2013 decrease of biogenic secondary organic aerosol in response to SO2 emission controls. Environ Res Lett 12. http://dx.doi.org/10.1088/1748-9326/aa69c8

Marple, VA; Olson, BA. (2011). Sampling and measurement using inertial, gravitational, centrifugal, and thermal techniques. In P Kulkami; PA Baron; K Willeke (Eds.), Aerosol measurement: Principles, techniques, and applications (3rd ed., pp. 129-151). Hoboken, NJ: Wiley. http://dx.doi.org/10.1002/9781118001684.ch8

Martin, RV. (2008). Satellite remote sensing of surface air quality. Atmos Environ 42: 7823-7843. http://dx.doi.org/10.1016/j.atmosenv.2008.07.018

ED_002220_00002287-00249

Maruf Hossain, AM; Park, S; Kim, JS; Park, K. (2012). Volatility and mixing states of ultrafine particles from biomass burning. J Hazard Mater 205-206: 189-197. http://dx.doi.org/10.1016/j.jhazmat.2011.12.061

Matte, TD; Ross, Z; Kheirbek, I; Eisl, H; Johnson, S; Gorczynski, JE; Kass, D; Markowitz, S; Pezeshki, G; Clougherty, JE. (2013). Monitoring intraurban spatial patterns of multiple combustion air pollutants in New York City: Design and implementation. J Expo Sci Environ Epidemiol 23: 223-231. http://dx.doi.org/10.1038/jes.2012.126

Matthias-Maser, S; Bogs, B; Jaenicke, R. (2000). The size distribution of primary biological aerosol particles in cloud water on the mountain Kleiner Feldberg/Taunus (FRG). Atmos Res 54: 1-13.

Mauldin, RL, III; Berndt, T; Sipilä, M; Paasonen, P; Petäjä, T; Kim, S; Kurtén, T; Stratmann, F; Kerminen, VM; Kulmala, M. (2012). A new atmospherically relevant oxidant of sulphur dioxide. Nature 488: 193-196. http://dx.doi.org/10.1038/nature11278

Mckendry, IG; Strawbridge, KB; O'Neill, NT; MacDonald, AM; Liu, PSK; Leaitch, WR; Anlauf, KG; Jaegle, L; Fairlie, TD; Westphal, DL. (2007). Trans-Pacific transport of Saharan dust to western North America: A case study. J Geophys Res 112: D01103. http://dx.doi.org/10.1029/2006JD007129

McMurry, PH; Kuang, C; Smith, JN; Zhao, J.; Eisele, F. (2011). Atmospheric new particle formation: physical and chemical measurements. In P Kulkami; PA Baron; K Willeke (Eds.), Aerosol measurement: Principles, techniques, and applications (3rd ed., pp. 681-695). Hoboken, NJ: Wiley. http://dx.doi.org/10.1002/9781118001684.ch31

McNeill, VF. (2015). Aqueous organic chemistry in the atmosphere: sources and chemical processing of organic aerosols. Environ Sci Technol 49: 1237-1244. http://dx.doi.org/10.1021/es5043707

Meier, R; Cascio, WE; Ghio, AJ; Wild, P; Danuser, B; Riediker, M. (2014). Associations of short-term particle and noise exposures with markers of cardiovascular and respiratory health among highway maintenance workers. Environ Health Perspect 122: 726-732. http://dx.doi.org/10.1289/ehp.1307100

Misra, C; Kim, S; Shen, S; Sioutas, C. (2002). A high flow rate, very low pressure drop impactor for inertial separation of ultrafine from accumulation mode particles. J Aerosol Sci 33: 735-752. http://dx.doi.org/10.1016/S0021-8502(01)00210-5

Moldanova, J; Fridell, E; Winnes, H; Holmin-Fridell, S; Boman, J; Jedynska, A; Tishkova, V; Demirdjian, B; Joulie, S; Bladt, H; Ivleva, NP; Niessner, R. (2013). Physical and chemical characterisation of PM emissions from two ships operating in European Emission Control Areas. Atmos Meas Tech 6: 3577-3596. http://dx.doi.org/10.5194/amt-6-3577-2013

Moore, K; Krudysz, M; Pakbin, P; Hudda, N; Sioutas, C. (2009). Intra-community variability in total particle number concentrations in the San Pedro Harbor Area (Los Angeles, California). Aerosol Sci Technol 43: 587-603. http://dx.doi.org/10.1080/02786820902800900

Morawska, L; Ristovski, Z; Jayaratne, ER; Keogh, DU; Ling, X. (2008). Ambient nano and ultrafine particles from motor vehicle emissions: Characteristics, ambient processing and implications on human exposure. Atmos Environ 42: 8113-8138. http://dx.doi.org/10.1016/j.atmosenv.2008.07.050

Morgan, TE; Davis, DA; Iwata, N; Tanner, JA; Snyder, D; Ning, Z; Kam, W; Hsu, YT; Winkler, JW; Chen, JC; Petasis, NA; Baudry, M; Sioutas, C; Finch, CE. (2011). Glutamatergic neurons in rodent models respond to nanoscale particulate urban air pollutants in vivo and in vitro. Environ Health Perspect 119: 1003-1009. http://dx.doi.org/10.1289/ehp.1002973

Morris, RE; Koo, B; Guenther, A; Yarwood, G; McNally, D; Tesche, TW; Tonnesen, G; Boylan, J; Brewer, P. (2006). Model sensitivity evaluation for organic carbon using two multi-pollutant air quality models that simulate regional haze in the southeastern United States. Atmos Environ 40: 4960-4972. http://dx.doi.org/10.1016/j.atmonsenv.2005.09.088

Mueller, K; Spindler, G; van Pinxteren, D; Gnauk, T; Iinuma, Y; Brueggemann, E; Herrmann, H. (2012). Ultrafine and fine particles in the atmosphere - sampling, chemical characterization and sources. Chem Ing Tech 84: 1130-1136. http://dx.doi.org/10.1002/cite.201100208

ED_002220_00002287-00250

Mwaniki, GR; Rosenkrance, C; Wallace, HW; Jobson, B; Erickson, MH; Lamb, BK; Hardy, RJ; Zalakeviciute, R; Vanreken, TM. (2014). Factors contributing to elevated concentrations of PM2.5 during wintertime near Boise, Idaho. Atmos Pollut Res 5: 96-103. http://dx.doi.org/10.5094/APR.2014.012

Myung, C; Kim, J; Jang, W; Jin, D; Park, S; Lee, J. (2015). Nanoparticle filtration characteristics of advanced metal foam media for a spark ignition direct injection engine in steady engine operating conditions and vehicle test modes. Energies 8: 1865-1881. http://dx.doi.org/10.3390/en8031865

Myung, CL; Ko, A; Park, S. (2014). Review on characterization of nano-particle emissions and pm morphology from internal combustion engines: Part 1. Int J Automot Tech 15: 203-218. http://dx.doi.org/10.1007/s12239-014-0022-x

Na, K; Cocker, DR, III. (2009). Characterization and source identification of trace elements in PM2.5 from Mira Loma, Southern California. Atmos Res 93: 793-800. http://dx.doi.org/10.1016/j.atmosres.2009.03.012

Nguyen, TB; Laskin, J; Laskin, A; Nizkorodov, SA. (2011). Nitrogen-containing organic compounds and oligomers in secondary organic aerosol formed by photooxidation of isoprene. Environ Sci Technol 45: 6908-6918. http://dx.doi.org/10.1021/es201611n

Nie, W, ei; Wang, T, ao; Gao, X; Pathak, RK; Wang, X; Gao, R, ui; Zhang, Q; Yang, L; Wang, W. (2010). Comparison among filter-based, impactor-based and continuous techniques for measuring atmospheric fine sulfate and nitrate. Atmos Environ 44: 4396-4403. http://dx.doi.org/10.1016/j.atmosenv.2010.07.047

Nolte, CG; Appel, KW; Kelly, JT; Bhave, PV; Fahey, KM; Collett, JL, Jr; Zhang, L; Young, JO. (2015). Evaluation of the Community Multiscale Air Quality (CMAQ) model v5.0 against size-resolved measurements of inorganic particle composition across sites in North America. GMD 8: 2877-2892. http://dx.doi.org/10.5194/gmd-8-2877-2015

NYDEC (New York Department of Environmental Conservation). (2016). Peace Bridge Study: Phase 2 final report September 2016. Albany, NY: New York Department of Environmental Conservation: Division of Air Resources.

O'Brien, RE; Laskin, A; Laskin, J; Liu, S; Weber, R; Russell, LM; Goldstein, AH. (2013). Molecular characterization of organic aerosol using nanospray desorption/electrospray ionization mass spectrometry: CalNex 2010 field study. Atmos Environ 68: 265-272. http://dx.doi.org/10.1016/j.atmosenv.2012.11.056

Oakes, M; Ingall, ED; Lai, B; Shafer, MM; Hays, MD; Liu, ZG; Russell, AG; Weber, RJ. (2012a). Iron solubility related to particle sulfur content in source emission and ambient fine particles. Environ Sci Technol 46: 6637-6644. http://dx.doi.org/10.1021/es300701c

Oakes, M; Weber, RJ; Lai, B; Russell, A; Ingall, ED. (2012b). Characterization of iron speciation in urban and rural single particles using XANES spectroscopy and micro X-ray fluorescence measurements: investigating the relationship between speciation and fractional iron solubility. Atmos Chem Phys 12: 745-756. http://dx.doi.org/10.5194/acp-12-745-2012

Olsen, Y; Karottki, DG; Jensen, DM; Bekö, G; Kjeldsen, BU; Clausen, G; Hersoug, LG; Holst, GJ; Wierzbicka, A; Sigsgaard, T; Linneberg, A; Møller, P; Loft, S. (2014). Vascular and lung function related to ultrafine and fine particles exposure assessed by personal and indoor monitoring: a cross-sectional study. Environ Health 13: 112. http://dx.doi.org/10.1186/1476-069X-13-112

Osan, J; Meirer, F; Groma, V; Torok, S; Ingerle, D; Streli, C; Pepponi, G. (2010). Speciation of copper and zinc in size-fractionated atmospheric particulate matter using total reflection mode X-ray absorption near-edge structure spectrometry. Spectrochim Acta Part B At Spectrosc 65: 1008-1013. http://dx.doi.org/10.1016/j.sab.2010.11.002

Paciorek, CJ; Liu, Y. (2009). Limitations of remotely-sensed aerosol as a spatial proxy for fine particulate matter. Environ Health Perspect unknown: unknown. http://dx.doi.org/10.1289/ehp.0800360

Paciorek, CJ; Yanosky, JD; Puett, RC; Laden, F; Suh, HH. (2009). Practical large-scale spatio-temporal modeling of particulate matter concentrations. Ann Appl Stat 3: 370-397. http://dx.doi.org/10.1214/08-AOAS204

ED_002220_00002287-00251

Pakbin, P; Hudda, N; Cheung, KL; Moore, KF; Sioutas, C. (2010). Spatial and temporal variability of coarse (PM10-2.5) particulate matter concentrations in the Los Angeles area. Aerosol Sci Technol 44: 514-525. http://dx.doi.org/10.1080/02786821003749509

Pang, W; Christakos, G; Wang, JF. (2010). Comparative spatiotemporal analysis of fine particulate matter pollution. Environmetrics 21: 305-317. http://dx.doi.org/10.1002/env.1007

Patel, MM; Chillrud, SN; Correa, JC; Feinberg, M; Hazi, Y; Kc, D; Prakash, S; Ross, JM; Levy, D; Kinney, PL. (2009). Spatial and temporal variations in traffic-related particulate matter at New York City high schools. Atmos Environ 43: 4975-4981 PMC - PMC2791330. http://dx.doi.org/10.1016/j.atmosenv.2009.07.004

Patton, AP; Perkins, J; Zamore, W; Levy, JI; Brugge, D; Durant, JL. (2014). Spatial and temporal differences in traffic-related air pollution in three urban neighborhoods near an interstate highway. Atmos Environ 99: 309-321. http://dx.doi.org/10.1016/j.atmosenv.2014.09.072

Pennington, MR; Bzdek, BR; Depalma, JW; Smith, JN; Kortelainen, AM; Ruiz, LH; Petaja, T; Kulmala, M; Worsnop, DR; Johnston, MV. (2013). Identification and quantification of particle growth channels during new particle formation. Atmos Chem Phys 13: 10215-10225. http://dx.doi.org/10.5194/acp-13-10215-2013

Petzold, A; Weingartner, E; Hasselbach, J; Lauer, P; Kurok, C; Fleischer, F. (2010). Physical properties, chemical composition, and cloud forming potential of particulate emissions from a marine diesel engine at various load conditions. Environ Sci Technol 44: 3800-3805. http://dx.doi.org/10.1021/es903681z

Pierce, J. R.; Leaitch, WR; Liggio, J; Westervelt, DM; Wainwright, CD; Abbatt, JPD; Ahlm, L; Al-Basheer, W; Cziczo, DJ; Hayden, KL; Lee, AKY; Li, SM; Russell, LM; Sjostedt, SJ; Strawbridge, KB; Travis, M; Vlasenko, A; Wentzell, JJB; Wiebe, HA; Wong, JPS; MacDonald, AM. (2012). Nucleation and condensational growth to CCN sizes during a sustained pristine biogenic SOA event in a forested mountain valley. Atmos Chem Phys 12: 3147-3163. http://dx.doi.org/10.5194/acp-12-3147-2012

Pierce, JR, JR; Riipinen, I; Kulmala, M; Ehn, M; Petaja, T; Junninen, H; Worsnop, DR; Donahue, NM. (2011). Quantification of the volatility of secondary organic compounds in ultrafine particles during nucleation events. Atmos Chem Phys 11: 9019-9036. http://dx.doi.org/10.5194/acp-11-9019-2011

Pirjola, L; Pajunoja, A; Walden, J; Jalkanen, JP; Ronkko, T; Kousa, A; Koskentalo, T. (2014). Mobile measurements of ship emissions in two harbour areas in Finland. Atmos Meas Tech 7: 149-161. http://dx.doi.org/10.5194/amt-7-149-2014

Pitchford, ML; Poirot, RL; Schichtel, BA; Maim, WC. (2009). Characterization of the winter midwestern particulate nitrate bulge. J Air Waste Manag Assoc 59: 1061-1069.

Pleim, JE; Bash, JO; Walker, JT; Cooter, EJ. (2013). Development and evaluation of an ammonia bidirectional flux parameterization for air quality models. J Geophys Res Atmos 118: 3794-3806. http://dx.doi.org/10.1002/jgrd.50262

Prospero, JM. (1999a). Long-range transport of mineral dust in the global atmosphere: Impact of African dust on the environment of the southeastern United States. Proc Natl Acad Sci USA 96: 3396-3403. http://dx.doi.org/10.1073/pnas.96.7.3396

Prospero, JM. (1999b). Long-term measurements of the transport of African mineral dust to the southeastern United States: implications for regional air quality. J Geophys Res 104: 15917-15927. http://dx.doi.org/10.1029/1999JD900072

Putaud, JP; Van Dingenen, R; Alastuey, A; Bauer, H; Birmili, W; Cyrys, J; Flentje, H; Fuzzi, S; Gehrig, R; Hansson, HC; Harrison, RM; Herrmann, H; Hitzenberger, R; Hüglin, C; Jones, AM; Kasper-Giebl, A; Kiss, G; Kousa, A; Kuhlbusch, TAJ; Löschau, G; Maenhaut, W; Molnar, A; Moreno, T; Pekkanen, J; Perrino, C; Pitz, M; Puxbaum, H; Querol, X; Rodriguez, S; Salma, I; Schwarz, J; Smolik, J; Schneider, J; Spindler, G; Ten Brink, H; Tursic, J; Viana, M; Wiedensohler, A; Raes, F. (2010). A European aerosol phenomenology 3: Physical and chemical characteristics of particulate matter from 60 rural, urban, and kerbside sites across Europe. Atmos Environ 44: 1308-1320. http://dx.doi.org/10.1016/j.atmosenv.2009.12.011

ED_002220_00002287-00252

Pye, HOT; Murphy, BN; Xu, L, u; Ng, N, gaL; Carlton, AG; Guo, H; Weber, R; Vasilakos, P; Appel, KW; Budisulistiorini, S, riH; Surratt, JD; Nenes, A; Hu, W; Jimenez, JL; Isaacman-Vanwertz, G; Misztal, PK; Goldstein, AH. (2017). On the implications of aerosol liquid water and phase separation for organic aerosol mass. Atmos Chem Phys 17: 343-369. http://dx.doi.org/10.5194/acp-17-343-2017

Pye, HOT; Zuend, A; Fry, JL; Isaacman-Vanwertz, G; Capps, SL; Appel, KW; Foroutan, H; Xu, L, u; Ng, N, gaL; Goldstein, AH. (2018). Coupling of organic and inorganic aerosol systems and the effect on gas-particle partitioning in the southeastern US. Atmos Chem Phys 18: 357-370. http://dx.doi.org/10.5194/acp-18-357-2018

Rattanavaraha, W; Chu, K; Budisulistiorini, H; Riva, M; Lin, YH; Edgerton, ES; Baumann, K; Shaw, SL; Guo, H; King, L; Weber, RJ; Neff, ME; Stone, EA; Offenberg, JH; Zhang, Z; Gold, A; Surratt, JD. (2016). Assessing the impact of anthropogenic pollution on isoprene-derived secondary organic aerosol formation in PM2.5 collected from the Birmingham, Alabama, ground site during the 2013 Southern Oxidant and Aerosol Study. Atmos Chem Phys 16: 4897-4914. http://dx.doi.org/10.5194/acp-16-4897-2016

Reid, CE; Jerrett, M; Petersen, ML; Pfister, GG; Morefield, PE; Tager, IB; Raffuse, SM; Balmes, JR. (2015). Spatiotemporal prediction of fine particulate matter during the 2008 northern California wildfires using machine learning. Environ Sci Technol 49: 3887-3896. http://dx.doi.org/10.1021/es505846r

Riccobono, F; Schobesberger, S; Scott, CE; Dommen, J; Ortega, IK; Rondo, L; Almeida, J; Amorim, A; Bianchi, F; Breitenlechner, M; David, A; Downard, A; Dunne, EM; Duplissy, J; Ehrhart, S; Flagan, RC; Franchin, A; Hansel, A; Junninen, H; Kajos, M; Keskinen, H; Kupc, A; Kürten, A; Kvashin, AN; Laaksonen, A; Lehtipalo, K; Makhmutov, V; Mathot, S; Nieminen, T; Onnela, A; Petäjä, T; Praplan, AP; Santos, FD; Schallhart, S; Seinfeld, JH; Sipilä, M; Spracklen, DV; Stozhkov, Y; Stratmann, F; Tomé, A; Tsagkogeorgas, G; Vaattovaara, P; Viisanen, Y; Vrtala, A; Wagner, PE; Weingartner, E; Wex, H; Wimmer, D; Carslaw, KS; Curtius, J; Donahue, NM; Kirkby, J; Kulmala, M; Worsnop, DR; Baltensperger, U. (2014). Oxidation products of biogenic emissions contribute to nucleation of atmospheric particles. Science 344: 717-721. http://dx.doi.org/10.1126/science.1243527

Ridley, DA; Heald, CL; Prospero, JM. (2014). What controls the recent changes in African mineral dust aerosol across the Atlantic? Atmos Chem Phys 14: 5735-5747. http://dx.doi.org/10.5194/acp-14-5735-2014

Rönkkö, T; Pirjola, L; Ntziachristos, L; Heikkilä, J; Karjalainen, P; Hillamo, R; Keskinen, J. (2014). Vehicle engines produce exhaust nanoparticles even when not fueled. Environ Sci Technol 48: 2043-2050. http://dx.doi.org/10.1021/es405687m

Rosenthal, FS; Kuisma, M; Lanki, T; Hussein, T; Boyd, J; Halonen, JI; Pekkanen, J. (2013). Association of ozone and particulate air pollution with out-of-hospital cardiac arrest in Helsinki, Finland: evidence for two different etiologies. J Expo Sci Environ Epidemiol 23: 281-288. http://dx.doi.org/10.1038/jes.2012.121

Ruehl, C; Herner, JD; Yoon, S; Collins, JF; Misra, C; Na, K; Robertson, WH; Biswas, S; Chang, MCO; Ayala, A. (2015). Similarities and differences between traditional and clean diesel PM. ECST 1: 17-23. http://dx.doi.org/10.1007/s40825-014-0002-7

Russell, A; Dennis, R. (2000). NARSTO critical review of photochemical models and modeling [Review]. Atmos Environ 34: 2283-2324. http://dx.doi.org/10.1016/S1352-2310(99)00468-9

Saffari, A; Hasheminassab, S; Shafer, MM; Schauer, JJ; Chatila, TA; Sioutas, C. (2016). Nighttime aqueous-phase secondary organic aerosols in Los Angeles and its implication for fine particulate matter composition and oxidative potential. Atmos Environ 133: 112-122. http://dx.doi.org/10.1016/j.atmosenv.2016.03.022

Saffari, A; Hasheminassab, S; Wang, D; Shafer, MM; Schauer, JJ; Sioutas, C. (2015). Impact of primary and secondary organic sources on the oxidative potential of quasi-ultrafine particles (PM0.25) at three contrasting locations in the Los Angeles Basin. Atmos Environ 120: 286-296. http://dx.doi.org/10.1016/j.atmosenv.2015.09.022

Saffaripour, M; Chan, TW; Liu, F; Thomson, KA; Smallwood, GJ; Kubsh, J; Brezny, R. (2015). Effect of drive cycle and gasoline particulate filter on the size and morphology of soot particles emitted from a gasoline-direct-injection vehicle. Environ Sci Technol 49: 11950-11958. http://dx.doi.org/10.1021/acs.est.5b02185

ED_002220_00002287-00253

Salma, I; Borsos, T; Weidinger, T; Aalto, P; Hussein, T; Dal Maso, M; Kulmala, M. (2011). Production, growth and properties of ultrafine atmospheric aerosol particles in an urban environment. Atmos Chem Phys 11: 1339-1353. http://dx.doi.org/10.5194/acp-11-1339-2011

Sander, SP; Abbatt, JPD; Barker, JR; Burkholder, JB; Friedl, RR; Golden, DM; Huie, RE; Kolb, CE; Kurylo, MJ; Moortgat, GK; Orkin, VL; Wine, PH. (2011). Chemical kinetics and photochemical data for use in atmospheric studies: Evaluation number 17. (JPL Publication 10-6). Pasadena, CA: Jet Propulsion Laboratory. http://jpldataeval.jpl.nasa.gov/pdf/JPL%2010-6%20Final%2015June2011.pdf

Satsangi, PG; Yadav, S. (2014). Characterization of PM2.5 by X-ray diffraction and scanning electron microscopy-energy dispersive spectrometer: its relation with different pollution sources. Int J Environ Sci Tech 11: 217-232. http://dx.doi.org/10.1007/s13762-012-0173-0

Sawvel, EJ; Willis, R; West, RR; Casuccio, GS; Norris, G; Kumar, N; Hammond, D; Peters, TM. (2015). Passive sampling to capture the spatial variability of coarse particles by composition in Cleveland, OH. Atmos Environ 105: 61-69. http://dx.doi.org/10.1016/j.atmosenv.2015.01.030

Schaumann, F; Frömke, C; Dijkstra, D; Alessandrini, F; Windt, H; Karg, E; Müller, M; Winkler, C; Braun, A; Koch, A; Hohlfeld, J; Behrendt, H; Schmid, O; Koch, W; Schulz, H; Krug, N. (2014). Effects of ultrafine particles on the allergic inflammation in the lung of asthmatics: results of a double-blinded randomized cross-over clinical pilot study. Part Fibre Toxicol 11: 39. http://dx.doi.org/10.1186/s12989-014-0039-3

Schiferl, LD; Heald, CL; Nowak, JB; Holloway, JS; Neuman, JA; Bahreini, R; Pollack, IB; Ryerson, TB; Wiedinmyer, C; Murphy, JG. (2014). An investigation of ammonia and inorganic particulate matter in California during the CalNex campaign. J Geophys Res Atmos 119: 1883-1902. http://dx.doi.org/10.1002/2013JD020765

Setyan, A; Song, C; Merkel, M; Knighton, WB; Onasch, TB; Canagaratna, MR; Worsnop, DR; Wiedensohler, A; Shilling, JE; Zhang, Q. (2014). Chemistry of new particle growth in mixed urban and biogenic emissions - insights from CARES. Atmos Chem Phys 14: 6477-6494. http://dx.doi.org/10.5194/acp-14-6477-2014

Shen, XJ; Sun, JY; Zhang, YM; Wehner, B; Nowak, A; Tuch, T; Zhang, XC; Wang, TT; Zhou, HG; Zhang, XL; Dong, F; Birmili, W; Wiedensohler, A. (2011). First long-term study of particle number size distributions and new particle formation events of regional aerosol in the North China Plain. Atmos Chem Phys 11: 1565-1580. http://dx.doi.org/10.5194/acp-11-1565-2011

Shilling, JE; Zaveri, RA; Fast, JD; Kleinman, L; Alexander, ML; Canagaratna, MR; Fortner, E; Hubbe, JM; Jayne, JT; Sedlacek, A; Setyan, A; Springston, S; Worsnop, DR; Zhang, Q. (2013). Enhanced SOA formation from mixed anthropogenic and biogenic emissions during the CARES campaign. Atmos Chem Phys 13: 2091-2113. http://dx.doi.org/10.5194/acp-13-2091-2013

Shirai, T; Yasueda, H; Saito, A; Taniguchi, M; Akiyama, K; Tsuchiya, T; Suda, T; Chida, K. (2012). Effect of exposure and sensitization to indoor allergens on asthma control level. Allergol Int 61: 51-56. http://dx.doi.org/10.2332/allergolint.11-OA-0313

Silcox, GD; Kelly, KE; Crosman, ET; Whiteman, CD; Allen, BL. (2011). Wintertime PM2.5 concentrations during persistent, multi-day cold-air pools in a mountain valley. Atmos Environ 46: 17-24. http://dx.doi.org/10.1016/j.atmosenv.2011.10.041

Singh, M; Misra, C; Sioutas, C. (2003). Field evaluation of a personal cascade impactor sampler (PCIS). Atmos Environ 37: 4781-4793. http://dx.doi.org/10.1016/j.atmosenv.2003.08.013

Singh, M; Phuleria, HC; Bowers, K; Sioutas, C. (2006). Seasonal and spatial trends in particle number concentrations and size distributions at the children's health study sites in Southern California. J Expo Sci Environ Epidemiol 16: 3-18. http://dx.doi.org/10.1038/sj.jea.7500432

Sioutas, C; Kim, S; Chang, M. (1999). Development and evaluation of a prototype ultrafine particle concentrator. J Aerosol Sci 30: 1001-1017. http://dx.doi.org/10.1016/S0021-8502(98)00769-1

Sioutas, C; Koutrakis, P; Burton, RM. (1994a). Development of a low cutpoint slit virtual impactor for sampling ambient fine particles. J Aerosol Sci 25: 1321-1330.

ED_002220_00002287-00254

Sioutas, C; Koutrakis, P; Burton, RM. (1994b). A high-volume small cutpoint virtual impactor for separation of atmospheric particulate from gaseous pollutants. Part Sci Technol 12: 207-221.

Sioutas, C; Koutrakis, P; Burton, RM. (1995a). A technique to expose animals to concentrated fine ambient aerosols. Environ Health Perspect 103: 172-177. http://dx.doi.org/10.2307/3432274

Sioutas, C; Koutrakis, P; Olson, BA. (1994c). Development and evaluation of a low cutpoint virtual impactor. Aerosol Sci Technol 21: 223-235. http://dx.doi.org/10.1080/02786829408959711

Sioutas, D; Koutrakis, P; Ferguson, ST; Burton, RM. (1995b). Development and evaluation of a prototype ambient particle concentrator for inhalation exposure studies. Inhal Toxicol 7: 633-644. http://dx.doi.org/10.3109/08958379509014470

Sipila, M; Berndt, T; Petaja, T; Brus, D; Vanhanen, J; Stratmann, F; Patokoski, J; Mauldin, R, III; Hyvarinen, AP; Lihavainen, H; Kulmala, M. (2010). The role of sulfuric acid in atmospheric nucleation. Science 327: 1243-1246. http://dx.doi.org/10.1126/science.1180315

Smith, JN; Dunn, MJ; Vanreken, TM; Iida, K; Stolzenburg, MR; McMurry, PH; Huey, LG. (2008). Chemical composition of atmospheric nanoparticles formed from nucleation in Tecamac, Mexico: evidence for an important role for organic species in nanoparticle growth. Geophys Res Lett 35: L04808. http://dx.doi.org/10.1029/2007GL032523

Snyder, DC; Rutter, AP; Worley, C; Olson, M; Plourde, A; Bader, RC; Dallmann, T; Schauer, JJ. (2010). Spatial variability of carbonaceous aerosols and associated source tracers in two cites in the Midwestern United States. Atmos Environ 44: 1597-1608. http://dx.doi.org/10.1016/j.atmosenv.2010.02.004

Solomon, PA. (2012). An overview of ultrafine particles in ambient air [Magazine]. EM Magazine, 5, 18-27.

Solomon, PA; Crumpler, D; Flanagan, JB; Jayanty, RK; Rickman, EE; McDade, CE. (2014). U.S. national PM2.5 Chemical Speciation Monitoring Networks-CSN and IMPROVE: Description of networks. J Air Waste Manag Assoc 64: 1410-1438. http://dx.doi.org/10.1080/10962247.2014.956904

Sorek-Hamer, M; Kloog, I; Koutrakis, P; Strawa, AW; Chatfield, R; Cohen, A; Ridgway, WL; Broday, DM. (2015). Assessment of PM2.5 concentrations over bright surfaces using MODIS satellite observations. Rem Sens Environ 163: 180-185. http://dx.doi.org/10.1016/j.rse.2015.03.014

Stanier, CO; Khlystov, AY; Pandis, SN. (2004). Ambient aerosol size distributions and number concentrations measured during the Pittsburgh Air Quality Study (PAQS). Atmos Environ 38: 3275-3284. http://dx.doi.org/10.1016/j.atmosenv.2004.03.020

Strand, TM; Larkin, N; Craig, KJ; Raffuse, S; Sullivan, D; Solomon, R; Rorig, M; Wheeler, N; Pryden, D. (2012). Analyses of BlueSky Gateway PM2.5 predictions during the 2007 southern and 2008 northern California fires. J Geophys Res Atmos 117. http://dx.doi.org/10.1029/2012JD017627

Sturtz, TM; Schichtel, BA; Larson, TV. (2014). Coupling Chemical Transport Model Source Attributions with Positive Matrix Factorization: Application to Two IMPROVE Sites Impacted by Wildfires. Environ Sci Technol 48: 11389-11396. http://dx.doi.org/10.1021/es502749r

Sullivan, RC; Pryor, SC. (2014). Quantifying spatiotemporal variability of fine particles in an urban environment using combined fixed and mobile measurements. Atmos Environ 89: 664-671. http://dx.doi.org/10.1016/j.atmosenv.2014.03.007

Surratt, JD; Gómez-González, Y; Chan, AW; Vermeylen, R; Shahgholi, M; Kleindienst, TE; Edney, EO; Offenberg, JH; Lewandowski, M; Jaoui, M; Maenhaut, W; Claeys, M; Flagan, RC; Seinfeld, JH. (2008). Organosulfate formation in biogenic secondary organic aerosol. J Phys Chem A 112: 8345-8378. http://dx.doi.org/10.1021/jp802310p

Surratt, JD; Kroll, JH; Kleindienst, TE; Edney, EO; Claeys, M; Sorooshian, A; Ng, NL; Offenberg, JH; Lewandowski, M; Jaoui, M; Flagan, RC; Seinfeld, JH. (2007). Evidence for organosulfates in secondary organic aerosol. Environ Sci Technol 41: 517-527. http://dx.doi.org/10.1021/es062081q

Tai, APK; Mickley, LJ; Jacob, DJ. (2010). Correlations between fine particulate matter (PM2.5) and meteorological variables in the United States: Implications for the sensitivity of PM2.5 to climate change. Atmos Environ 44: 3976-3984. http://dx.doi.org/10.1016/j.atmosenv.2010.06.060

ED_002220_00002287-00255

Tai, APK; Mickley, LJ; Jacob, DJ. (2012a). Impact of 2000-2050 climate change on fine particulate matter (PM2.5) air quality inferred from a multi-model analysis of meteorological modes. Atmos Chem Phys 12: 11329-11337. http://dx.doi.org/10.5194/acp-12-11329-2012

Tai, APK; Mickley, LJ; Jacob, DJ; Leibensperger, EM; Zhang, L; Fisher, JA; Pye, HOT. (2012b). Meteorological modes of variability for fine particulate matter (PM2.5) air quality in the United States: implications for PM2.5 sensitivity to climate change. Atmos Chem Phys 12: 3131-3145. http://dx.doi.org/10.5194/acp-12-3131-2012

TFHTAP (Task Force on Hemispheric Transport of Air Pollution). (2006). Hemispheric transport of air pollution 2010. Part A: Ozone and particulate matter. (Air Pollution Studies No. 17). Geneva, Switzerland: United Nations Publications.

TFHTAP (Task Force on Hemispheric Transport of Air Pollution). (2007). Hemispheric transport of air pollution 2007. Convention on Long-range Transboundary Air Pollution, 17-19 October 2007, Juelich, Germany.

Thornburg, J; Rodes, CE; Lawless, PA; Williams, R. (2009). Spatial and temporal variability of outdoor coarse particulate matter mass concentrations measured with a new coarse particle sampler during the detroit exposure and aerosol research study. Atmos Environ 43: 4251-4258. http://dx.doi.org/10.1016/j.atmosenv.2009.06.026

Tolocka, MP; Turpin, B. (2012). Contribution of organosulfur compounds to organic aerosol mass. Environ Sci Technol 46: 7978-7983. http://dx.doi.org/10.1021/es300651v

Tuccella, P; Curci, G; Grell, GA; Visconti, G; Crumeyrolle, S; Schwarzenboeck, A; Mensah, AA. (2015). A new chemistry option in WRF-Chem v. 3.4 for the simulation of direct and indirect aerosol effects using VBS: evaluation against IMPACT-EUCAARI data. GMD 8: 2749-2776. http://dx.doi.org/10.5194/gmd-8-2749-2015

Tuet, WY; Chen, Y; Xu, L, u; Fok, S; Gao, D; Weber, RJ; Ng, N, gaL. (2017). Chemical oxidative potential of secondary organic aerosol (SOA) generated from the photooxidation of biogenic and anthropogenic volatile organic compounds. Atmos Chem Phys 17: 839-853. http://dx.doi.org/10.5194/acp-17-839-2017

Tyler, CR; Zychowski, KE; Sanchez, BN; Rivero, V; Lucas, S; Herbert, G; Liu, J; Irshad, H; Mcdonald, JD; Bleske, BE; Campen, MJ. (2016). Surface area-dependence of gas-particle interactions influences pulmonary and neuroinflammatory outcomes. Part Fibre Toxicol 13: 64. http://dx.doi.org/10.1186/s12989-016-0177-x

U.S. EPA (U.S. Environmental Protection Agency). (1996). Air quality criteria for particulate matter [EPA Report]. (EPA/600/P-95/001aF-cF. 3v). Research Triangle Park, National Center for Environmental Assessment-RTP Office NC.

U.S. EPA (U.S. Environmental Protection Agency). (1998). SLAMS/NAMS/PAMS network review guidance [EPA Report]. (EPA/454/R-98/003). Research Triangle Park, NC.

U.S. EPA (U.S. Environmental Protection Agency). (2004). Air quality criteria for particulate matter [EPA Report]. (EPA/600/P-99/002aF-bF). Research Triangle Park, NC: U.S. Environmental Protection Agency, Office of Research and Development, National Center for Environemntal Assessment- RTP Office. http://cfpub.epa.gov/ncea/cfm/recordisplay.cfm?deid=87903

U.S. EPA (U.S. Environmental Protection Agency). (2008a). Integrated science assessment for oxides of nitrogen and sulfur: Ecological criteria [EPA Report]. (EPA/600/R-08/082F). Research Triangle Park, NC: U.S. Environmental Protection Agency, Office of Research and Development, National Center for Environmental Assessment- RTP Division. http://cfpub.epa.gov/ncea/cfm/recordisplay.cfm?deid=201485

U.S. EPA (U.S. Environmental Protection Agency). (2008b). Integrated science assessment for sulfur oxides: Health criteria [EPA Report]. (EPA/600/R-08/047F). Research Triangle Park, NC: U.S. Environmental Protection Agency, Office of Research and Development, National Center for Environmental Assessment- RTP. http://cfpub.epa.gov/ncea/cfm/recordisplay.cfm?deid=198843

U.S. EPA (U.S. Environmental Protection Agency). (2009). Integrated science assessment for particulate matter [EPA Report]. (EPA/600/R-08/139F). Research Triangle Park, NC: U.S. Environmental Protection Agency, Office of Research and Development, National Center for Environmental Assessment- RTP Division. http://cfpub.epa.gov/ncea/cfm/recordisplay.cfm?deid=216546

ED_002220_00002287-00256

U.S. EPA (U.S. Environmental Protection Agency). (2014). Policy assessment for the review of the ozone national ambient air quality standards. (NTIS/13360097). U.S. Environmental Protection Agency, Office of Air Quality Planning and Standards.

U.S. EPA (U.S. Environmental Protection Agency). (2015). Pilot study on coarse PM monitoring [EPA Report]. (EPA-454/R-15-001). Research Triangle Park, NC: U.S. EPA Office of Air Quality Planning and Standards.

U.S. EPA (U.S. Environmental Protection Agency). (2016a). 2014 National Emissions Inventory (NEI) data. Washington, DC. Retrieved from https://www.epa.gov/air-emissions-inventories/2014-national-emissions-inventory-nei-data

U.S. EPA (U.S. Environmental Protection Agency). (2016b). Integrated review plan for the national ambient air quality standards for particulate matter [EPA Report]. (EPA-452/R-16-005). Research Triangle Park, NC. https://yosemite.epa.gov/sab/sabproduct.nsf/0/eb862b233fbd0cde85257dda004fcb8c!OpenDocument&TableRow=2.0

U.S. EPA (U.S. Environmental Protection Agency). (2017). Integrated science assessment for sulfur oxides: Health criteria [EPA Report]. (EPA/600/R-17/451). Research Triangle Park, NC: U.S. Environmental Protection Agency, Office of Research and Development, National Center for Environmental Assessment- RTP. https://www.epa.gov/isa/integrated-science-assessment-isa-sulfur-oxides-health-criteria

U.S. EPA (U.S. Environmental Protection Agency). (2018). 2014 National Emissions Inventory (NEI) data (Version 2). Washington, DC. Retrieved from https://www.epa.gov/air-emissions-inventories/2014-national-emissions-inventory-nei-data

Uno, I; Eguchi, K; Yumimoto, K; Liu, Z; Hara, Y; Sugimoto, N; Shimizu, A; Takemura, T. (2011). Large Asian dust layers continuously reached North America in April 2010. Atmos Chem Phys 11: 7333-7341. http://dx.doi.org/10.5194/acp-11-7333-2011

Vakkari, V; Tiitta, P; Jaars, K; Croteau, P; Beukes, JP; Josipovic, M; Kerminen, VM; Kulmala, M; Venter, AD; van Zyl, PG; Worsnop, DR; Laakso, L. (2015). Reevaluating the contribution of sulfuric acid and the origin of organic compounds in atmospheric nanoparticle growth. Geophys Res Lett 42. http://dx.doi.org/10.1002/2015GL066459

van Donkelaar, A; Martin, RV; Levy, RC; da Silva, AM; Krzyzanowski, M; Chubarova, NE; Semutnikova, E; Cohen, AJ. (2011). Satellite-based estimates of ground-level fine particulate matter during extreme events: A case study of the Moscow fires in 2010. Atmos Environ 45: 6225-6232. http://dx.doi.org/10.1016/j.atmosenv.2011.07.068

Vancuren, RA; Cahill, TA. (2002). Asian aerosols in North America: Frequency and concentration of fine dust. J Geophys Res 107: 4804. http://dx.doi.org/10.1029/2002JD002204

Vanderpool, RW; Ellestad, TG; Harmon, MK; Hanley, TD; Scheffe, RD; Hunike, ET; Solomon, PA; Murdoch, RW; Natarajan, S; Noble, CA; Ambs, JL; Sem, GJ; Tisch, J. (2004). Multi-site evaluations of candidate methodologies for determining coarse particulate matter (PMc) concentrations [First draft] [EPA Report]. (EPA/600/A-04/059). Research Triangle Park, NC: U.S. Environmental Protection Agency.

Vanhanen, J; Mikkila, J; Lehtipalo, K; Sipila, M; Manninen, HE; Siivola, E; Petaja, T; Kulmala, M. (2011). Particle size magnifier for nano-CN detection. Aerosol Sci Technol 45: 533-542. http://dx.doi.org/10.1080/02786826.2010.547889

Vecchi, R; Valli, G; Fermo, P; D'Alessandro, A; Piazzalunga, A; Bernardoni, V. (2009). Organic and inorganic sampling artefacts assessment. Atmos Environ 43: 1713-1720. http://dx.doi.org/10.1016/j.atmosenv.2008.12.016

Vedantham, R, am; Hagler, GSW; Holm, K; Kimbrough, S, ue; Snow, R. (2015). Adaptive Decomposition of Highly Resolved Time Series into Local and Non-Local Components. Aerosol Air Qual Res 15: 1270-+. http://dx.doi.org/10.4209/aaqr.2015.02.0103

Vehkamaki, H; Riipinen, I. (2012). Thermodynamics and kinetics of atmospheric aerosol particle formation and growth. Chem Soc Rev 41: 5160-5173. http://dx.doi.org/10.1039/c2cs00002d

ED_002220_00002287-00257

Verma, V; Ning, Z, hi; Cho, AK; Schauer, JJ; Shafer, MM; Sioutas, C. (2009). Redox activity of urban quasi-ultrafine particles from primary and secondary sources. Atmos Environ 43: 6360-6368. http://dx.doi.org/10.1016/j.atmosenv.2009.09.019

Verma, V; Wang, Y; El-Afifi, R; Fang, T; Rowland, J; Russell, AG; Weber, RJ. (2015). Fractionating ambient humic-like substances (HULIS) for their reactive oxygen species activity - Assessing the importance of quinones and atmospheric aging. Atmos Environ 120: 351-359. http://dx.doi.org/10.1016/j.atmosenv.2015.09.010

Viana, M; Rivas, I; Querol, X; Alastuey, A; Alvarez-Pedrerol, M; Bouso, L; Sioutas, C; Sunyer, J. (2015). Partitioning of trace elements and metals between quasi-ultrafine, accumulation and coarse aerosols in indoor and outdoor air in schools. Atmos Environ 106: 392-401. http://dx.doi.org/10.1016/j.atmosenv.2014.07.027

Vogel, AL; Schneider, J; Müller-Tautges, C; Phillips, GJ; Pöhlker, ML; Rose, D; Zuth, C; Makkonen, U; Hakola, H; Crowley, JN; Andreae, MO; Pöschl, U; Hoffmann, T. (2016). Aerosol chemistry resolved by mass spectrometry: Linking field measurements of cloud condensation nuclei activity to organic aerosol composition. Environ Sci Technol. http://dx.doi.org/10.1021/acs.est.6b01675

Vu, TV; Delgado-Saborit, JM; Harrison, R, oyM. (2015). Review: Particle number size distributions from seven major sources and implications for source apportionment studies. Atmos Environ 122: 114-132. http://dx.doi.org/10.1016/j.atmosenv.2015.09.027

Vukovic, A; Vujadinovic, M; Pejanovic, G; Andric, J; Kumjian, MR; Djurdjevic, V; Dacic, M; Prasad, AK; El-Askary, HM; Paris, BC; Petkovic, S; Nickovic, S; Sprigg, WA. (2014). Numerical simulation of "an American haboob". Atmos Chem Phys 14: 3211-3230. http://dx.doi.org/10.5194/acp-14-3211-2014

Wagner, J; Casuccio, G. (2014). Spectral imaging and passive sampling to investigate particle sources in urban desert regions. Environ Sci Process Impacts 16: 1745-1753. http://dx.doi.org/10.1039/c4em00123k

Wang, Y; Hopke, PK; Chalupa, DC; Utell, MJ. (2011). Long-term study of urban ultrafine particles and other pollutants. Atmos Environ 45: 7672-7680. http://dx.doi.org/10.1016/j.atmosenv.2010.08.022

Wang, Y; Hopke, PK; Utell, MJ. (2012). Urban-scale seasonal and spatial variability of ultrafine particle number concentrations. Water Air Soil Pollut 223: 2223-2235. http://dx.doi.org/10.1007/s11270-011-1018-z

Wang, Y; Xie, Y; Cai, L; Dong, W; Zhang, Q; Zhang, L, in. (2015). Impact of the 2011 Southern US Drought on Ground-Level Fine Aerosol Concentration in Summertime. J Atmos Sci 72: 1075-1093. http://dx.doi.org/10.1175/JAS-D-14-0197.1

Watson, JG; Chow, JC; Chen, LW; Frank, NH. (2009). Methods to assess carbonaceous aerosol sampling artifacts for IMPROVE and other long-term networks. J Air Waste Manag Assoc 59: 898-911. http://dx.doi.org/10.3155/1047-3289.59.8.898

Weakley, AT; Takahama, S; Dillner, A, nnM. (2016). Ambient aerosol composition by infrared spectroscopy and partial least-squares in the chemical speciation network: Organic carbon with functional group identification. Aerosol Sci Technol 50: 1096-1114. http://dx.doi.org/10.1080/02786826.2016.1217389

Weber, RJ; Guo, H; Russell, AG; Nenes, A. (2016). High aerosol acidity despite declining atmospheric sulfate concentrations over the past 15 years. Nat Geosci 9: 282-285. http://dx.doi.org/10.1038/NGEO2665

Weber, RJ; Sullivan, A; Peltier, RE; Russell, A; Yan, B; Zheng, M; de Gouw, J; Warneke, C; Brock, C; Holloway, JS; Atlas, EL; Edgerton, E. (2007). A study of secondary organic aerosol formation in the anthropogenic-influenced southeastern United States. J Geophys Res Atmos 112. http://dx.doi.org/10.1029/2007JD008408

Weinstock, L. (2012). Putting multipollutant monitoring into practice: EPA's NCore network. EM Magazine May 2012: 26-31.

Welz, O; Savee, JD; Osborn, DL; Vasu, SS; Percival, CJ; Shallcross, DE; Taatjes, CA. (2012). Direct kinetic measurements of Criegee intermediate (CHOO) formed by reaction of CHI with O. Science 335: 204-207. http://dx.doi.org/10.1126/science.1213229

ED_002220_00002287-00258

Westervelt, DM; Pierce, JR, JR; Adams, PJ. (2014). Analysis of feedbacks between nucleation rate, survival probability and cloud condensation nuclei formation. Atmos Chem Phys 14: 5577-5597. http://dx.doi.org/10.5194/acp-14-5577-2014

Whitby, KT. (1978). The physical characteristics of sulfur aerosols. Atmos Environ 12: 135-159. http://dx.doi.org/10.1016/0004-6981(78)90196-8

Whitby, KT; Husar, RB; Liu, BYH. (1972). The aerosol size distribution of Los Angeles smog. J Colloid Interface Sci 39: 177-204.

Whitefield, PD; Lobo, P; Hagen, DE; Taylor, C; Ratliff, G; Lukachko, S; Sequeira, C; Hileman, J; Waitz, I; Webb, S; Thrasher, TG; Ohsfeldt, MR; Kaing, HK; Essama, SC. (2008). Summarizing and interpreting aircraft gaseous and particulate emissions data. ACRP Report 9. Washington, D.C.: Transportation Research Board of the National Academies. http://dx.doi.org/10.17226/14197

Whiteman, CD; Hoch, SW; Horel, JD; Charland, A. (2014). Relationship between particulate air pollution and meteorological variables in Utah's Salt Lake Valley. Atmos Environ 94: 742-753. http://dx.doi.org/10.1016/j.atmosenv.2014.06.012

Wiedensohler, A; Birmili, W; Nowak, A; Sonntag, A; Weinhold, K; Merkel, M; Wehner, B; Tuch, T; Pfeifer, S; Fiebig, M; Fjaraa, AM; Asmi, E; Sellegri, K; Depuy, R; Venzac, H; Villani, P; Laj, P; Aalto, P; Ogren, JA; Swietlicki, E; Williams, P; Roldin, P; Quincey, P; Hueglin, C; Fierz-Schmidhauser, R; Gysel, M; Weingartner, E; Riccobono, F; Santos, S; Gruening, C; Faloon, K; Beddows, D; Harrison, RM; Monahan, C; Jennings, SG; O'Dowd, CD; Marinoni, A; Horn, HG; Keck, L; Jiang, J; Scheckman, J; McMurry, PH; Deng, Z; Zhao, CS; Moerman, M; Henzing, B; de Leeuw, G; Loeschau, G; Bastian, S. (2012). Mobility particle size spectrometers: harmonization of technical standards and data structure to facilitate high quality long-term observations of atmospheric particle number size distributions. Atmos Meas Tech 5: 657-685. http://dx.doi.org/10.5194/amt-5-657-2012

Wiedensohler, A; Cheng, YF; Nowak, A; Wehner, B; Achtert, P; Berghof, M; Birmili, W; Wu, ZJ; Hu, M; Zhu, T; Takegawa, N; Kita, K; Kondo, Y; Lou, S. R.; Hofzumahaus, A; Holland, F; Wahner, A; Gunthe, SS; Rose, D; Su, H; Poeschl, U. (2009). Rapid aerosol particle growth and increase of cloud condensation nucleus activity by secondary aerosol formation and condensation: A case study for regional air pollution in northeastern China. J Geophys Res 114: D00G08. http://dx.doi.org/10.1029/2008JD010884

Wilson, WE; Suh, HH. (1997). Fine particles and coarse particles: Concentration relationships relevant to epidemiologic studies. J Air Waste Manag Assoc 47: 1238-1249. http://dx.doi.org/10.1080/10473289.1997.10464074

Wong, DC; Pleim, J; Mathur, R; Binkowski, F; Otte, T; Gilliam, R; Pouliot, G; Xiu, A; Young, JO; Kang, D. (2012). WRF-CMAQ two-way coupled system with aerosol feedback: Software development and preliminary results. GMD 5: 299-312. http://dx.doi.org/10.5194/gmd-5-299-2012

Woodward, NC; Pakbin, P; Saffari, A; Shirmohammadi, F; Haghani, A; Sioutas, C; Cacciottolo, M; Morgan, TE; Finch, CE. (2017). Traffic-related air pollution impact on mouse brain accelerates myelin and neuritic aging changes with specificity for CA1 neurons. Neurobiol Aging 53: 48-58. http://dx.doi.org/10.1016/j.neurobiolaging.2017.01.007

Woody, MC; Baker, KR; Hayes, PL; Jimenez, JL; Koo, B; Pye, HOT. (2016). Understanding sources of organic aerosol during CalNex-2010 using the CMAQ-VBS. Atmos Chem Phys 16: 4081-4100.

Wyat Appel, K; Bhave, PV; Gilliland, AB; Sarwar, G; Roselle, SJ. (2008). Evaluation of the Community Multiscale Air Quality (CMAQ) model version 45: Sensitivities impacting model performance; Part II - particulate matter. Atmos Environ 42(24): 6057-6066. http://dx.doi.org/10.1016/j.atmosenv.2008.03.036

Xie, M; Coons, TL; Dutton, SJ; Milford, JB; Miller, SL; Peel, JL; Vedal, S; Hannigan, MP. (2012). Intra-urban spatial variability of PM2.5-bound carbonaceous components. Atmos Environ 60: 486-494. http://dx.doi.org/10.1016/j.atmosenv.2012.05.041

ED_002220_00002287-00259

Xing, J; Mathur, R; Pleim, J; Hogrefe, C; Gan, CM; Wong, DC; Wei, C; Gilliam, R; Pouliot, G. (2015). Observations and modeling of air quality trends over 1990-2010 across the Northern Hemisphere: China, the United States and Europe. Atmos Chem Phys 15: 2723-2747. http://dx.doi.org/10.5194/acp-15-2723-2015

Yanosky, JD; Paciorek, CJ; Laden, F; Hart, JE; Puett, RC; Liao, D; Suh, HH. (2014). Spatio-temporal modeling of particulate air pollution in the conterminous United States using geographic and meteorological predictors. Environ Health 13: 63. http://dx.doi.org/10.1186/1476-069X-13-63

Yanosky, JD; Paciorek, CJ; Suh, HH. (2009). Predicting chronic fine and coarse particulate exposures using spatiotemporal models for the northeastern and midwestern United States. Environ Health Perspect 117: 522-529. http://dx.doi.org/10.1289/ehp.11692

Yasmeen, F; Vermeylen, R; Szmigielski, R; Iinuma, Y; Boege, O; Herrmann, H; Maenhaut, W; Claeys, M. (2010). Terpenylic acid and related compounds: precursors for dimers in secondary organic aerosol from the ozonolysis of alpha- and beta-pinene. Atmos Chem Phys 10: 9383-9392. http://dx.doi.org/10.5194/acp-10-9383-2010

Ying, Q; Li, J; Kota, SH. (2015). Significant contributions of isoprene to summertime secondary organic aerosol in eastern United States. Environ Sci Technol 49: 7834-7842. http://dx.doi.org/10.1021/acs.est.5b02514

Yli-Juuti, T; Nieminen, T; Hirsikko, A; Aalto, PP; Asmi, E; Horrak, U; Manninen, HE; Patokoski, J; Dal Maso, M; Petaja, T; Rinne, J; Kulmala, M; Riipinen, I. (2011). Growth rates of nucleation mode particles in Hyytiala during 2003-2009: variation with particle size, season, data analysis method and ambient conditions. Atmos Chem Phys 11: 12865-12886. http://dx.doi.org/10.5194/acp-11-12865-2011

Young, DE; Kim, H; Parworth, C; Zhou, S; Zhang, X; Cappa, CD; Seco, R; Kim, S; Zhang, Q, i. (2016). Influences of emission sources and meteorology on aerosol chemistry in a polluted urban environment: results from DISCOVER-AQ California. Atmos Chem Phys 16: 5427-5451. http://dx.doi.org/10.5194/acp-16-5427-2016

Yu, F. (2010). Ion-mediated nucleation in the atmosphere: Key controlling parameters, implications, and look-up table. J Geophys Res Atmos 115. http://dx.doi.org/10.1029/2009JD012630

Yu, H; Chin, M; Bian, H; Yuan, T; Prospero, JM; Omar, A, liH; Remer, LA; Winker, DM; Yang, Y; Zhang, Y, an; Zhang, Z. (2015). Quantification of trans-Atlantic dust transport from seven-year (2007-2013) record of CALIPSO lidar measurements. Rem Sens Environ 159: 232-249. http://dx.doi.org/10.1016/j.rse.2014.12.010

Yu, H; Remer, LA; Chin, M; Bian, H; Kleidman, RG; Diehl, T. (2008). A satellite-based assessment of transpacific transport of pollution aerosol. J Geophys Res 113: 1-15. http://dx.doi.org/10.1029/2007JD009349

Yu, L; Smith, J; Laskin, A; Anastasio, C; Laskin, J; Zhang, Q. (2014a). Chemical characterization of SOA formed from aqueous-phase reactions of phenols with the triplet excited state of carbonyl and hydroxyl radical. Atmos Chem Phys 14: 13801-13816. http://dx.doi.org/10.5194/acp-14-13801-2014

Yu, L, u; Smith, J; Laskin, A; George, KM; Anastasio, C; Laskin, J; Dillner, A, nnM; Zhang, Q, i. (2016). Molecular transformations of phenolic SOA during photochemical aging in the aqueous phase: competition among oligomerization, functionalization, and fragmentation. Atmos Chem Phys 16: 4511-4527. http://dx.doi.org/10.5194/acp-16-4511-2016

Yu, S; Mathur, R; Pleim, J; Wong, D; Gilliam, R; Alapaty, K; Zhao, C; Liu, X. (2014b). Aerosol indirect effect on the grid-scale clouds in the two-way coupled WRF-CMAQ: model description, development, evaluation and regional analysis. Atmos Chem Phys 14: 11247-11285. http://dx.doi.org/10.5194/acp-14-11247-2014

Yue, D; Hu, M; Wu, Z; Wang, Z; Guo, S; Wehner, B; Nowak, A; Achtert, P; Wiedensohler, A; Jung, J; Kim, YJ; Liu, S. (2009). Characteristics of aerosol size distributions and new particle formation in the summer in Beijing. J Geophys Res 114: D00G12. http://dx.doi.org/10.1029/2008JD010894

Yumimoto, K; Takemura, T. (2015). Long-term inverse modeling of Asian dust: Interannual variations of its emission, transport, deposition, and radiative forcing : Supplemental materials [Supplemental Data]. J Geophys Res Atmos 120: 1582-1607.

ED_002220_00002287-00260

Zhang, H; Hu, D; Chen, J; Ye, X; Wang, S; Hao, J, iM; Wang, L, in; Zhang, R; An, Z. (2011a). Particle Size Distribution and Polycyclic Aromatic Hydrocarbons Emissions from Agricultural Crop Residue Burning. Environ Sci Technol 45: 5477-5482. http://dx.doi.org/10.1021/es1037904

Zhang, H; Liu, H; Davies, KJ; Sioutas, C; Finch, CE; Morgan, TE; Forman, HJ. (2012a). Nrf2-regulated phase II enzymes are induced by chronic ambient nanoparticle exposure in young mice with age-related impairments. Free Radic Biol Med 52: 2038-2046. http://dx.doi.org/10.1016/j.freeradbiomed.2012.02.042

Zhang, Q; Jimenez, JL; Canagaratna, MR; Allan, JD; Coe HL Ulbrich, I; Alfarra, MR; Takami, A; Middlebrook, AM; Sun, YL; Dzepina, K; Dunlea, E; Docherty, K; Decarlo, PF; Salcedo, D; Onasch, T; Jayne, J. R.; Miyoshi, T; Shimono, A; Hatakeyama, S; Takegawa, N; Kondo, Y; Schneider, J; Drewnick, F; Borrmann, S; Weimer, S; Demerjian, K; Williams, P; Bower, K; Bahreini, R; Cottrell, L; Griffin, RJ; Rautiainen, J; Sun, J. R.; Zhang, YM; Worsnop, DR. (2007). Ubiquity and dominance of oxygenated species in organic aerosols in anthropogenically-influenced Northern Hemisphere midlatitudes. Geophys Res Lett 34: L13801. http://dx.doi.org/10.1029/2007GL029979

Zhang, R; Khalizov, A; Wang, L, in; Hu, M, in; Xu, W, en. (2012b). Nucleation and Growth of Nanoparticles in the Atmosphere. Chem Rev 112: 1957-2011. http://dx.doi.org/10.1021/cr2001756

Zhang, X; Kim, H; Parworth, CL; Young, DE; Zhang, Q, i; Metcalf, AR; Cappa, CD. (2016). Optical Properties of Wintertime Aerosols from Residential Wood Burning in Fresno, CA: Results from DISCOVER-AQ 2013. Environ Sci Technol 50: 1681-1690. http://dx.doi.org/10.1021/acs.est.5b04134

Zhang, YM; Zhang, XY; Sun, JY; Lin, WL; Gong, SL; Shen, XJ; Yang, S. (2011b). Characterization of new particle and secondary aerosol formation during summertime in Beijing, China. Tellus B Chem Phys Meteorol 63: 382-394. http://dx.doi.org/10.1111/j.1600-0889.2011.00533.x

Zhao, Y; Hennigan, CJ; May, AA; Tkacik, DS; de Gouw, JA; Gilman, JB; Kuster, WC; Borbon, A; Robinson, AL. (2014). Intermediate-volatility organic compounds: a large source of secondary organic aerosol. Environ Sci Technol 48: 13743-13750. http://dx.doi.org/10.1021/es5035188

Zhu, Y; Hinds, WC. (2002). Concentration and size distribution of ultrafine particles near a major highway. J Air Waste Manag Assoc 52: 1032-1042.

Zou, B; Wilson, JG; Zhan, FB; Zeng, YN. (2009). Spatially differentiated and source-specific population exposure to ambient urban air pollution. Atmos Environ 43: 3981-3988. http://dx.doi.org/10.1016/j.atmosenv.2009.05.022

ED_002220_00002287-00261

CHAPTER 3 EXPOSURE TO AMBIENT PARTICULATE MATTER

Overall Conclusions regarding Exposure to Ambient PM

- Recent and existing evidence indicate that exposure error typically produces *underestimation* of health effects in epidemiologic studies of short-term and long-term PM exposure. Bias away from the null can sometimes occur for long-term exposure studies if a monitor or model underestimates population exposure.
- New developments in PM exposure assessment methods, including hybrid spatiotemporal models that incorporate satellite observations of AOD, land use variables, surface monitoring data from FRMs, and/or CTMs, have reduced bias and uncertainty in health effect estimates by improving the spatial resolution and accuracy of exposure predictions.
- High correlations of $PM_{2.5}$ with some gaseous copollutants necessitate evaluation of the impact of confounding on health effect estimates.
- There is typically more uncertainty for health effect estimates for exposure to $PM_{10-2.5}$ and UFP, because their concentrations tend to be more spatially variable than $PM_{2.5}$ concentrations and concentration data for $PM_{10-2.5}$ and UFP are less frequently available and/or more uncertain.

3.1 Introduction

Assessment of exposure to ambient PM builds from the characterization of concentrations and atmospheric chemistry presented in CHAPTER 2. The primary conclusions from CHAPTER 2 were that $PM_{2.5}$ concentrations continue to decrease over time with few areas exceeding the level of the current NAAQS, sulfates comprise a smaller proportion of total $PM_{2.5}$ throughout the country including in the eastern half of the country, $PM_{10-2.5}$ contributes most substantially to PM_{10} in the southwestern U.S. but is highly variable across urban areas, and substantial uncertainty still exists regarding UFP sources, composition, and concentrations.

This chapter presents new developments in exposure assessment methodology and interpretation of epidemiological study results given strengths and limitations of the exposure assessment data. The chapter describes concepts and terminology relating to exposure (Section 3.2), methodological considerations for use of exposure data (Section 3.3), and exposure assessment and interpretation of epidemiologic study results (Section 3.4). This chapter focuses on the ambient component of personal exposure to PM, because the NAAQS pertains to ambient PM. However, studies using total personal PM measurements or indoor PM concentrations to represent exposure can also inform the understanding of the relationship between exposure and health effects and so are included as supporting evidence if ambient PM exposure can be deduced from the information provided in the studies. This chapter focuses on studies of exposure among the general population. Exposure of groups potentially at increased risk of PM-related health effects, based for example on socioeconomic status and race, is addressed in CHAPTER 12. Intake of PM based on ventilation rate, and in relation to physical activity, is described in CHAPTER 4. The information provided in this chapter will be used to help interpret the evidence for the

ED_002220_00002287-00262

health effects of PM exposure presented in the health chapters that follow (CHAPTER 5, CHAPTER 6, CHAPTER 7, CHAPTER 8, CHAPTER 9, CHAPTER 10, and CHAPTER 11).

3.2 Conceptual Overview of Human Exposure

The 2009 PM ISA (U.S. EPA, 2009b) provided a conceptual model of exposure to form a distinction between ambient PM exposure and total personal exposure. This section illustrated that exposure is integrated over time and across the microenvironments in which a person spends time. This section also introduced the concept of an infiltration factor that depends on both penetration of PM indoors and the ventilation and deposition characteristics that influence indoor PM concentration. That discussion is currently updated and presented in Section 3.2.2.

This ISA contains two new sections to orient the reader to concepts relevant to exposure. Section 3.2.1 introduces terminology that is used throughout the chapter when describing exposure assessment studies. Section 3.2.3 highlights facets of exposure assessment that are particularly relevant to PM.

3.2.1 Exposure Terminology

A variety of metrics and terms are used to characterize air pollution exposure. They are described here at the beginning of the chapter to provide clarity for the subsequent discussion.

The *concentration* of PM is defined as the mass of the pollutant in a given volume of air (e.g., $\mu g/m^3$). Concentrations observed in outdoor locations accessible to the public are referred to as ambient concentrations. The term exposure refers to contact at the interface of the breathing zone with the ambient concentration of a specific pollutant over a certain period of time (Zartarian et al., 2005), in single or multiple locations. For example, contact with a concentration of 10 $\mu g/m^3$ $PM_{2.5}$ for 1-hour would be referred to as a 1-hour exposure to 10 $\mu g/m^3$ $PM_{2.5}$, and 10 $\mu g/m^3$ is referred to as the *exposure concentration*. As discussed in CHAPTER 4, dose incorporates the concept of intake into the body (via inhalation).

A location where exposure occurs is referred to as a *microenvironment*, and an individual's daily exposure consists of the time-integrated concentrations in each of the microenvironments visited during the day. Ambient air pollution may penetrate indoors (see Section 3.4.1.1 on infiltration), where it combines with air pollution from indoor sources (*nonambient air pollution*) to produce the total measured indoor concentration. Exposure to the ambient fraction of total indoor concentration, together with exposure to ambient concentrations in outdoor microenvironments such as parks, yards, sidewalks, and bicycles or motorcycles, is referred to as ambient exposure (Wilson et al., 2000). *Total personal exposure to ambient PM* is the concentration of PM emitted from ambient sources or formed in the atmosphere that

ED_002220_00002287-00263

is encountered by an individual over a given time. This differs from overall total personal exposure, which may also include exposure to nonambient air pollution. Personal exposure to ambient PM is influenced by several factors, including:

- Time-activity in different microenvironments (e.g., vehicle, residence, workplace, outdoor);
- climate (e.g., weather, season);
- characteristics of indoor microenvironments (e.g., window openings, draftiness, air conditioning); and
- microenvironmental emission sources (e.g., roadways, construction equipment, indoor gas stoves) and concentrations.

Because personal exposures are not routinely measured, the term *exposure surrogate* is used in this chapter to describe a quantity meant to estimate or represent exposure, such as $PM_{2.5}$ concentration measured at an ambient monitor (Sarnat et al., 2000). A *fixed-site monitor* (i.e., a monitor with a fixed position) is a type of *ambient monitor* used to estimate population average exposure concentrations and their trends over neighborhood- and urban-scales for epidemiologic studies.

When surrogates are used for exposure estimation in epidemiologic studies, exposure error or exposure misclassification can result. *Exposure error* refers to the bias and uncertainty associated with using concentration metrics to represent the actual exposure of an individual or population (Lipfert and Wyzga, 1996). Exposure misclassification refers to exposure error that occurs when exposure conditions such as location, timing, or population grouping are incorrectly assigned. *Exposure misclassification* due to exposure assignment methods and spatial and temporal variability in pollutant concentrations may be either differential (i.e., systematic), or nondifferential (i.e., random). *Differential misclassification* refers to the situation where exposure errors differ between groups. An example of differential misclassification is the use of geocoding to estimate air pollution exposure by proximity to roadways, because concentrations decrease with distance from roadways and are different upwind and downwind of a major roadway (Lane et al., 2013; Singer et al., 2004). *Nondifferential misclassification* refers to the situation where exposure characterization has the same probability of being misclassified to a similar degree across all groups.

Exposure misclassification and exposure error can result in bias and reduced precision of the effect estimate in epidemiologic studies. *Bias* refers to the difference between the population-average measured and true exposure, while precision is a measure of the variation of measurement error in the population (Armstrong et al., 1992). Bias toward the null, or attenuation of the effect estimate, indicates an underestimate of the magnitude of the effect, and is characteristic of nondifferential measurement error. Bias away from the null can occur through differential exposure measurement error, such as may occur when an exposed person or group of people are located far from a source that is captured by a fixed-site monitor (Armstrong et al., 1992).

ED_002220_00002287-00264

Exposure error has two components: (1) exposure measurement error derived from uncertainty in the metric being used to represent exposure and (2) use of a surrogate parameter of interest in the epidemiologic study in lieu of the true exposure, which may be unobservable. *Classical error* is defined as error scattered around the true personal exposure and independent of the measured exposure. Classical error results in bias of the epidemiologic health effect estimate. Because variation in the measurements tends to be greater than variation in the true exposures, classical error typically biases the health effect estimate towards the null (no effect of the exposure). This would cause the health effect estimate to be underestimated. Classical error can also cause inflation or reduction of the standard error of the health effect estimate. For example, classical error may occur when a fixed-site monitor measuring exposure concentration is imprecise. *Berkson error* is defined as error scattered around the measured exposure surrogate (in most cases, the ambient monitoring measurement) and independent of the true exposure (Goldman et al., 2011; Reeves et al., 1998). Pure Berkson error is not expected to bias the health effect estimate. Berkson error tends not to cause bias in the health effect estimate. For example, Berkson error may occur when personal monitors used in a panel study capture ambient and nonambient exposures, if the objective of the study is to evaluate the effect of ambient exposures on health and the ambient and nonambient exposures are independent of each other.

Definitions for *classical-like* and *Berkson-like errors* were developed for modeled exposures. These errors depend on how exposure metrics are averaged across space. Classical-like errors can add variability to predicted exposures and can bias health effect estimates in a manner similar to pure classical errors, but they differ from pure classical errors in that the variability in estimated exposures is also not independent across space. Szpiro et al. (2011a) defined Berkson-like and classical-like errors as errors sharing some characteristics with Berkson and classical errors, respectively, but with some differences. Specifically, Berkson-like errors occur when the modeled exposure does not capture all of the variability in the true exposure. Berkson-like errors increase the variability around the health effect estimate in a manner similar to pure Berkson error, but Berkson-like errors are spatially correlated and not independent of predicted exposures, unlike pure Berkson errors. Berkson-like error can lead to bias of the health effect estimate in either direction (Szpiro and Paciorek, 2013).

The influence of these types of exposure errors on health effect estimates for specific short-term and long-term exposure study designs is evaluated in Section 3.4.5. This review of the influence of error on exposure estimates used in epidemiology studies informs evaluation of confounding and other biases and uncertainties when considering the health effects evidence in CHAPTER 5, CHAPTER 6, CHAPTER 7, CHAPTER 8, CHAPTER 9, CHAPTER 10, and CHAPTER 11.

ED_002220_00002287-00265

3.2.2 Conceptual Model of Total Personal Exposure

A conceptual model of personal exposure is presented to highlight measurable quantities and the uncertainties that exist in this framework. An individual's time-integrated total exposure to PM can be described based on a compartmentalization of the person's activities throughout a given time period:

$$E_T = \int_1^n C_j dt$$

Equation 3-1

where E_T = total exposure over a time-period of interest, C_j = airborne PM concentration at microenvironment j, n = total number of microenvironments, and dt = portion of the time-period spent in microenvironment j. Total exposure (E_T) can be decomposed into a model that accounts for exposure to PM of ambient (E_a) and nonambient (E_{na}) origin of the form:

$$E_T = E_a + E_{na}$$

Equation 3-2

Indoor combustion, such as cooking, smoking, or candle burning, as well as cleaning, and other activities are nonambient sources of PM (see Section 3.4.1.2, indoor-outdoor [I/O] relationships on indoor PM) that are specific to individuals and result in variable nonambient exposures across the population. Assuming steady-state outdoor conditions, E_a can be expressed in terms of the fraction of time spent in various outdoor and indoor microenvironments (U.S. EPA, 2006; Wilson et al., 2000):

$$E_a = \Sigma f_o C_o + \Sigma f_i F_{inf,i} C_{o,i}$$

Equation 3-3

where f_o = fraction of the relevant time period (equivalent to dt in Equation 3-1) in outdoor microenvironments; f_i = fraction of the relevant time period (equivalent to dt in Equation 3-1) in indoor microenvironments; C_o = PM concentration in outdoor microenvironments; $C_{o,I}$ = PM concentration in outdoor microenvironments adjacent to an indoor microenvironment i; and $F_{inf,i}$ = infiltration factor for indoor microenvironment i. Equation 3-3 is subject to the constraint $\Sigma_{fo} + \Sigma_{fi} = 1$ to reflect the total exposure over a specified time period, and each term on the right hand side of the equation has a summation because it reflects various microenvironmental exposures. Here, "indoors" refers to being inside any aspect of the built environment, [e.g., homes, schools, office buildings, enclosed vehicles (automobiles, trains, buses), and/or recreational facilities (movie theaters, restaurants, bars)], while "outdoors" refers to outdoor microenvironments (e.g., parks, yards, sidewalks, and bicycles or motorcycles). Assuming steady state ventilation conditions, the infiltration factor (F_{inf}) is a function of the penetration (P) of PM into the microenvironment, the air exchange rate (a) of the microenvironment, and the rate of PM loss (k) in the microenvironment:

ED_002220_00002287-00266

$$F_{inf} = \frac{Pa}{(a+k)}$$

Equation 3-4

In epidemiologic studies, the ambient PM concentration, Ca, is often used in lieu of outdoor microenvironmental data to represent these exposures based on the availability of data. Thus, it is often assumed that $C_o = C_a$ and that the fraction of time spent outdoors can be expressed cumulatively as f_o; the indoor terms still retain a summation because infiltration differs for different microenvironments. If an epidemiologic study employs only C_a, then it is assumed that exposure to ambient PM, E_a given in Equation 3-3, is re-expressed solely as a function of C_a:

$$E_a = (f_o + \Sigma f_i F_{inf,i}) C_a$$

Equation 3-5

Equation 3-5 encapsulates several facets of the relationship between ambient concentration and E_a. First, C_a represents all ambient PM concentrations combined. Measurements and models to quantify C_a may assign one uniform PM concentration in the region of study (e.g., Section 3.3.1.1), or it might be modeled to represent how it varies outdoors across space (Section 3.4.2.2). Second, exposure is related to both concentration encountered and time spent in a given microenvironment. Outdoor exposure is directly influenced by ambient concentration and time spent outdoors. Indoor exposure occurs where infiltration of ambient PM into the envelope of an enclosed space (e.g., building, bus) likely reduces ambient PM exposure by filtering out a fraction of the ambient PM, but the influence of ambient concentration and time of exposure is still present. The components of indoor and outdoor exposure to ambient PM to comprise total ambient PM exposure, E_a. Further combining these factors with human activity level influences dose (Section 4.1.7).

Certain factors influence whether Equation 3-5 is a reasonable approximation for Equation 3-3, including the spatial variability of outdoor PM concentrations due to spatial distribution of sources; meteorology, topography, oxidation rates, and the design of the epidemiologic study. These equations also assume steady-state microenvironmental concentrations. Errors and uncertainties inherent in using Equation 3-5 in lieu of Equation 3-3 are described in Section 3.4. with respect to implications for interpreting epidemiologic studies. Epidemiologic studies often use concentration measured at an ambient monitor to represent ambient concentration; thus α, the ratio between personal exposure to ambient PM and the ambient concentration of PM, is defined as:

$$\alpha = \frac{E_a}{C_a}$$

Equation 3-6

Combining Equation 3-5 and Equation 3-6 yields:

ED_002220_00002287-00267

$$\alpha = f_o + \Sigma f_i F_{inf,i}$$

Equation 3-7

where α varies between 0 and 1. If a person's exposure occurs in a single microenvironment, the ambient component of the microenvironmental PM concentration can be represented as the product of the ambient concentration and F_{inf}. Time-activity data and corresponding estimates of F_{inf} for each microenvironmental exposure are needed to compute an individual's α with accuracy (U.S. EPA, 2006). In epidemiologic studies, α is assumed to be constant in lieu of time-activity data and estimates of F_{inf}, which can vary spatially (between homes) and temporally (within a home) based on building and meteorology-related air exchange characteristics.

The conceptual model presented in Equation 3-1 through Equation 3-7 establish a framework for considering the influence of exposure measurement error on statistical models used in epidemiology studies. Exposure measurement error occurs when there is an absence of information for the variables in this framework, so assumptions must be made regarding ambient exposures. If important local outdoor sources and sinks exist but are not captured by ambient monitors, then the ambient component of the local outdoor concentration may be estimated using dispersion models, land use regression (LUR) models, chemical transport models (CTMs), satellite data, or some combination of these techniques, which are described in Section 3.3.2.

3.2.3 Exposure Considerations Specific to PM

The inhalation exposure route relevant for PM is influenced by sources, chemistry, particle size distribution, meteorology, and ambient concentrations, as described in detail in Chapter 2 and briefly summarized here.

The polydisperse size distribution (Section 2.2) and composition (Section 2.3) of PM interact to influence several aspects of exposure. UFP dominates the number concentration (NC) distribution of PM, while $PM_{2.5}$ typically dominates the mass distribution. Combustion via energy production, mobile sources, and industrial processes is the main primary anthropogenic source of UFP and $PM_{2.5}$. Brake, tire, and clutch wear can also contribute to primary UFP, $PM_{2.5}$, and $PM_{10-2.5}$. Secondary production of NO_3^-, NH_4^+, and SO_4^{2-} are also major contributors to $PM_{2.5}$, and the magnitude of those contributions varies by region, time of day, and season. UFP will also grow to the accumulation mode following emissions on time scales of hours to days. Road and construction dust are important anthropogenic sources of $PM_{10-2.5}$ in urban areas, while agricultural dust is an anthropogenic source of $PM_{10-2.5}$ in rural areas. Biogenic $PM_{10-2.5}$ from pollen can also be a substantial contributor to overall $PM_{10-2.5}$.

The size distribution influences transport and dispersion of PM, therefore affecting spatial and temporal variability of PM concentration and hence exposure (U.S. EPA, 2009b). UFP has a short lifetime because it either readily evaporates or undergoes rapid growth into the accumulation mode via

ED_002220_00002287-00268

agglomeration of UFP into larger particles, condensation or adsorption of vapors onto UFP, or reaction of gases in or on the particles (Section 2.2). $PM_{2.5}$ will tend to follow the wind unless evaporating, participating in a surface reaction, and/or accumulating to a larger size. Particle growth may enhance deposition. $PM_{10-2.5}$ in dust can settle out of the air at a faster rate than $PM_{2.5}$. Resuspension by vehicle-generated turbulence, tire motion, or other activities may occur for particles of any size but are more likely for $PM_{10-2.5}$, which forms more readily via mechanical generation (Section 2.3.3). As a result, spatial and temporal variability of PM exposure concentration tends to be greater for UFP and $PM_{10-2.5}$ compared with $PM_{2.5}$ (Section 2.5).

Size distribution will also affect what fraction of the ambient air penetrates indoors (U.S. EPA, 2009b). Because $PM_{2.5}$ navigates changes in direction more easily, more $PM_{2.5}$ tends to infiltrate indoors compared with $PM_{10-2.5}$, which impacts onto building envelope surfaces more easily. UFP is more likely to diffuse onto building envelope surfaces compared with $PM_{2.5}$, so it would be expected that a lower proportion of UFP would infiltrate indoors compared with $PM_{2.5}$.

In summary, variability and uncertainties in accounting for PM emissions, chemistry, transport, and dispersion (noted here and described in detail in CHAPTER 2) leads to variability and uncertainties in estimates of exposure concentrations. For PM, uncertainties extend to characterization of the statistical distribution of particles by size and concentration (spatially and temporally). Because they have shorter lifetimes compared with $PM_{2.5}$, spatial and temporal variability is more pronounced for the lower (UFP) and upper ($PM_{10-2.5}$) segments of the particle size distribution compared with the accumulation mode ($PM_{2.5}$). Such uncertainties may complicate estimation of exposure concentrations using models such as CTMs (Section 3.3.2.4) or satellite-based methods where a relationship between $PM_{2.5}$ and surface measurements is derived (Section 3.3.3). Errors associated with these factors are described further in Section 3.4.2, and their influence on epidemiologic study results is considered in Section 3.4.5.

3.3 Methodological Considerations for Use of Exposure Data and Models

This section describes methods for estimating human exposure to PM, along with their strengths and limitations, which are important to understand when developing associations between PM exposure and health endpoints in epidemiologic analyses. The 2009 PM ISA (U.S. EPA, 2009b) and other literature [e.g., Madrigano et al. (2013); Hubbell (2012); Tagaris et al. (2009)] presented information about ambient and personal monitoring, as well as models for data averaging, spatial interpolation, LUR, CTM, and dispersion models. The current section extends that presentation by updating the assessment with discussion of new methodology and a more detailed consideration of features, strengths, and limitations of measurement and modeling techniques for PM exposure assessment.

For epidemiologic analyses, accurately assigning air pollutant exposure concentrations to individuals is difficult given the limited spatial and temporal resolution of the available observations.

ED_002220_00002287-00269

Applications can vary in scale, from personal (Baxter et al., 2013; Brown et al., 2012; Dons et al., 2012; Kaur and Nieuwenhuijsen, 2009) to national (Fann et al., 2012; Bell et al., 2011b) to global (Lelieveld et al., 2015; Brauer et al., 2012; Lim et al., 2012). In some studies, personal monitoring has been used, but study limitations (e.g., expense, recruiting subjects to participate) typically constrain the size of the population studied in panel studies (Baxter et al., 2013; Ozkaynak et al., 2013; Jerrett et al., 2005a; Sarnat et al., 2000). Thus, methods are employed that use the limited observational data available from ambient air quality monitoring regulatory networks (Solomon et al., 2011) and special, often intensive studies that may be designed to provide data for exposure assessment and/or spatial characterization (Vedal et al., 2013; Hansen et al., 2006; Edgerton et al., 2005; Jerrett et al., 2005b; Butler et al., 2003; Hansen et al., 2003). In addition, health studies are taking advantage of satellite data [e.g., Madrigano et al. (2013); Liu et al. (2009)], mobile monitoring data [e.g., Levy et al. (2014); Bergen et al. (2013)], and models [e.g., Jerrett et al. (2016); Turner et al. (2016); Villeneuve et al. (2015); Pope et al. (2014)].

Modeling PM exposure concentrations can be challenging because PM may contain a mixture of components and is found in a continuum of sizes (Section 2.2). Approaches for modeling PM exposure concentration can generally be used for different sized particles ($PM_{10-2.5}$, $PM_{2.5}$, UFP) and components, though additional considerations may be involved. For example, there are very limited observational data on UFP for cross-validation (Section 2.5); $PM_{2.5}$ composition data from ambient monitoring networks are typically available every few days (e.g., every third or every sixth day) using 24-hour integrated measurements. Different observational techniques for $PM_{10-2.5}$, $PM_{2.5}$, and UFP have different biases and uncertainties, and composition may influence biases and uncertainties within a given size fraction. Some observed components (e.g., OC) are composed of multiple compounds that behave differently in the environment.

There are a range of approaches used to model PM exposure that are applied for specific purposes, and their uses depend upon available data. Ozkaynak et al. (2013) developed a hierarchy of methods based upon complexity, ranging from using ambient monitoring data as an exposure surrogate to human exposure models accounting for time-activity data and microenvironmental exposure concentrations (Figure 3-1). This list can be extended to include source apportionment models. The amount and complexity of model input data increases with increasing complexity of the models. Increasing the complexity of the exposure modeling methods may reduce exposure error in some cases (Sarnat et al., 2013b).

This section includes discussions of surface measurements (including fixed-site and personal monitoring [Section 3.3]), modeling approaches (increasing in complexity from data averaging techniques through microenvironmental models [Section 3.3.2]), and satellite-based methods (Section 3.3.3). Each of these approaches has strengths and limitations, and several new studies discussed in Section 3.3.2.4.3 and Section 3.3.3 blend observations and air quality model results to reduce exposure measurement error. An analysis of the relative strengths and limitations of these methods for application in epidemiologic studies is provided in Section 3.3.5.

ED_002220_00002287-00270

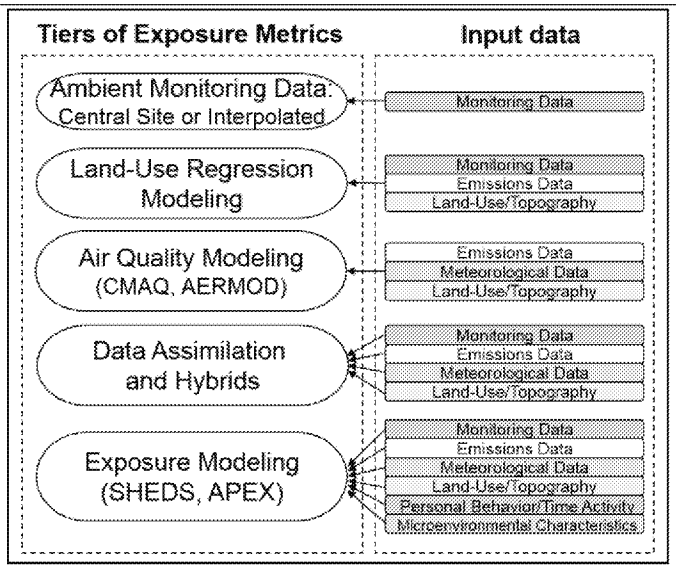

Source: Permission pending, Adapted from Ozkaynak et al. (2013).

Figure 3-1 Tiers of exposure models relevant to epidemiology studies and input data types for each exposure model tier.

3.3.1 Surface Measurement

The 2009 PM ISA (U.S. EPA, 2009b) discussed the use of ambient PM concentration data measured at FRMs and FEMs and used as surrogates for PM exposures, and main points are summarized in Section 2.4. The technology for measuring ambient PM at fixed-site monitors has largely stayed the same. More attention is given in Section 2.4.3 to measuring UFP concentrations. New insights to help interpret $PM_{2.5}$, $PM_{10-2.5}$, and UFP concentration data for use in exposure assessment studies are provided in Section 3.4.1.1.

The 2009 PM ISA (U.S. EPA, 2009b) described developments in using personal monitors for exposure assessment. Specifically, developments in light scattering continuous monitoring instrumentation, passive sampling, cascade impactor sampling for $PM_{10-2.5}$ and $PM_{2.5}$, and use of GPS for estimating time-activity were presented. Since then, new developments have been made in active sampling of $PM_{10-2.5}$, $PM_{2.5}$, and UFP. Important developments include reducing the size and increasing portability and battery life of samplers. These are described in Section 3.3.1.2.

3.3.1.1 Ambient Monitoring

Ambient PM data from FRM or FEM from individual sites continue to be used widely in health studies as a surrogate for PM exposure concentration. (Pope et al., 2009; Zanobetti and Schwartz, 2009) provide a number of reasons for the continued use of fixed-site monitor data as exposure surrogates:

ED_002220_00002287-00271

(1) instrument error is typically small compared to spatiotemporal modeling error, (2) an ambient monitor may provide a comprehensive set of measurements, (3) the need to capture temporal variation is typically greater than the need to capture spatial variation in short-term exposure studies, and (4) ambient monitor data provide a useful reference for comparing population exposure concentration estimates in long-term exposure studies. The ambient monitor approach is the least data intensive approach among all exposure concentration estimation methods because it only requires data from a single monitor to represent exposures to a large area (on the order of 100 km^2).

Differences in sampler design for $PM_{2.5}$, $PM_{10-2.5}$, and UFP influence the quality of exposure concentration data available for epidemiologic studies of each respective size cut. For $PM_{2.5}$ samplers, quality assurance testing has demonstrated that $PM_{2.5}$ concentration measurements are replicable [(U.S. EPA, 2004), Section 2.4.1.1], lending confidence to their frequent application in exposure assessment studies. In contrast, $PM_{10-2.5}$ exposure concentration has been measured in three ways [dichotomous samplers, differencing using concentrations from collocated PM_{10} and $PM_{2.5}$ monitors, and subtracting area-wide (e.g., county-wide) $PM_{2.5}$ concentration from area-wide PM_{10} concentration] with large differences in quality assurance (Section 2.4.2). It is expected that dichotomous samplers would produce the most accurate measure of $PM_{10-2.5}$ concentration for use as an exposure surrogate, because dichotomous samplers are designed for isokinetic flow appropriate for each PM cut point. However, a systematic study comparing all three methods has not yet been performed. Differences in spatial variability of $PM_{2.5}$ and $PM_{10-2.5}$ (Section 2.5) coupled with low-moderate correlation (Section 3.4.3.1) suggest that area-wide differences would provide the least accurate measure of $PM_{10-2.5}$ concentration for use in exposure assessment studies. UFP is usually measured by condensation particle counters (CPC) (Section 2.4.3.1) and at times by inertial impaction (Section 2.4.3.3). Testing of CPCs has shown that CPCs may operate at 95% counting efficiency. However, concentrations measured by UFP samplers are also more susceptible to negative bias due to larger evaporative losses compared with $PM_{2.5}$ or $PM_{10-2.5}$ concentration measurements. Hence, there is generally higher confidence in $PM_{2.5}$ concentration measurements than in $PM_{10-2.5}$ and UFP concentration measurements used as exposure surrogates.

3.3.1.2 Personal Monitoring

Methods for personal PM monitoring were described in the 2009 PM ISA (U.S. EPA, 2009b). At that time, filter-based personal monitors were used most frequently. Developments at the time of the 2009 PM ISA included size selectivity of personal samples using a Personal Cascade Impactor Sampler that can sample down to a cut point of 250 nm (Singh et al., 2003), a mini-cyclone with the capability of sampling down to 210 nm (Hsiao et al., 2009), and a two-stage cascade impactor for $PM_{10-2.5}$ sampling (Case et al., 2008). A passive monitor had also been adapted for $PM_{10-2.5}$ sampling (Ott et al., 2008; Leith et al., 2007) based on a passive sampler developed earlier that can be used for user-defined size fractions including $PM_{2.5}$ (Wagner and Leith, 2001a, b). Light-scattering detection devices for continuous monitoring, such as the Personal DataRam (pDR, Thermo Scientific, Waltham, MA), the DustTrak (TSI,

ED_002220_00002287-00272

Inc., Shoreview, MN), and the SidePak (TSI, Inc., Shoreview, MN) for PM_{10} or $PM_{2.5}$ mass concentration and the P-Trak (TSI, Inc., Shoreview, MN) or personal CPC Model 3007 (TSI, Inc., Shoreview, MN) for UFP count concentration were also described in the 2009 PM ISA. The P-Trak samples between 20 nm and 1 μm, and the CPC samples between 10 nm and 1 μm. However, it is anticipated that the majority of particles are smaller than 100 nm when measuring NC (see Preface). Additionally, the 2009 PM ISA detailed new methodologies used by investigators to enhance personal sampling by incorporating videotape (Sabin et al., 2005) or Global Positioning Systems (GPS) (Westerdahl et al., 2005) into their sampling protocols to estimate personal exposure by using simultaneous measures of exposure concentration and time-activity data. Techniques discussed in the 2009 PM ISA are widely in use, and development of new samplers have largely built upon these techniques. Table 3-1 lists these new techniques with sampling size fraction, speciation, mechanism, and error characteristics.

Table 3-1 New or innovative methods for personal sampling of PM exposure concentrations published since the 2009 PM ISA.

Reference	Active or Passive Sampling	Sampler	Size Fraction	Species	Mechanism	Error Characteristics
Thornburg et al. (2009)	Active	Coarse Particulate Exposure Monitor (CPEM)	$PM_{10-2.5}$, $PM_{2.5}$	NA	Three-stage impactor	$PM_{10-2.5}$: −23% (R^2 = 0.81) $PM_{2.5}$: −3% (R^2 = 0.91) compared with a dichotomous $PM_{10-2.5}$ sampler
Volckens et al. (2016)	Active	Ultrasonic Personal Aerosol Sampler (UPAS)	$PM_{2.5}$	NA	Miniature piezoelectric pump with a cyclone for 2.5 μm size cut plus additional sensors for air flow, sunlight, temperature, pressure, relative humidity, and acceleration	−1.4% compared with a $PM_{2.5}$ FRM
Ryan et al. (2015b)	Active	Personal UFP Sampler (PUFP)	UFP	NA	Water-based CPC plus GPS for location	+16% (R^2 = 0.99)

ED_002220_00002287-00273

Table 3-1 (Continued): New or innovative methods for personal sampling of PM exposure concentrations published since the 2009 PM ISA.

Reference	Active or Passive Sampling	Sampler	Size Fraction	Species	Mechanism	Error Characteristics
Nash and Leith (2010)	Passive	Algorithm to modify output from the Wagner-Leith passive sampler to UFP	UFP	Yes	Model of deposition flux developed the passive sampler's size range	6% compared with SMPS
Cai et al. (2014); Cai et al. (2013)	Active	Modification to the Microaethalometer (AethLabs, Berkeley, CA)	$PM_{2.5}$	BC	Reduced humidity and temperature fluctuations through addition of a diffusion dryer	53 ± 238% difference in 1-min readings between the original and diffusion dryer inlet on 97−100% RH day and 5 ± 33% difference between original and diffusion dryer inlet on 65% RH day. The differences reduce to approximately 1% when data are averaged over an hour.
Hagler et al. (2011);Cheng and Lin (2013)	Active	Algorithm to modify output from the Microaethalometer (AethLabs, Berkeley, CA)	$PM_{2.5}$	BC	Introduced a data cleaning algorithm to reduce erroneous fluctuations in the signal (i.e., noise)	Comparison between 1-min data with optimized noise reduction algorithm was comparable to 5-min data averaged with noise
Sameenoi et al. (2012)	Active	Microfluidic electrochemical sensor to detect oxidative potential of PM	Any	ROS	Incorporated DTT assay into Particle into Liquid Sampler (PILS)	Comparison with traditional DTT assay: $R^2 = 0.98$
Sameenoi et al. (2013)	Active	Microfluidic paper-based analytical device (μPAD) to detect oxidative potential of PM	Any	ROS	Collected $PM_{2.5}$ and PM_{10} on filters, desorbed, then pipetted onto μPAD	Comparison with traditional DTT assay: bias = 10.5%, $R^2 = 0.98$

ED_002220_00002287-00274

Table 3-1 (Continued): New or innovative methods for personal sampling of PM exposure concentrations published since the 2009 PM ISA.

Reference	Active or Passive Sampling	Sampler	Size Fraction	Species	Mechanism	Error Characteristics
Landreman et al. (2008)	Active	Expose rat macrophages to collected aerosol sample to detect oxidative potential of PM	Any	ROS	Collected $PM_{2.5}$ onto filters, desorbed, then pipetted onto a 96-well plate seeded with rat macrophages	Response corresponded to spikes for samples exposed to different numbers of macrophages (not quantitative)

BC = black carbon; DTT = dithiothreitol; ROS = reactive oxygen species.

Prevalent field usage of continuous personal PM monitors using optical techniques necessitates validation of these instruments, since calibration is not possible given that ambient PM does not have replicable optical properties. Wallace et al. (2011) tested the 6 pDR and 14−16 DustTrak (number varied with tests) for $PM_{2.5}$ (with a size-selective inlet), and 14 P-Trak personal samplers for particle number to measure UFP exposure concentrations to establish operational parameters (MDL, bias, precision, drift) for each sampler compared with the median. MDL for the DustTrak and pDR were estimated to be 5 $\mu g/m^3$ and 5.5 $\mu g/m^3$, respectively (not detected for the P-Trak), and relative precision was within 10% for all four monitors. The pDR measurements were 60% higher than collocated personal gravimetric samples from the field tests ($R^2 = 0.7$), and the DustTrak measurements were 164% higher than personal gravimetric measurements ($R^2 = 0.9$). The authors pointed out that the higher readings from the light-scattering instruments relative to the gravimetric measurements are due in part to the lower density of ambient PM relative to the density of the aerosol standard used for laboratory calibration. Another factor Wallace et al. (2011) noted to influence the performance of light-scattering personal PM monitors is relative humidity (RH). High RH results in sorption of water to particles and an increase in volume and mass detected by the instrument. Quintana et al. (2000) found that pDRs produced much higher readings than a gravimetric TEOM instrument when RH was above 85%, but that pDR readings tracked the TEOM readings relatively well at RH values below 60%. Since indoor RH is generally maintained below 60%, the influence of RH is likely to mainly affect outdoor light-scattering measurements, particularly in morning, evening, and overnight hours when RH is highest. Optical personal samplers are subject to errors given the inability to calibrate the monitors for ambient characteristics. The characterization work described above has been done for optical sampling of $PM_{2.5}$, so uncertainties are greater for the $PM_{10-2.5}$ and UFP size fractions. Instrument error and replicability and the factors that affect them must be evaluated for each use in panel studies.

ED_002220_00002287-00275

3.3.2 Modeling

At the time of the 2009 PM ISA (U.S. EPA, 2009b), fine-scale exposure prediction models were still relatively nascent in their development. Methods reviewed include time-weighted microenvironmental models and stochastic exposure models for estimation of PM exposure and dispersion models, LUR, and GIS-based modeling approaches for estimation of PM exposure concentration, and attention was given to the models' limitations in adequately capturing spatial variability of PM concentration, particularly for more variable UFP and $PM_{10-2.5}$. Since the 2009 PM ISA, more approaches to spatial averaging of concentrations used for estimating exposure concentrations (Section 3.3.2.1), and new developments in spatiotemporal interpolation of exposure concentration surfaces (Section 3.3.2.2), LUR (Section 3.3.2.3), and dispersion models (Section 3.3.2.4.2) have appeared in the peer-reviewed literature. Additionally, there has been growing use of chemical transport models (CTMs) in exposure assessment studies (Section 3.3.2.4.1) in recent years. Table 3-2 provides an overview of the modeling approaches discussed in this section.

The models discussed in the following sections are typically validated by the study authors using surface monitoring data, but model validation is not performed consistently across the literature. Table 3-3 lists performance measures that have been utilized in the recent PM exposure modeling literature. Model performance is typically evaluated for bias or error using both absolute and relative (or normalized) metrics.

Table 3-2 Comparison of models used for estimating exposure concentration or exposure.

	Type of Model						
Factors[a]	Data averaging	IDW/ Kriging	LUR/ ST	CTM and Hybrid	Dispersion	Satellite and Hybrid	Microenvironmental
Type of model	C	C	C	C	C	C	E
Distance from source	X	X	X	X	X	X	X
Emission rate			X	X	X	X	X
Terrain or land use			X	X	X	X	X
Dispersion				X	X	X	X
Chemistry				X	X	X	X

ED_002220_00002287-00276

	Type of Model						
Factors[a]	Data averaging	IDW/ Kriging	LUR/ ST	CTM and Hybrid	Dispersion	Satellite and Hybrid	Microenvironmental
Human activity							X
Infiltration							X
Inhalation							X

C = concentration model, CTM = chemical transport model, E = exposure model, IDW = inverse distance weighting, LUR = land use regression, ST = spatiotemporal models.

[a]Factors that may be available in each model are checked.

Table 3-3 Statistical measures used for air quality model performance evaluation.

Performance Measures	Definition[a]
Mean bias (MB)	$\frac{1}{N}\sum_{i=1}^{N}(P_i - O_i)$
Mean error (ME)	$\frac{1}{N}\sum_{i=1}^{N}\lvert P_i - O_i\rvert$
Root mean square error (RMSE)	$\sqrt{\frac{1}{N}\sum_{i=1}^{N}(P_i - O_i)^2}$
Coefficient of determination (R^2)	$\frac{\left\{\sum_{i=1}^{N}(O_i - \overline{O})(P_i - \overline{P})\right\}^2}{\sum_{i=1}^{N}(O_i - \overline{O})^2 \sum_{i=1}^{N}(P_i - \overline{P})^2}$

[a]P_i and O_i are prediction and observation at the ith monitoring site, respectively; N is the number of monitoring sites.

ED_002220_00002287-00277

3.3.2.1 Data Averaging

Averaging measurements from all monitors in a study area is frequently used to mitigate some of the errors associated with using data from a single ambient monitor to estimate exposure concentrations for a population. There are many averaging approaches in use to provide more representative exposure concentration estimates than those derived from a fixed-site ambient monitor. For example, Strickland et al. (2011) compared nearest fixed-site monitor concentrations of $PM_{2.5}$ and $PM_{2.5}$ components (SO_4^{2-}, OC, EC) averaged over 24 hours with concentrations averaged over three monitors (unweighted). They found that $PM_{2.5}$ and $PM_{2.5}$–SO_4^{2-} mass concentrations were within 8% of each other, with strong correlations between the concentration obtained by a fixed-site monitor and with that obtained by a population-weighted average Spearman $R = 0.969$. Reported $PM_{2.5-OC}$ concentrations had a Spearman correlation of $R = 0.847$, but more spatially varying $PM_{2.5-EC}$ had a Spearman correlation of $R = 0.831$. Goldman et al. (2012) had similar findings when comparing nearest monitor with unweighted averaging. Strickland et al. (2013) compared unweighted averages across monitors with concentrations measured at fixed-site monitors and concentrations estimated to be the "true" exposure concentrations at grid cells within the study domain. The fixed-site monitor produced $PM_{2.5}$ concentrations with the largest biases of −31.3%, in comparison with the unweighted average (−9.0%). Biases for $PM_{2.5}$ components (SO_4^{2-}, NO_3^-, NH_4^+, EC, OC) were similar for both the fixed-site monitor and unweighted average. In the unweighted averaging technique studied by Strickland et al. (2013), temporal variability may be dampened, leading to Berkson errors. As described below, more spatial heterogeneity inherent to the exposure concentration field implies greater Berkson errors.

Spatial averaging techniques include area-weighting and population-weighting (Vaidyanathan et al., 2013). Such schemes require some type of spatial modeling of data before averaging. For example, area and population-weighting might involve use of a regression model of PM or PM component concentration and population density, land use, or emission estimates to develop exposure concentration estimates at grid locations. Concentrations for census tracts, zip codes, or counties can then be averaged and weighted by the associated areas or populations. In such schemes, the objective of the spatial modeling is to develop more representative area or population estimates.

Population-weighted averaging is designed to reduce bias in the health effect estimate by giving greater weight to the locations where more people live. As part of the study referenced above, Strickland et al. (2013) compared population-weighted averages across monitors with concentrations measured at fixed-site monitors and concentrations estimated to be the "true" exposure concentrations at grid cells within the study domain. The population-weighted average produced $PM_{2.5}$ concentrations with biases of −8.1% in comparison with the true $PM_{2.5}$ exposure concentrations. Biases for $PM_{2.5}$ components (SO_4^{2-}, NO_3^-, NH_4^+, EC, OC) were similar for both the fixed-site monitor and unweighted average. Strickland et al. (2011) compared nearest fixed-site monitor concentrations of $PM_{2.5}$ and $PM_{2.5}$ components (SO_4^{2-}, OC, EC) averaged over 24 hours with concentrations averaged using population-weighted averages. They found that $PM_{2.5}$ and $PM_{2.5}$–SO_4^{2-} mass concentrations were within 8% of each other, with correlations

ED_002220_00002287-00278

among the three spatial representations ranging from Spearman $R = 0.963–0.995$. Reported $PM_{2.5-OC}$ concentrations had Spearman correlations of $R = 0.891$, but more spatially varying $PM_{2.5-EC}$ had Spearman $R = 0.804$. Goldman et al. (2012) had similar findings when comparing nearest monitor, unweighted, and population-weighted averaging. These results suggest that population-weighted averaging may provide a small improvement over unweighted averaging for estimation of exposure concentration.

Spatial averaging approaches may influence exposure measurement error (Goldman et al., 2010) and associations between short-term $PM_{2.5}$ exposure and health outcomes (Goldman et al., 2012). In the latter study, the authors noted improved population-weighted R^2 values (relative to the fixed-site ambient monitoring method) between exposure concentration metrics estimated using data averaging methods and the simulated "true" ambient concentration field. For example, the R^2 values increased from 0.25 for a fixed-site ambient monitoring method to approximately 0.38 for data averaging methods.

Various methods can be chosen for temporal averaging, such as straight arithmetic averaging or methods that account for site-specific variability and that also account for the lack of some observations during the period. Temporal averaging is used to estimate exposure concentrations over different time intervals. Hourly and daily measures are averaged to provide metrics of interest (e.g., daily, weekly, monthly, seasonal, and annual). Darrow et al. (2011) tested different averaging intervals and found that 1-hour daily max $PM_{2.5}$ concentrations had high correlation with 24-hour average (Spearman $R = 0.82$) and moderate correlations (Spearman $R = 0.75$ and 0.68) with commuting time (7:00–10:00 and 16:00–19:00) and daytime (8:00–19:00) average $PM_{2.5}$ concentrations, respectively. As with the development of spatial averages, the objective of temporal averaging is to minimize error that might be introduced due to missing data from a time-series, so that diurnal, weekly, seasonal, or annual trends can be well characterized.

Spatial and temporal averaging methods provide a mechanism for interpolating where data are missing over space or in a time-series, respectively. The literature shows that averaging techniques produce some bias when compared with true exposure concentrations, but averaging techniques do present an improvement over using data from a single fixed-site monitor.

3.3.2.2 Spatial Interpolation Methods

The single fixed-site ambient monitor and methods that average concentration data across monitoring sites in an area both lead to exposure concentration estimates with no spatial variation. When spatially resolved estimates of PM exposure concentration are desired, a variety of approaches are available for two-dimensional interpolation of observations ranging from smoothing techniques (described here) to statistical modeling techniques involving additional data (Section 3.3.2.4). Various spatial interpolation methods exist that use multiple monitors to provide spatially varying fields. Such

ED_002220_00002287-00279

methods include: inverse distance weighting (IDW), inverse distance squared weighting (ID2W) (Hoek et al., 2002), and kriging (Mercer et al., 2011; Whitworth et al., 2011).

IDW, in which ambient PM concentration at a receptor point is calculated as the weighted average of ambient PM concentration measured at monitoring locations, is a commonly used simple interpolation method [e.g., Tai et al. (2010)]. Several variations of IDW have been used to estimate exposure based on ambient PM concentration surfaces. The weighting factor is an inverse function of distance between the receptor and the monitor. For example, Brauer et al. (2008) and MacIntyre et al. (2011) estimated exposure to ambient $PM_{2.5}$ and other industrial pollutants within 10 km of point sources using an IDW sum of ambient $PM_{2.5}$ concentration and the three closest monitors within 50 km. Often, the weighting factor is the inverse distance raised to some power, and a higher power is applied to increase the weight on monitors that are closer to the receptor. Rivera-González et al. (2015) applied an ID2W model and compared the results with a citywide average, use of the nearest monitor, or kriging for development of an ambient $PM_{2.5}$ concentration surface. The results from IDW were correlated with the other city-wide averaging, nearest monitor, and ordinary kriging (Pearson $R = 0.83–0.99$), and the mean ambient $PM_{2.5}$ concentration estimated with IDW was within 5% of the mean computed with the other methods. Neupane et al. (2010) compared estimates of the ambient $PM_{2.5}$ concentration surface calculated using IDW with a $PM_{2.5}$ concentration surface calculated using both bicubic spline interpolation. Bicubic spline interpolation produced a lower mean ambient $PM_{2.5}$ concentration and larger IQR compared with IDW. Because there is no reference value in these studies, it is difficult to conclude that IDW presents any substantial improvement in prediction accuracy compared with other methods. These findings indicate that the results of IDW are comparable to methods that average concentrations across monitors and to methods that smooth concentration surfaces when estimating $PM_{2.5}$ concentration.

Kriging is a set of well-established methods that use observed covariance for geostatistical interpolation [e.g., Beelen et al. (2009)]. Recent developments have been made to improve kriging techniques. Pang et al. (2010) developed a space-time Bayesian Maximum Entropy (BME) model and compared it with ordinary kriging (OK). OK assumes linearity between data points, and it also assumes that the data are normally distributed. BME is not restricted to linearity or normality and so can draw on different sources of information, such as space-time relationships between variables and probability distributions describing the concentration dataset, to address missing data. Pang et al. (2010) found that estimation errors were 2–4 times larger for OK compared with BME. The ability to apply nonlinear models to address missing data thus provide BME-kriging approaches greater accuracy in modeling $PM_{2.5}$ concentration surfaces.

Berkson-like error in the estimated exposure concentration may arise from smoothing inherent to spatial interpolation models, such as IDW and kriging (see Section 3.2.1 for definition of Berkson-like error). The potential for Berkson-like error may be evaluated by cross-validation across receptor locations distributed over space, and the statistical performance of spatial interpolation methods may vary from study to study. When an interpolation model is fit using a relatively sparsely distributed monitoring

ED_002220_00002287-00280

network, Berkson-like errors in estimated exposure concentration can be substantial (Alexeeff et al., 2015; Whitworth et al., 2011). All of the spatial interpolation approaches will produce spatially smoothed pollutant exposure concentration fields from monitoring data. However, spatial and temporal variabilities not captured by monitors are also not captured by these approaches.

If the quantity of data is small in each given site, or if the quality of the data obtained at the monitors is low, then classical-like error may arise (Szpiro et al., 2011a). If there are few observations, all of the interpolation methods suffer. This includes kriging, which depends on developing a variogram. With few observations at the monitoring locations, there is limited information to determine the functional coefficients used for kriging (e.g., the nugget, sill, and range). Weighting schemes for the interpolation models may amplify these errors (Wong et al., 2004).

3.3.2.3 Land Use Regression and Spatiotemporal Modeling

Direct spatial interpolation of PM exposure concentration and methods that employ static parameters to capture spatial variance can lead to excessive spatial autocorrelation when spatial variability of PM is high (Krewski et al., 2009). $PM_{2.5}$ tends to have less spatial heterogeneity than $PM_{10-2.5}$ or UFP (Section 3.4.2) given secondary production (U.S. EPA, 2009b), but high concentrations can still occur near primary sources. Statistical approaches that utilize data that vary over space and time can address this limitation. Geographic information system (GIS) models are being used to incorporate land use, emissions data, and geographic covariates into PM exposure concentration estimates. Two types of models are covered in this section, LUR and spatiotemporal models. LUR models regress observed PM concentrations on land use (and sometimes additional geographic) covariates and then use the model to predict exposure concentrations where PM is not measured (Hoek et al., 2008a; Ryan and Lemasters, 2007). Spatiotemporal models tend to incorporate kriging or autocorrelation into the response variable, which is then fit to the land use and geographic covariates [e.g., Sampson et al. (2013)].

3.3.2.3.1 Land Use Regression

LUR is an empirical approach to estimate exposure concentrations, often at very high resolution in more densely populated locations, by relating observed concentrations to the detailed information on land use. The basic approach is to develop an equation, via regression, relating observed pollutant concentrations (Hoek et al., 2008a; Ryan and Lemasters, 2007) to land use characteristics and other inputs:

$$Y(s_i, t_j) = \beta_0(s_i, t_j) + \sum_k \beta_{1,k}(s_i, t_j) X_k(s_i, t_j) + \epsilon(s_i, t_j)$$

Equation 3-8

ED_002220_00002287-00281

Here, $Y(s_i,t_j)$ is the observed concentration at location (monitor) s_i (where i is a monitor location) and time t_j, β_0 and $\beta_{1,k}$ are the regression coefficients (intercept and slopes that are potentially spatially and temporally varying, but may also be constant in time and space), X are the independent variables (e.g., land use or meteorological parameters that may vary in time and/or space), k is the index indicating type of land use, and ϵ is the residual error term. β_0 is also called the additive bias and $\beta_{1,k}$ the multiplicative bias. Other forms of LUR models are also used. While the regression equation often is linear in the independent variables (as shown above), it can include nonlinear and mixed terms, particularly if there is specific knowledge of the relationship between a concentration and a variable that would suggest a specific functional form. The resulting regression equation can then be used to predict exposure concentrations at other times (t) and locations (s) where observations are not available.

Recent studies demonstrate typical LUR model performance, performance evaluation, and variability between cities. Eeftens et al. (2012) evaluated the application of LUR models in 20 cities in Europe for $PM_{2.5}$, PM_{10}, $PM_{2.5}$ absorbance, and $PM_{10-2.5}$. First, the models for the various cities had substantially different independent variables used in the final models, as well as coefficients associated with similar independent variables, demonstrating the location-specific nature of the models. Second, the in-sample R^2 of the various city models varied between 35 and 89% for $PM_{2.5}$ and between 32 and 81% for $PM_{10-2.5}$. Evaluation using a leave one out cross-validation (LOOCV) produced R^2 levels of 21 to 79% for $PM_{2.5}$ and 3 to 73% for $PM_{10-2.5}$. R^2 was not consistent between each city. Wang et al. (2014) expanded on the same model for $PM_{2.5}$ in thirty-six European cities. They found a LOOCV R^2 of 81% (RMSE = 2.38 $\mu g/m^3$) for cities where the model was fit. However, Wang et al. (2014) tested transferability of the model to areas where the model was not fit, and R^2 dropped to 42% (RMSE = 1.14 $\mu g/m^3$). Estimation of $PM_{10-2.5}$ in the LUR can be accomplished using the difference between the PM_{10} and $PM_{2.5}$ LUR models, since each model was trained using PM_{10} and $PM_{2.5}$ concentration data. However, low LOOCV R^2 for $PM_{10-2.5}$ in select cities may have been related to how measured $PM_{10-2.5}$ concentration was calculated for the validation dataset. If reference $PM_{10-2.5}$ concentration was calculated by the difference of two collocated monitors rather than by a dichotomous sampler, flow rate differences could cause some error in the reported $PM_{10-2.5}$ concentrations. If $PM_{10-2.5}$ was calculated by the difference between concentrations measured by PM_{10} and $PM_{2.5}$ monitors that were not collocated, then errors would likely be larger.

Several features of LUR have the potential to limit the accuracy of modeled exposure concentrations. Beckerman et al. (2013a) noted that two major limitations with LUR are variable selection and how to best deal with unbalanced repeated measures, potentially involving arbitrary decisions in the model building process. They used a generalized linear model with a deletion/substitution/addition machine learning algorithm to model $PM_{2.5}$, resulting in an out-of-sample R^2 of 0.65 based on fivefold cross-validation (n-fold cross-validation means that 1/n of the data are reserved for validation with the rest used for model training, and the process is repeated n times). The ability of an LUR method to relate air pollutant concentrations to specific land uses, and thus estimate high resolution exposure concentration fields, is directly dependent on having sufficient numbers of observations in time and/or space to develop

ED_002220_00002287-00282

the regression equation with reasonable uncertainties in each of the coefficients (Wang et al., 2014). The sparseness of the routine monitoring networks may incur Berkson-like error in the exposure estimates. More intensive studies may be conducted where additional monitoring data are available (sometimes called saturation monitoring if the additional monitors lead to extensive spatial coverage). Saturation sampling can also lead to introduction of classical-like error in the exposure predictions if different measurement methods are used and differences in the methods are not fully understood (Vedal et al., 2013; Levy et al., 2010).

A related weakness of LUR is its limited generalizability when the monitor and study participant locations are different. The developed regression equations are usually restricted to the study region (typically city-scale) alone and may not be directly applied to another region, due largely to the empirical nature of LUR (Wu et al., 2011; Jerrett et al., 2005a). Local PM data are required to calibrate LUR models, and measurements must be available that estimate the spatial patterns of exposure concentrations. For example, Patton et al. (2015) found during estimation of UFP exposure concentrations in Boston urban neighborhoods that models fit to one neighborhood did not necessarily provide robust estimates of particle NC for another neighborhood, and acceptable model performance required calibration with local data. Hoek et al. (2008a) also reviewed the performance of the LUR model regarding their application for $PM_{2.5}$ given differences between where the model was fit and where it was used for predictions. R^2 values for the developed LUR models for $PM_{2.5}$ ranges from 0.17 to 0.69, with substantially lower out-of-sample R^2 in evaluation (0.09−0.47, with fewer studies performed evaluation/cross-validation). This suggests that comparing performance statistics between cities, even when using one method (in this case, LUR) can yield very different performance and that using cross-validation reduces performance, but to a degree that is not predicable from the full model R^2. This work was extended by Wang et al. (2015) to show the association between the LOOCV R^2 and a health outcome (forced vital capacity: FVC). For models of $PM_{2.5}$, Wang et al. (2015) note that cross-holdout validation, where the model is rebuilt after removing data from a site and retraining the model using the same variables, may be more appropriate than traditional LOOCV for assessing LUR performance, particularly when there are a small number of training sites, because it makes use of all data in the model evaluation process instead of leaving out a portion of the data. In summary, LUR models can have relatively good validation ($0.4 < R^2 < 0.7$), even for spatially variable $PM_{10-2.5}$, but good validation will only occur when the model is used to predict concentrations in the same geographic area where it was fit.

Although LUR models have been used to estimate long-term (e.g., annual) average PM exposure concentrations within large metropolitan areas by using variables such as road type, traffic count, land cover, and topography (Gulliver et al., 2011; Hoek et al., 2008a) and can be applied to current or historical conditions (Hystad et al., 2013), LUR has been used less frequently for time-series exposure studies. Land use variables (e.g., elevation, road-type, distance to road, land cover) usually do not vary in time. Temporal variation in the model is gained by including both the available observations and other temporally-varying inputs, such as meteorological parameters. As part of the New York City Community Air Survey (NYCCAS) in which $PM_{2.5}$ samples were collected from 150 sites across the five boroughs of

ED_002220_00002287-00283

New York City, Ross et al. (2013) built a LUR for application in a birth defects exposure study and developed a temporal adjustment procedure to increase the temporal resolution of $PM_{2.5}$ exposure concentration estimates to 2 weeks. This was accomplished by multiplying an LUR derived for one year by the ratio of 2-week averages to annual averages. Validation of the method using data from a second year of measurements produced out-of-sample R^2 of 0.83 ($R^2 = 0.88$ if two outliers were removed from the dataset). Dons et al. (2013) aimed to fit a LUR model of black carbon (BC) concentration to hourly data for a time-activity exposure study. However, they observed that many variables became insignificant when inputting hourly data into an annual model. Dons et al. (2013) instead built a LUR for hourly data using static and dynamic variables in different models. They found that LOOCV R^2 varied from 0.13 to 0.78. Higher R^2 but also higher RMSE were observed during the late morning to evening hours for the model with dynamic variables. These studies demonstrate that LUR can be extended to study temporal variability of $PM_{2.5}$ and BC, but caution must be used for application in time-series studies since model accuracy is sometimes low.

Recently, LUR has been applied to predict spatial distribution of $PM_{2.5}$ components. As part of the NYCCAS study, Ito et al. (2016) speciated the collected $PM_{2.5}$ samples and built a LUR model to predict $PM_{2.5}$ components concentrations across New York City. The temporal adjustment described above from Ross et al. (2013) was applied in the Ito et al. (2016) study, as well. LOOCV was used to test the models, and models for $PM_{2.5}$ mass and several components (Ca, Ni, V, and Zn) produced $R^2 > 0.8$. Several other components produced R^2 in the range of 0.6–0.7 (Cu, Fe, K, S, and Si), and others produced $R^2 \leq 0.5$ (Al, Br, Mn, Pb, and Ti). Spatial coefficient of variation (CV) was calculated for each component model, and high spatial variability did not always correspond to low LOOCV. For example, Ni had a spatial CV of 0.70 and LOOCV R^2 of 0.85, while Mn had a spatial CV of 0.68 and LOOCV R^2 of 0.36. The LUR models were then applied to a source attribution analysis in which 50–1,000 m buffers were placed around sources, and then annual average concentrations for each component modeled by the LUR were compared to the sources within those buffers.

In summary, new developments for LUR include adaptation of LUR models for short time resolutions and for spatially variable size fractions (UFP, $PM_{10-2.5}$) of PM and $PM_{2.5}$ components (e.g., Ca, Cu, Fe, K, Ni, S, Si, V, Zn). At the same time, several studies have improved characterization of errors and uncertainties in LUR modeling and how best to quality assure those models. Several studies drew attention to poor validations produced when LUR models were fit to one geographic area and then applied to another. Similarly, lack of spatial correlation between predicted concentrations at the model receptors and actual exposure concentrations of study participants can lead to Berkson-like error, and incompatibility of methods to model and measure PM can lead to classical-like errors (see error type definitions in Section 3.2.1).

ED_002220_00002287-00284

3.3.2.3.2 Spatiotemporal Modeling

A GIS-based spatiotemporal model provides a useful tool for large-scale spatiotemporal analysis. GIS-based mapping such as kriging utilizes the covariogram for statistical smoothing but may lead to invalid spatial features due to insufficient data for characterizing spatial variation. Generalized additive models that describe regional and small-scale spatial and temporal (monthly) gradients (and corresponding uncertainties) were developed for $PM_{10-2.5}$ and $PM_{2.5}$ over the U.S. for 1998−2007 for use in health studies (Yanosky et al., 2014). Model validation was higher for $PM_{2.5}$ (out-of-sample $R^2 = 0.77$, normalized mean bias factor, NMBF = −1.6%) compared with $PM_{10-2.5}$ (out-of-sample $R^2 = 0.52$, NMBF = −3.2%). Bias increased and precision decreased for $PM_{10-2.5}$ compared with $PM_{2.5}$. Spatial covariates, including elevation, urbanized land use within 1 km, county-level population density, distance to roadways of moderate to heavy traffic, and point-source emissions density were all determined by the authors to be important predictors of $PM_{2.5}$, although the authors did not present data for the relative contribution of each variable to the model. Yanosky et al. (2009) developed spatially and temporally resolved concentration fields of $PM_{2.5}$ and $PM_{10-2.5}$ to be used as exposure concentration estimates in long-term exposure studies for the northeastern and Midwestern U.S. Out-of-sample R^2 for the $PM_{2.5}$ model was 0.77 with precision of 2.2 $\mu g/m^3$ for 1999 to 2002, compared with out-of-sample R^2 for the $PM_{10-2.5}$ model of 0.39 with precision of 5.5 $\mu g/m^3$. The IDW method was applied as an alternative to compare with a semiempirical model. For a $PM_{2.5}$ concentration field developed for 1999 to 2002, cross-validation results for IDW show reasonable performance with out-of-sample $R^2 = 0.60$ (and cross-validation results for IDW were not available for $PM_{10-2.5}$).

Recent studies have attempted to estimate spatially resolved $PM_{2.5}$ exposure across larger regions of the U.S. for application in epidemiologic studies. For example, Sampson et al. (2013) developed a model combining universal kriging that builds from regional partial least squares regression LUR models with categorical variables describing land use, population, emissions, vegetative index, roadway type, impervious surfaces, and proximity to features. Results of cross-validation with 10-fold cross-validation produced out-of-sample $R^2 = 0.52−0.63$ at the national scale and $R^2 = 0.84−0.88$ at the regional scale. Keller et al. (2015) applied this model to $PM_{2.5}$ and BC prediction in the six MESA Air cities (Baltimore, MD, Chicago, IL, Los Angeles, CA, New York City, NY, St. Paul, MN, and Winston-Salem, NC) and obtained out-of-sample R^2 of 0.82−0.91 for $PM_{2.5}$ and 0.79−0.99 for BC (using both AQS and MESA Air monitors for cross-validation). Bergen et al. (2013) applied a similar method for four $PM_{2.5}$ components: EC, OC, silicon, and sulfur, and the out-of-sample R^2 ranges from 0.62 to 0.95. Kim et al. (2015) examined $PM_{2.5}$ component networks for suitability of the data inputs for applying spatiotemporal models for PM component exposure concentrations, and they found that the Chemical Speciation Network (CSN) and Interagency Monitoring of Protected Visual Environments (IMPROVE) networks were too sparse to fit the model. They found that the greater density of the National Particle Component Toxicity (NPACT) study network, set up outside study participants' homes, would be needed to fit the model. Additionally, differences among the three networks with respect to averaging times, quality assurance, and pump flow rates, complicates the ability to combine networks into one database for fitting the model.

ED_002220_00002287-00285

Recent developments in spatiotemporal modeling have enabled modeling of larger geographic regions and to overcome some of the limitations of kriging. In some cases, these models have been fit with good accuracy and precision. However, differences in model calibration in different regions introduce model errors, and sparse networks have been found insufficient for model fitting.

3.3.2.4 Mechanistic Models

Improvements in computational resources have led to mechanistic models (see Section 2.4.7 for a description) that are more amenable to exposure assessment studies, because they provide finer spatial resolution over larger domains and can include more components, more sources, and longer time periods compared with previous versions of CTMs (Garcia-Menendez et al., 2015; Ivey et al., 2015; Li et al., 2015; Turner et al., 2015; Hu et al., 2014d; Burr and Zhang, 2011; Civerolo et al., 2010; Wagstrom et al., 2008). Such models computationally solve the atmospheric-diffusion-reaction equations that describe the transport and physical and chemical transformations of pollutants (Seinfeld and Pandis, 2006). Turbulent diffusion is typically treated by using atmospheric dispersion coefficients or diffusivities. Mechanistic models may be used to characterize exposure concentrations where monitoring data are limited or not available.

3.3.2.4.1 Chemical Transport Model Applications for Exposure Concentration Estimation

CTMs commonly utilized for exposure concentration modeling in the U.S. include the Community Multiscale Air Quality (CMAQ) model, Particulate Matter-Comprehensive Air Quality Model with Extensions (PM-CAMx), and the University of California at Davis/California Institute of Technology (UCD/CIT) CTM (Gaydos et al., 2007; Byun and Schere, 2006; Kleeman and Cass, 2001; Russell et al., 1988) at the urban-to-regional scales and global models such as the Goddard Earth Observing System CTM (GEOS-Chem) and Comprehensive Air Quality Chemistry Model (CAM-Chem) (Garcia-Menendez et al., 2015; Bey et al., 2001). The European Air Pollution Dispersion and Chemistry Transport Model (EURAD-CTM) has been used in Europe for PM and related exposure concentration modeling (Weinmayr et al., 2015; Nonnemacher et al., 2014), and GEM-MACH is being used in Canada (Peng et al., 2017). More specialized models may also be used to model specific sources, such as forest fires (Rappold et al., 2014).

CTMs are typically applied over grid sizes of 1 km or more, depending upon the application (while grid resolutions of less than 10 km are used over urban areas, continental scale applications typically are done at about 10−40 km, and global scale applications with larger grids yet). Nested grids are used to achieve a range of resolutions in many applications (Isakov et al., 2007; Byun and Schere, 2006; Zhang et al., 2004). In some applications, CTMs are coupled directly (i.e., on-line) to a meteorological model to provide meteorological fields, commonly WRF and CMAQ (Mathur et al.,

ED_002220_00002287-00286

2010). Inputs include meteorological parameters (e.g., wind speed and direction, temperature, relative humidity, etc.) throughout the vertical layers of the atmosphere up to and including portions of the stratosphere and source emissions. The model outputs are the pollutant concentrations, and how they vary in space and/or time (Figure 3-1). The resulting fields are then used for epidemiologic studies and other studies of air quality. The ambient concentration fields are also used as inputs to microenvironmental models for estimating exposure (Baxter et al., 2013; Jones et al., 2013; Georgopoulos et al., 2005; Burke et al., 2002).

CTM models have been used for estimation of exposure concentrations, including for use in epidemiologic studies, both in North America and abroad (Ostro et al., 2015; Weinmayr et al., 2015; Anenberg et al., 2014; Marshall et al., 2014; Nonnemacher et al., 2014; Silva et al., 2013; West et al., 2013; Lim et al., 2012; Tagaris et al., 2010). For studies covering a large geographic area, CTM models can provide location-specific estimates without gaps in coverage. Issues with using CTM models relevant for exposure assessment studies are discussed below. Hu et al. (2015) used the UCD/CIT model to develop a 9-year set of simulated pollutant concentration fields, which were then used by Ostro et al. (2015) to assess the associations of $PM_{2.5}$ and UFP with health in a cohort epidemiologic study. When evaluating the model against monitoring data, they observed low error for $PM_{2.5}$ mass compared with error for individual components, such as SO_4^{2-}. In general, errors were higher when matching observations and simulated values on a daily basis compared with monthly and annual averaging periods, suggesting that model results are more accurate over longer averaging times. They did not report RMSEs or R^2. They noted one advantage of using model results over ambient monitoring was the availability of PM component concentrations every day, versus one out of three. Hou et al. (2015) extended the application of CMAQ to the study of human health effects by using the emissions input data to calculate the sensitivity of $PM_{2.5}$ concentrations to EGU and non-EGU emissions from four regions of the U.S. The sensitivities were then used to estimate changes in mortality as a function of $PM_{2.5}$ exposure concentrations and sensitivity of mortality to regional EGU and non-EGU emissions. Bravo et al. (2012) simulated $PM_{2.5}$ over the eastern U.S. using a 12 km× 12 km grid with a normalized mean bias of 2.1% over the course of a year. However, $PM_{2.5}$ concentrations were underestimated by up to 27% in summer and by up to 32% in late fall. In a related study, Mannshardt et al. (2013) compared results using observations and CMAQ-estimated exposure concentration fields in a study of $PM_{2.5}$ and O_3 associations on emergency hospital emissions in three counties of New York City for 2002–2006. CMAQ was run for the eastern U.S. using 12 km grids and used as input to a human exposure model, SHEDS-PM.

Results from CTMs can be biased and subject to various errors due to inputs and model parameterizations, but factors leading to simulation errors continue to be identified and reduced [e.g., Yu et al. (2014); Barsanti et al. (2013); Baek et al. (2011); Foley et al. (2010)]. For example, PM chemistry modules in CMAQ have been added and revised to address limitations in modeling secondary organic PM formation and nitrate chemistry. Nonetheless, biases and errors persist that may have weekly and seasonal trends due to limitations in emission inventory specifications and chemical and meteorological inputs, respectively. Nolte et al. (2015) compared MOUDI measurements of PM size distribution with

ED_002220_00002287-00287

predictions of size distribution (ranging from 0.05 to 20 μm) for several PM components (SO_4^{2-}, NO_3^-, NH_4^+, Na^+, Cl^-, Mg_2^+, Ca_2^+, K^+) at different sites. Nolte et al. (2015) observed discrepancies between the modeled and monitored size distributions where the emissions data were not accurate. Typically, where data were omitted from the NEI, modeled size fractions were negatively biased so that exposure concentrations would be underestimated for those size fractions. Differential bias may also be observed across regions in space. Many such biases can be corrected for using adjustment factors based on comparisons of simulation results with observational data.

The dearth of ambient UFP observations, given that necessary instrumentation is not standard to routine monitoring networks (Section 2.4.5), has limited development and validation of CTMs at this size fraction. UFPs are derived from both direct emissions as well as atmospheric nucleation, and they coagulate on shorter time scales than larger particles (Section 2.3.4). Their concentrations can vary rapidly, and there is an observed steep spatial gradient in NC near sources, e.g., within a few hundred meters of highways (Karner et al., 2010; Zhou and Levy, 2007), suggesting finer resolution modeling should be used when using models to estimate exposure fields for UFPs. The lack of emissions information on UFPs also complicates CTM development. Hu et al. (2014a) and Hu et al. (2014b) developed source-based CTMs to predict $PM_{0.1}$ mass concentration surfaces for estimation of exposure concentrations that were used in an epidemiologic study by Ostro et al. (2015). The model included emissions, advection, diffusion, wet deposition, and dry deposition, but it omitted gas-to-particle phase chemistry, gas-to-particle phase conversion, nucleation, and coagulation. Hu et al. (2014b) used a 4 km × 4 km grid, which creates uncertainties because it is larger than the spatial scale over which UFPs evolve. They noted the need for either fine grid resolution or a subgrid scale model such as large eddy simulation to capture finer-scale dynamics. Hu et al. (2014b) reported Pearson $R = 0.92$ for comparison of $PM_{0.1}$ mass concentration predictions with measurements and Pearson $R = 0.94$ for comparison of $PM_{0.1}$ EC mass concentration predictions with measurements. Bias was not reported, but the authors noted that model performance degrades for $PM_{0.1}$ mass concentration >4 μg/m^3 or <1 μg/m^3 and for $PM_{0.1}$ EC mass concentration >1 μg/m^3 or <0.2 μg/m^3. Using SEARCH data to evaluate CMAQ performance for application in epidemiologic studies, Park et al. (2006) found that CMAQ did not capture UFP dynamics well, finding biases of an order of magnitude and more in NC. Elleman and Covert (2010, 2009a), and Elleman and Covert (2009b) also found that CMAQ did not accurately predict UFP numbers. They linked the biases to the treatment of particle nucleation, emissions estimates, and how the size distribution is captured. Stanier et al. (2014) developed a nonlinear, Lagrangian trajectory model designed to capture the size distribution of UFPs, and applied it to simulate UFPs in the Los Angeles area for a period when more detailed observations existed. They were able to reproduce NC within a factor of two 94% of the time at the four sites being used in the evaluation. In a comparison of 12 different nucleation parameterizations, Zhang et al. (2010a) found that the predicted NC of Aitken mode particles can vary by three orders of magnitude. These recent efforts illustrate that the large uncertainties in UFPs are still a great limitation in applying CTMs to model UFP exposure concentration.

ED_002220_00002287-00288

Several new developments in CTM have made the technology more amenable for application in exposure assessment, such as improvements to the model through bias correction methods. However, several limitations still exist, including large grid sizes, uncertainties regarding emissions inputs, and uncertainties in modeling UFP. Specific modeling decisions must therefore be evaluated when CTMs are employed in epidemiologic studies.

3.3.2.4.2 Dispersion Modeling Applications for Exposure Concentration Estimation

Dispersion modeling has been performed to develop relatively fine resolution PM exposure concentration fields (Jerrett et al., 2005a). Dispersion models describe the relationship between emissions, meteorology and the resulting pollutant concentrations using algebraic relationships (e.g., the Gaussian Plume Equation), but they typically have limited ability to model chemistry (if any) (Holmes and Morawska, 2006). Examples of dispersion models include AERMOD, Research LINE-Source Model (or R-LINE), Community LINE-source Model (C-LINE), and California LINE Source Dispersion Model (CALINE) (Barzyk et al., 2015; Snyder et al., 2013; Cimorelli et al., 2005; Perry et al., 2005; Benson, 1992).

Model intercomparison has more recently focused on near-road dispersion modeling. Heist et al. (2013) conducted an intermodel comparison of AERMOD, CALINE, ADMS, and R-LINE for tracer (SF6) dispersion and found that the more recently developed ADMS and R-LINE exhibited lower error and better validation compared with CALINE and AERMOD. The models were each compared with results from a tracer study in Idaho Falls, ID (for open field and constructed barrier conditions) under different convective mixing conditions and near Highway 99 in Sacramento, CA and showed that ADMS, R-LINE, and both versions of AERMOD performed better than the CALINE models for both sites (Table 3-4). ADMS and R-LINE were further compared for near-neutral, weakly stable, convective, and moderately-to-strongly stable convective mixing conditions. At low concentrations (<1 pbb), both models exhibited a tendency for positive bias except for the moderately-to-strongly stable conditions, where both models exhibited some negative bias with more scatter. Chen et al. (2009) tested the performance of three dispersion models, CALINE4, CAL3QHC and AERMOD, at Sacramento, CA and London, U.K. regarding their application in modeling near road $PM_{2.5}$ concentrations. All three models produced R^2 values ranges from 0.85 to 0.90 comparing with measurement data (without adding background concentrations) in Sacramento, CA. However, the models perform less well at London, U.K. with R^2 value at around 0.03 without background concentrations due to the influence of street canyons on receptor performance.

Dispersion models are typically applied over smaller domains (near-source to urban) than CTMs (urban to global). For example, AERMOD is designed for simulating "near source" dispersion from point and area sources, and is most useful for assessing source impacts within 20 km of the source (Silverman et al., 2007), although it has been evaluated for distances up to 50 km for certain applications (Perry et al.,

ED_002220_00002287-00289

2005). R-LINE is used for line source modeling, and was originally evaluated by Snyder et al. (2013) for distances of 200 m, though applications have applied it to urban scale (Batterman et al., 2014). While AERMOD is designed to simulate point and area/volume sources, it has been used to estimate the impacts of road networks by approximating road segments as area or volume sources (Isakov et al., 2014; Chen et al., 2009). Rowangould (2015) proposed a new dispersion modeling method for urban environments by breaking the city into coarse and fine grid cells (depending on the roadway density) and modeling dispersion from roadway sources in each roster in parallel. No validation was presented in the Rowangould (2015) paper.

Table 3-4 Comparison of dispersion models with data from a tracer study in Idaho Falls, ID and a near road study in Sacramento, CA and an UFP study in Somerville, MA and Chinatown in Boston, MA.

	Idaho Falls, ID		Sacramento, CA		Somerville, MA		Boston, MA	
Model	NMSE	*R*	NMSE	*R*	NMSE	R^2	NMSE	R^2
CALINE3	NR	NR	2.26	0.29	NR	NR	NR	NR
CALINE4	1.94	0.76	0.86	0.47	0.06	0.54	0.02	0.78
AERMOD-V	1.26	0.84	0.28	0.77	0.11	0.57	0.02	0.81
AERMOD-A	1.25	0.82	0.31	0.72	NR	NR	NR	NR
ADMS	1.14	0.88	0.20	0.78	NR	NR	NR	NR
R-LINE	0.96	0.85	0.34	0.75	0.13	0.58	0.02	0.81

NMSE = normalized mean squared error; NR = not reported, *R* = correlation (not specified if Pearson or Spearman); R^2 = coefficient of determination.

Sources: Data reproduced with permission of Heist et al. (2013); data reprinted with permission from Patton, AP, Milando, C, Durant, JL, Kumar, P. Assessing the suitability of multiple dispersion and land use regression models for urban traffic-related ultrafine particles. Environ Sci Technol. 2017;51:384-392. Copyright (2017) American Chemical Society. (Patton et al., 2017).

Several studies have used dispersion models at urban or neighborhood scales to estimate exposure concentrations. For example, Isakov et al. (2014) applied both AERMOD and R-LINE in Detroit, MI to estimate exposure concentrations to $PM_{2.5}$, EC, OC and pollutant gases at homes and schools of children with asthma participating in the Near Road Exposure of Urban Air Pollutants Study (NEXUS). CMAQ and kriging of observations were used to define regional air pollutant levels. Comparison between model results and measurement show reasonable performance with Pearson *R* range from 0.78 to 0.94 (daily average $PM_{2.5}$ concentrations) at different monitor sites. Simulated concentrations of PM are often used in conjunction with other estimates of regional PM because dispersion models are the more limited in spatial extent and so not designed for PM transport over large distances. For example, in an Atlanta application

ED_002220_00002287-00290

(Dionisio et al., 2013; Sarnat et al., 2013b), a variety of approaches were used to estimate exposure concentrations. One approach used AERMOD to model impacts of traffic emissions and added the resulting concentrations to background concentrations (developed from observations) to construct a high-resolution PM field for use in an epidemiologic study. Sarnat et al. (2013b) used the fine-scale resolution to help identify potential health disparities linked to socioeconomic status that were not apparent when using a single fixed-site monitor. Maroko (2012) used AERMOD to simulate $PM_{2.5}$ impacts from point sources in the New York City area to assess environmental justice issues. Dispersion models can also be used to simulate components of PM, assuming that they do not undergo a chemical reaction in the atmosphere. For example, Colledge et al. (2015) used AERMOD to estimate particulate manganese exposure in two Ohio towns.

A recent development in dispersion modeling is the inclusion of UFP when modeling PM dispersion in the vicinity of a road. Patton et al. (2017) evaluated CALINE4, R-LINE, and AERMOD for UFP transport near roads in the greater Boston, MA area (Somerville, MA and Chinatown, within Boston). They found similar performance among all three models (Table 3-4). Stanier et al. (2014) recognized that it is challenging to model UFP emitted from mobile sources, because the UFP size distribution rapidly evolves upon emission from vehicle tailpipes. They fit emissions factors based on existing data for cruising and acceleration of heavy-duty and light-duty vehicles, estimating across a size distribution down to 7 nm and correcting for coagulation and deposition. The emissions factors were incorporated into a dispersion term in the model. Modeled particle NC was compared with measured concentration at two sites within the Los Angeles, CA metropolitan area and showed underestimation of the model (below a factor of 1:2) at one location and modeled data within a factor of two at the other site. Stanier et al. (2014) propose that the model is suitable for estimating spatially resolved UFP exposure concentrations on a daily basis.

Dispersion modeling continues to be used in exposure assessment studies, often in conjunction with CTMs to provide fine-scale spatial resolution. Recent improvements have been made in modeling dispersion of traffic-related air pollution and applying dispersion models at urban scales. However, dispersion models are still limited when applied in dense urban environments since dispersion models are not designed to deal with complex built topography (Kakosimos et al., 2010), and they are limited in their ability to represent UFP transport because they are not designed to capture size-specific UFP dynamics (Stanier et al., 2014).

3.3.2.4.3 Hybrid Approaches

Although spatiotemporal and LUR models have been applied to estimate long-term (e.g., monthly and annual) spatially-resolved ambient PM exposure concentrations, these techniques are typically not as successful for short-term (e.g., hourly and daily) applications as they do not include the impacts of changing source emissions and meteorology. PM data from ambient monitors provide accurate information on temporal trends at monitoring sites but little information on spatial patterns.

ED_002220_00002287-00291

Emissions-based models provide spatial information consistent with emissions, chemistry, and meteorology but subject to limitations in the accuracy of these inputs as well as in the ability of models to simulate air pollution physical and chemical processes. "Hybrid" approaches that combine observational data with emissions-based model results are being developed and used to provide better estimates of single component and mixtures along with estimates of the associated uncertainties. These approaches range from rescaling model results to correction for known biases to combining observational and simulation data and optimizing spatiotemporal exposure concentration estimates.

Fusion of Model Outputs for Exposure Concentration Estimation

As noted above, CTMs by themselves typically have spatial resolution of 4 km or greater due to computational limitations, but they provide regional variations in PM (and PM component levels) and capture the formation of secondary PM, while dispersion models provide near-source impacts with a finer resolution. Given these complementary characteristics, it is natural to couple them (though care must be taken to not double count emissions) (Isakov et al., 2009).

Several recent studies have merged CMAQ with dispersion models. For example, Beevers et al. (2013) combined CMAQ results with the ADMS (a dispersion model) in London, England. They found that the combination could capture the spatial and temporal variations in air quality, with a mean bias of 0.6 $\mu g/m^3$ when comparing the model to monitors at five sites. Similarly, Zhai et al. (2016) combined R-LINE results with CMAQ-data fusion fields to estimate $PM_{2.5}$ exposure concentration fields for Atlanta, GA for a birth cohort study, with Pearson $R^2 = 0.72$ between the model and monitoring data with LOOCV normalized RMSE = 0.50 and normalized mean bias of 12%. A combined AERMOD-CMAQ application to New Haven, CT, was conducted (Lobdell et al., 2011; Isakov et al., 2009) to develop local scale (census block level) PM exposure concentrations in a base year (2001) and future years (2010, 2020 and 2030 to assess pollutant control programs). They noted the uncertainties due to model inputs, with coefficients of variation (standard deviation of concentration/mean concentration) ranging from 10−70% within different census tracts, but no estimates of model uncertainty with respect to $PM_{2.5}$ were provided. They linked their results to the HAPEM (Ozkaynak et al., 2008) and SHEDS (Isakov et al., 2009) exposure models, as described further in Section 3.3.4.

Another method of addressing the low spatial resolution of a CTM is to combine the model results with dispersion model results and LUR modeling output for exposure concentration. Wang et al. (2016) combined CTM with LUR using a hierarchical spatiotemporal modeling technique in which the 2-week average LUR-derived $PM_{2.5}$ concentration is modeled as a function of spatiotemporal trends and spatiotemporal residual terms, where the trend terms can be decomposed into an average and a spatially-varying trend (Keller et al., 2015). Wang et al. (2016) incorporated the CTM predictions into the spatially-varying trend term. The advantage of combining these two models is that the CTM is a mechanistic model employing principles of transport, dispersion, and atmospheric chemistry with finer temporal resolution (daily for this study), while the LUR offers fine-scale spatial resolution. The LUR

ED_002220_00002287-00292

was fit to fixed-site $PM_{2.5}$ monitoring data in AQS and from the MESA Air study and incorporated a variable for long-term average concentration derived from the CAL3QHCR near-road line source dispersion model. Wang et al. (2016) found that addition of the CTM to the spatiotemporal model of Keller et al. (2015) only produced a marginal improvement in the prediction ability of the model for capturing $PM_{2.5}$ exposure concentrations. Di et al. (2016b) combined GEOS-Chem simulations, based on a 28 km × 25 km grid, with land use and meteorological variables to improve resolution to 1 km × 1 km across the northeastern U.S. Di et al. (2016b) compared the model results with monitoring data when the GEOS-Chem model was used alone and when it was combined with land use and meteorological variables. Out-of-sample R^2 for $PM_{2.5}$ improved from 0.47 for GEOS-Chem alone to 0.85 for the hybrid model. Out-of-sample R^2 ranged from 0.13–0.33 for $PM_{2.5}$ components (EC, OC, NO_3^-, SO_4^{2-}, NH_4^+, dust, sea salt) for GEOS-Chem alone, and R^2 improved to 0.41–0.83 across the $PM_{2.5}$ components for the hybrid model.

Fusion of Chemical Transport Model Predictions with Surface Observation Data

To take greater advantage of the strengths of observational data and model simulations, various data fusion approaches have been developed and applied. Such model-data fusion approaches used in estimating exposure concentration fields for health studies have frequently used CMAQ.

Downscaling approaches have been used frequently in recent years to correct biases in CTM output. Berrocal et al. (2009) proposed a downscaling approach combining monitoring and CMAQ modeling data to improve the accuracy of spatially resolved O_3 model data. Specifically, a Bayesian model was developed to regress CMAQ model estimates of O_3 concentration on monitoring data, and then the regression model was used to predict concentrations using the CMAQ model results as an input field. Although the downscaling method was originally developed for to model O_3 concentration, this technique has since been applied for modeling $PM_{2.5}$ concentration surfaces and found to have low NMB (0.95%) with mean correlation between model output and monitoring data of 0.97 (Bravo et al., 2017). Berrocal et al. (2010) extended the approach to include two pollutants (ozone and $PM_{2.5}$) in a single modeling framework. Predictive mean absolute error (PMAE) for $PM_{2.5}$ concentration in the bivariate model was 2.3 $\mu g/m^3$, compared with observations at 65 monitoring sites. PMAE for $PM_{2.5}$ was 2.4 $\mu g/m^3$ for the comparison of the single-pollutant model with the monitoring sites. Berrocal et al. (2012) also added smoothing processes that incorporate spatial autocorrelation and correction for spatial misalignment between monitoring and modeled data. Bentayeb et al. (2014) applied a similar data assimilation method in which local measurements and elevation data were combined with CTM output in a geostatistical forecasting model. This algorithm was applied for $PM_{2.5}$, PM_{10}, NO_2, SO_2, C_6H_6, and O_3. For the years 1989–2008, correlation between assimilated $PM_{2.5}$ concentration and local observations at 2 km resolution ranged from Pearson $R = 0.12$ to 0.85, with correlations decreasing with year. Bentayeb et al. (2014) explained the low correlations by a small number of $PM_{2.5}$ monitoring stations producing anomalous data and low correlations between emissions and concentration data.

ED_002220_00002287-00293

Bias correction methods are variations on downscaling that have been developed to address spatiotemporal bias in the CMAQ model. For example, Crooks and Oezkaynak (2014) developed a statistical method of spatiotemporal bias correction of $PM_{2.5}$ mass and its major components for CMAQ fields. The correction uses speciated data from ambient monitors. Mass conservation for $PM_{2.5}$ observations constrains the sum of the $PM_{2.5}$ components' concentrations in locations without speciation monitors. The Crooks and Oezkaynak (2014) method is similar to downscaling methods in that it is a calibration method, but it corrects to the grid-scale rather than receptor points. The method was developed for use in an epidemiologic study investigating the association between $PM_{2.5}$ component ambient concentrations and birth outcomes throughout the state of New Jersey based on 1-month averages, so the focus was on addressing seasonal bias trends rather than daily biases. The bias-corrected CMAQ results were more accurate than the original CMAQ output (calculated as mean bias and RMSE using monitored concentrations as a reference), and a cross-validation study found that predictions improved when enforcing mass conservation. Comparison between the bias-corrected CMAQ and other downscaling or bias correction methods was not provided. Hogrefe et al. (2009) used a combined model-observation approach to estimate historic gridded fields of $PM_{2.5}$ mass and component concentrations, with corrections varying by component, season, and location. $PM_{2.5}$ mass concentration had a median bias of -0.3 $\mu g/m^3$ and median RMSE of 7.5 $\mu g/m^3$ compared with monitor values. Hogrefe et al. (2009) reported high relative biases and larger uncertainties for nitrate and organic carbon, compared with sulfate and ammonium. This was especially pronounced at remote IMPROVE sites, compared with urban CSN sites that have more monitors. Although more development is needed, these methods present additional options for applying CTMs for modeling $PM_{2.5}$ species.

A hierarchical Bayesian model (HBM) to predict daily $PM_{2.5}$ exposure concentrations for use in the Environmental Public Health Tracking Network has been developed through a CDC-EPA collaboration. This model integrates U.S. EPA monitor data with CMAQ simulation results to generate daily $PM_{2.5}$ concentration and error fields for a 36 km grid across the conterminous U.S. and for a 12 km grid across an eastern portion of the U.S. (Vaidyanathan et al., 2013; McMillan et al., 2010). In the application of HBM over a section of the eastern U.S., McMillan et al. (2010) found that the mean squared error using the HBM field was similar to a field developed using kriging, though the HBM outperformed kriging by 10–15% for bias. They found that 59% of the validation data was captured in the kriging prediction intervals as compared to 80–90% when using HBM. For the U.S.-wide application at 36 km resolution, the HBM method had Pearson R's ranging from 0.91 to 0.94, depending upon the method used to impute the CMAQ data (Vaidyanathan et al., 2013), while the 12 km application over the eastern portion had Pearson R's of 0.84 to 0.86.

Data fusion methods sometimes include fusing CTM modeling results with observations for exposure predictions. Chen et al. (2014) evaluated an observation-CMAQ fusion for population air pollution exposure assessment using an inverse distance weighting method on observation-CMAQ differences, concluding that data fusion improved the estimation of population-weighted average exposure concentrations. On average, $PM_{2.5}$ mass was estimated to be negatively biased by about 30%,

ED_002220_00002287-00294

and individual components had a range of positive and negative biases from −150 to 100%. Nitrate and OC tended to see the largest biases and errors. After data fusion, the bias for $PM_{2.5}$ was near zero. Performance for individual components was similarly improved. Friberg et al. (2016) also fused CMAQ results to observations in a study focused on $PM_{2.5}$ exposures in Georgia. In this study, daily spatial exposure concentration fields for $PM_{2.5}$ mass, $PM_{2.5}$ components, and various gases were constructed from two blended fields. For one field, the temporal variance is driven by observations, while the spatial structure is driven by the annual mean CMAQ fields. The second field is constructed by scaling daily CMAQ simulated fields using mean observations to reduce bias. The final step blends the two fields based on using the temporal variance. The method intentionally does not force the fields to the observations at each monitor as they can be impacted by local emissions. The original CMAQ application for $PM_{2.5}$ was biased low about 12% with an RMSE of about 50% and an R^2 of 0.3. Typically, performance for individual $PM_{2.5}$ components was not as good. After applying the data fusion, the bias was almost totally removed, the RMSEs were about 20% for $PM_{2.5}$ and most PM components (though NO_3^- and EC were substantially higher), and the R^2 was about 0.92 (similar to individual components, though R^2 for EC was about 0.8). The method was tested using a 10−fold cross validation. In this case, the $PM_{2.5}$ R^2 was 0.75 and the RMSE was 30%.

Data fusion techniques have been tested in several other locations. Friberg et al. (2017) compared the fused CMAQ with original CMAQ model runs for five cities (Atlanta, GA, Birmingham, AL, Dallas, TX, Pittsburgh, PA, and St. Louis, MO) and found that the RMSE for $PM_{2.5}$ ranged from 2.21 to 3.76 μg/m^3 for the fused CMAQ, compared with 6.93 to 7.86 μg/m^3 for the original CMAQ.Huang et al. (2018) applied this method to North Carolina. In addition to doing the traditional 10-fold cross-validation, they also used spatial grouping of the 10% of monitors being removed to account for monitor clustering. In this case, the simulated $PM_{2.5}$ from the base CMAQ application had an RMSE of 6.3 μg/m^3 and an R^2 of 0.3, while after data fusion the RMSE decreased to 1.8 μg/m^3 and R^2 improved to 0.95. They also conducted 10-fold cross validation, both with and without (i.e., randomly withheld) spatial grouping. Finally, they compared the CMAQ-based data fusion fields with fields developed using a Bayesian-based method incorporating aerosol optical depth (AOD) from satellite data and found that the CMAQ-based approach performed slightly better (e.g., R^2 of 0.97 vs. 0.90 for AOD) using all of the data. The application of the same method in multiple locations shows that performance varies by domain.

Hybrid approaches can involve merging CTMs with dispersion and/or LUR models, merging CTMs with observational data, or some combination therein. Hybrid approaches improved CTM validation for $PM_{2.5}$ mass concentration when CTM was merged with either models or observational data. However, validation was not as good for $PM_{2.5}$ mass components, possibly due to the sparseness of validation data and limited data for $PM_{2.5}$ component emissions.

ED_002220_00002287-00295

3.3.3 Satellite-based Methods for Exposure Concentration Estimation

At present, spatiotemporal methods for predicting exposure concentration based on satellite observations have been applied primarily to $PM_{2.5}$ using AOD information supplied by various satellite-based instruments [see Section 2.4.4 and (Lin et al., 2015; Hu et al., 2014c; van Donkelaar et al., 2014; Lee et al., 2012a; Mao et al., 2012; Liu et al., 2009)]. Satellite data (Section 2.4.5), obtained twice per day over the U.S., has been used in recent exposure assessment studies to estimate exposure concentrations in rural regions where monitoring is not conducted, to improve estimates of spatial variability in exposure concentrations, and to cover larger geographic regions. For example, Hystad et al. (2012) used a composite satellite image of AOD over the years 2001 to 2006 to estimate $PM_{2.5}$ exposure concentration across Canada, which includes urban and rural areas. The authors adjusted the satellite data by annual average $PM_{2.5}$ (or estimated $PM_{2.5}$ based on TSP measurements prior to $PM_{2.5}$ measurements, which began in 1984) and then used the study cohorts' residential locations to estimate their exposures based on their residential histories and exposure concentrations corresponding to those locations. Hystad et al. (2012) noted that incorrect assignment of exposure based on failure to account for movement between residences over time and space through this method resulted in 50% of individuals being classified in the wrong $PM_{2.5}$ exposure quintile. Prud'homme et al. (2013) computed the correlation of $PM_{2.5}$ exposure concentration predicted at a residential location with the nearest fixed-site monitor and found that the correlation decreased from $R = 0.74$ (not stated if Pearson or Spearman) when the home was within 1 km of the monitor and decreased to 0.60 for distances of 30−40 km between the home and the monitor. This result implies that the $PM_{2.5}$ exposure concentration predicted using AOD is a better predictor of exposure concentration within a given grid cell compared with exposure concentrations further away.

Errors in the relationship between $PM_{2.5}$ and AOD are related to variation in retrieval due to resolution of the satellite image and variation in meteorology, topography, and reflectance (Section 2.4.4). Hu (2009) calculated the correlation between surface $PM_{2.5}$ and AOD at 877 monitoring sites across the U.S. and found that average correlation east of the 100°W longitude line was Pearson $R = 0.67$, compared with Pearson $R = 0.22$ west of the 100°W longitude line. Negative correlations between $PM_{2.5}$ and AOD were calculated at several sites west of the 100°W longitude line but at only three locations east of the 100°W longitude line. van Donkelaar et al. (2010) also noted this discrepancy between satellite data quality in the eastern and western U.S. They used population-weighting to determine national and global estimates of exposure concentration. Population density happens to be lower in mountainous parts of the western U.S., where the highest biases in AOD were noted.

Improving the relationship between AOD and surface PM observations to estimate exposure concentrations has led to the use of more advanced statistical methods for fusion of satellite data with CTM output and surface data in recent years. Satellite-based exposure concentration models now use AOD and other information (e.g., direct pollutant observations, meteorology, and land-use). For example, van Donkelaar et al. (2012) applied a smoothed bias correction to satellite-derived $PM_{2.5}$ exposure

ED_002220_00002287-00296

concentrations by first applying a 90-day moving average to the AOD prior to fitting $PM_{2.5}$ concentration estimates, and then smoothing the $PM_{2.5}$ exposure concentration field using IDW. The bias correction alone reduced the positive bias in the estimate to +29% with an estimated uncertainty of 54%. This is compared to the uncorrected $PM_{2.5}$ exposure concentration estimate, which had a bias of 97% with an estimated uncertainty of 67%. Incorporation of smoothing reduced the bias further to +14% with an uncertainty of 42%. An LUR approach to derive spatiotemporal pollutant fields accounts for the complexities in the AOD-PM relationships, including spatially and temporally varying conditions (Lee et al., 2016; Hu et al., 2014e; Ma et al., 2014; Chudnovsky et al., 2012; Hystad et al., 2011). Similar to LUR models, the approach is to develop a regression relationship between the observed $PM_{2.5}$ and AOD that includes the AOD field available from satellite observations and, potentially, other variables (e.g., those used in traditional LUR modeling). The regression coefficients can vary in time and space.

Not accounting for spatial and temporal variability in the relationship between $PM_{2.5}$ and AOD may lead to poor model performance (Hu et al., 2014d). Liu et al. (2009) recommended use of a two-stage general additive model including land use variables, with a stage one temporal model and stage two spatial model, so that the temporal and spatial variability are both addressed by the model, with an out-of-sample R^2 of 0.78, which was close to the model fit R^2 of 0.79 (stage one model-fit $R^2 = 0.77$, stage two model-fit $R^2 = 0.73$). Given the large spatial and temporal coverage of satellites, a large number of observations are typically available to develop the model. Additional spatial variation, particularly at scales finer than the resolution of the satellite observations, is provided by using fine scale land use variables. Lee et al. (2011) also recognized that the relationship between $PM_{2.5}$ and AOD is governed by time varying parameters affecting the vertical profile, the temporal variability of surface $PM_{2.5}$ over the course of a day. They developed a day-specific mixed effects model with random intercepts and slopes to quantify the relationship between surface $PM_{2.5}$ measured by surface monitors and AOD over New England in 2003. They assumed that temporal variability in properties that most strongly affect this relationship are much larger than their spatial variability over the domain of interest. In their model, the AOD fixed effect represents the average effect of AOD on $PM_{2.5}$ for all study days and the AOD random effects explain the daily variability in the $PM_{2.5}$-AOD relationship. Since some ground-based $PM_{2.5}$ monitors are located near strong sources, but Moderate Resolution Imaging Spectroradiometer (MODIS) samples represent an average over a 10 km × 10 km grid, an additional site specific random effects term is added to correct possible bias. Site specific out-of-sample R^2 varied from 0.87 to 1.0 with precision ranging from 8.8 to 38.6% for measured mean $PM_{2.5}$ at 26 urban sites (range: 9 to 19.5 $\mu g/m^3$).

Satellite observations of AOD have also been incorporated into hybrid modeling approaches. For example, Beckerman et al. (2013b) combined LUR, based on AOD observations, GEOS-Chem model output, land use data, and surface measurements of $PM_{2.5}$ concentration, with BME to predict $PM_{2.5}$ concentrations. BME was added to the model to improve spatiotemporal variability at scales smaller than the satellite's spatial resolution. Beckerman et al. (2013b) did not observe a substantial added benefit to including satellite data in an LUR model that also drew from land use data, surface measurements of $PM_{2.5}$ concentrations, and GEOS-Chem simulations. In this study, $PM_{2.5}$ concentrations were predicted

ED_002220_00002287-00297

throughout the contiguous U.S. using an LUR-BME with and without satellite data. The LUR with inclusion of satellite data produced an out-of-sample R^2 of 0.27 compared with R^2 of 0.05 without inclusion of satellite data. When BME was incorporated in the LUR to interpolate between spatiotemporal residuals from the training model, out-of-sample R^2 improved to 0.79. R^2 was the same for the simulations both including and excluding satellite data. Using a similar hybrid satellite-modeling approach, Lee et al. (2012a) found that during the period 2000–2008 in the New England region of the U.S., a densely populated study domain with high traffic areas, $PM_{2.5}$ exposure concentrations were predicted with an out-of-sample R^2 value of 0.83 and a mean relative error of 3.5%. Chang et al. (2014) describe a statistical downscaling approach that incorporates LUR models utilizing AOD and statistical techniques for combining air quality data sets that have different spatial resolutions. In cross-validation experiments for a 3-year time period over the southeastern U.S., the model performed well (out-of-sample $R^2 = 0.78$ and RMSE = 3.61 $\mu g/m^3$ between observed and predicted daily $PM_{2.5}$ concentrations), with a 10% decrease in RMSE attributed to the use of AOD as a predictor. Validation of hybrid models has been inconsistent across studies.

Recent studies have tested the effect of satellite image resolution on $PM_{2.5}$ mass concentration predictions. Hu et al. (2014c), using a two-stage model, compared the more traditional MODIS AOD at 10 km resolution with a Multiangle Implementation of Atmospheric Correction (MAIAC) algorithm at 1 km in the Southeastern U.S. and found that, when using 10-fold cross-validation, the out-of-sample R^2 was slightly lower for the 1 km MAIAC observations (0.67 vs. 0.69), though the R^2 for model fitting was the same (0.83). This can be contrasted against Chudnovsky et al. (2013), discussed in Section 2.4.4 Alexeeff et al. (2015) also used the 1 km MAIAC fields to estimate exposure concentration fields, comparing their results to fields developed using kriging. They found that using the MAIAC-based fields had a higher cross-validation than kriging, and that the low out-of-sample R^2 yielded biases in areas with lower covariance in the concentration field. Lv et al. (2016) used MODIS AOD and a statistical method similar to Chang et al. (2014) in an application in China. It is discussed here in terms of how the evaluation was performed. Using all data (no withholding), the R^2 was 0.78 and the normalized mean error was 0.27. When they used a random leave 10% out procedure, the method led to an R^2, normalized mean error (NME) and RMSE of 0.68, 0.26 and 21.40 $\mu g/m^3$, respectively (like $PM_{2.5}$ concentrations, RMSE is much higher in China than in the U.S.). Using a process where monitors were removed after being grouped by city led to somewhat worse performance: 0.61, 0.28 and 23.53 $\mu g/m^3$, respectively. This suggests that method and application evaluations should use cross-validation methods that consider spatial groupings of monitors as a more stringent evaluation approach.

Recent efforts have fused satellite data with LUR model results and surface observations to maximize available data for estimation of exposure concentrations. Kloog et al. (2011) built a three-stage regression model using surface measurements as the response variable and including MODIS-derived AOD, land use variables, and a daily calibration $PM_{2.5}$ concentration from surface measurements to estimate $PM_{2.5}$ exposure concentration on a 1 km × 1 km grid across New England, and Kloog et al. (2012a) extended the model across the Mid-Atlantic states. When AOD was available, the

ED_002220_00002287-00298

cross-validation out-of-sample R^2 was 0.83 for New England and 0.87 for the Mid-Atlantic states; when AOD was unavailable, cross-validation out-of-sample R^2 was still 0.81 for New England and 0.85 for the Mid-Atlantic states. When running the model for the two regions combined, Kloog et al. (2012b) found cross-validation out-of-sample R^2 was 0.81 for the total model of $PM_{2.5}$ and 0.81 for the LUR stage of the model. Kloog et al. (2014) built upon this method by first calibrating the AOD on daily measurements of $PM_{2.5}$ and adjusting for land use and meteorological variables for the Northeastern U.S. (New Jersey to Maine) for 2003–2011. Where AOD data were available, this model was used to predict $PM_{2.5}$ exposure concentration. The second model used the AOD–$PM_{2.5}$ calibration to predict AOD, which was then input into the regression model for a 1 km × 1 km grid. Finally, a 200 m × 200 m resolution prediction was developed by taking the residuals at each monitoring site and regressing them against the fine-scale resolution predictors to estimate fine-scale $PM_{2.5}$ exposure concentration. The models were built separately for temporal and spatial variables, and each had an average cross-validation out-of-sample $R^2 = 0.87$.

Similar to BME, machine learning approaches can be used to merge satellite observations with land use and other data for prediction of $PM_{2.5}$ mass concentration. For example, Reid et al. (2015) used a machine learning approach to estimate spatiotemporal $PM_{2.5}$ exposure concentration fields over the central region of California during a period of wildfires in the region by building spatiotemporal models using 11 model types from a set of 29 independent variables and selecting the optimal one for each model type. Input data included $PM_{2.5}$ and meteorological predictions from a CTM (WRF-Chem), land use data, and satellite AOD observations [three sets: the Geostationary Operational Environmental Satellite West Aerosol/Smoke Product (GASP) with a resolution of 4 km, the MODIS AOD product with a resolution of 10 km, and a local AOD product developed from MODIS data at a 500 m resolution, $PM_{2.5}$ and meteorological predictions from WRF-Chem, land use data, and distance to the nearest fire cluster]. The data were put in to each of the methods to develop a best model. Ten-fold cross-validation out-of-sample R^2 ranged from 0.387 to 0.803, and RMSE ranged from 1.49 μg/m^3 to 2.03 μg/m^3. It was found that similar model performance (within 1.5% of the RMSE) was achieved using only 13 variables, compared with a model of all 29 variables, with highest out-of-sample R^2 and lowest RMSE. They found that the variable most correlated with the $PM_{2.5}$ observations was the GASP followed by the distance to nearest active fire cluster, then the local AOD product and WRF-Chem $PM_{2.5}$ contributed equally. Di et al. (2016a) used a similar approach for a model of $PM_{2.5}$ exposure concentration across the contiguous U.S. GEOS-Chem simulation results were merged with satellite data for AOD, surface reflectance, and aerosol absorbance index, as well as with surface data from monitors reporting to AQS and data for meteorology and land use. For 2000–2012, out-of-sample $R^2 = 0.84$ with RMSE of 2.94 μg/m^3. The relationship between predicted and measured $PM_{2.5}$ concentrations was approximately linear until measured $PM_{2.5}$ concentrations were above approximately 60 μg/m^3. At that point, the predictions were insensitive to measured $PM_{2.5}$, but limited $PM_{2.5}$ concentration data were available above concentrations of 60 μg/m^3. These studies illustrate that the most important variables change, depending on the scenario modeled and the specific variables included.

ED_002220_00002287-00299

Several other studies have devised novel methods to fuse observational data and results from models for estimation of exposure concentrations. Pirani et al. (2014) performed Bayesian spatiotemporal modeling for the assessment of short-term exposure to PM_{10} in London, U.K. using mass concentration measurements and output from the high spatial resolution air dispersion modeling system. They found exposure concentration estimates in urban areas are improved by including city-scale particle component and long-range transport component with covariates to account for residual spatiotemporal variation. Crooks and Isakov (2013) developed a novel method using wavelets to blend CMAQ, AERMOD, and observation fields to capture intra-urban transport of pollutants across a spectrum of spatial scales. They used it to estimate block group and zip code centroid exposure concentrations in Atlanta, GA and found that it captured the concentrations down to scales on the order of 100 m.

Several studies using AOD observations to predict $PM_{2.5}$ have been published in recent years. Progress in this approach includes incorporation of AOD with LUR, BME, and geostatistical modeling approaches that also may include surface measurements. Most applications of these hybrid models were designed to make comparisons across space for long-term exposure studies, where the temporal averages were more stable than for short-term exposure studies. Still, validation results across these studies were inconsistent, so attention must be given to the strengths and limitations of individual exposure models and their appropriateness for a given scenario (e.g., urban vs. rural, where monitoring for use in model training and validation may be sparse in the latter case) rather than assuming that the predicted $PM_{2.5}$ exposure concentration is accurate if it includes satellite data.

3.3.4 Microenvironmental Exposure Modeling

Indoor air exposures to total PM may be measured directly or estimated based on infiltration rates that typically use some level of mass balance model, potentially with chemistry, deposition, and other processes that can affect individual exposure. Inputs to indoor air mass balance models include ambient PM concentrations (observed or estimated), air exchange rates, indoor source emissions, and other factors that can affect the dynamics of pollutants. Such indoor air models are included in integrated exposure models (such as U.S. EPA's Stochastic Human Exposure and Dose Simulation [SHEDS] and Air Pollutants Exposure [APEX] models) or individual models (such as the Exposure Model for Individuals [EMI]), that also incorporate factors such as human activity patterns (Baxter et al., 2013). In Baxter et al. (2013), mean $PM_{2.5}$ exposure estimates obtained from models that considered time spent indoors and indoor-outdoor air exchange rates with no indoor sources were approximately half of the concentrations from ambient monitor measurements.

Personal exposure occurs in multiple microenvironments that people encounter through their daily activities (e.g., indoors, outdoors, in vehicles). Methods have been developed to simulate potential total exposures through such environments by tracking "representatives" of population groups as they move between indoor and outdoor microenvironments, using estimated pollutant concentrations in each

ED_002220_00002287-00300

location to develop a time-weighted exposure profile for that population group. How individuals "move" though the different microenvironments is taken from studies of personal activity data [e.g., the Consolidated Human Activity Database, or CHAD (Isaacs, 2014)]. This database has information on sequential patterns of individual activities. This allows simulating not only "average" individual exposures, but also the distribution of exposures for different individuals or population groups over time.

Residential air exchange rate (AER) is a critical parameter for exposure models, such as APEX, SHEDS, and EMI (Breen et al., 2015; U.S. EPA, 2011, 2009a; Burke et al., 2001), with people spending the majority of their time indoors (Section 3.4.2.1). Since the appropriate AER measurements may not be available for exposure models, mechanistic, and empirical (i.e., regression-based) AER models can be used for exposure assessments. Empirical AER models do not consider the driving forces from the wind and indoor-outdoor temperature differences. Instead, a scaling constant can be used based on factors such as building age and floor area (Chan et al., 2005). Single-zone mechanistic models, such as the Lawrence Berkeley Laboratory (LBL) model, represent a building as a single well-mixed volume(Breen et al., 2010; Sherman and McWilliams, 2007; Sherman and Grimsrud, 1980). Recently, the LBL air infiltration model was linked with a leakage area model using population-level census and residential survey data (Sherman and McWilliams, 2007) and individual-level questionnaire data (Breen et al., 2010). Variations on the LBL model were compared with daily AER measurements in North Carolina (Breen et al., 2010) to find mean absolute differences of 40−43%.

The Hazardous Air Pollutant Exposure Model (HAPEM, now Version 6) is a screening level approach for modeling long-term inhalation exposures to ambient air pollutants, including PM. It can take modeled ambient pollutant concentrations as inputs or can use a parameterization of National Air Toxics Assessment (NATA)-generated PM estimates based on the near-road and far-from-road census tract populations (Rosenbaum and Huang, 2007). To develop exposure concentration estimates in microenvironments (e.g., commuting), microenvironmental factors are used to modify outdoor concentrations (e.g., provided by developing ambient exposure concentration fields). HAPEM has been used for nationwide assessments of exposure to sources of specific PM components and other pollutants (Ozkaynak et al., 2008) and, as noted above, coupled with a CMAQ/AERMOD combination (Isakov et al., 2009).

The SHEDS model and APEX model (which is now part of the Total Risk Integrated Methodology, or TRIM-Expo) both simulate individual movements though multiple microenvironments. APEX uses either a mass balance approach or a ratio to estimate in-vehicle or indoor concentrations (Che et al., 2015). Differences in subpopulation sampling methods between APEX and SHEDS produce small differences in predictions for population exposure concentrations (12.2 vs. 12.9 $\mu g/m^3$, respectively). SHEDS includes an activity-dependent ventilation rate to estimate dose. SHEDS-PM (the PM version of SHEDS) has a linear relationship between ambient concentrations and in-vehicle concentrations as well as in offices, restaurants/bars, schools, and stores. When analyzing contributions to exposure based on application of SHEDS-PM with daily $PM_{2.5}$ from CMAQ, Jiao et al. (2012) found that spatial variability

ED_002220_00002287-00301

of ambient concentrations within urban areas was not substantial, but inter-individual variability in estimated exposures was substantial. Daily estimates of the ratio of ambient exposure to ambient concentration differed by a factor of 4–5 across the simulated individuals. SHEDS uses time-activity data from the CHAD database. Jiao et al. (2012) noted that there were not sufficient data in the CHAD database to quantify how time-activity patterns varied as a function of sex, region, or season when limited to the three areas studied, although statistically significant differences in time spent indoors or time spent outdoors by sex, region, and season were seen for CHAD data aggregated across large geographic regions. Liu and Frey (2011) proposed a method to estimate in-vehicle $PM_{2.5}$ exposure concentrations that combines using ambient concentrations and a local incremental concentration that accounts for near road enhancements in lieu of assuming a linear relationship between $PM_{2.5}$ concentration measured at fixed-site monitors and exposure concentrations estimated on the road using the CALINE4 dispersion model. Liu and Frey (2011) found that in-vehicle exposures contribute 10–20% of average daily $PM_{2.5}$ exposures. Georgopoulos et al. (2009) linked SHEDS with an environmental risk model (MENTOR) to estimate exposures (and the related risks) for $PM_{2.5}$ in Philadelphia, using a CTM to provide the $PM_{2.5}$ field. For those individuals with the highest 5% of $PM_{2.5}$ exposures, the major microenvironment was indoors, and environmental tobacco smoke was the dominant source. Ozkaynak et al. (2009) evaluated the uncertainty inherent in the coupled model formulation and compared it with a "crude" estimation of uncertainty when the models are run separately and with CMAQ outputs being used for SHEDS inputs. Uncertainty for the crude method was 1.2–4.4 times higher than for the coupled formulation.

The EMI model simulates individual exposure to $PM_{2.5}$ as the aggregate of exposures in multiple microenvironments (Breen et al., 2015). The EMI uses a five-tier system to model individual exposures. AER is predicted in Tier 1 based on surveys and variations on the LBL model for each microenvironment. Infiltration factors are predicted in Tier 2, and those values are used to predict outdoor concentrations infiltrated indoors measured immediately outside each microenvironment and measured at fixed-site monitors in Tier 3. A weighted average of the infiltration factor over time spent in different microenvironments is produced for each individual in Tier 4, and then personal exposures to pollution from directly outside the microenvironment and from the fixed-site concentration measurement are computed in Tier 5 for each individual. Personal monitoring and time-activity surveys are necessary inputs for the EMI. The Tier 2–5 metrics were observed to have approximately 15–25% error (Breen et al., 2018; Breen et al., 2015).

The trade-off between computational accuracy and efficiency in exposure and risk models has received limited discussion in the exposure model literature. Chang et al. (2012) described a simulation process incorporating SHEDS exposure simulation into two risk models: an "exposure simulator" in which an exposure time series was simulated stochastically and then incorporated into an ensemble average risk, and a two-stage "Bayesian" approach in which the computed time series was used as a prior in an exposure model. Risk of mortality (CHAPTER 11) associated with short-term $PM_{2.5}$ exposure was estimated using the exposure simulator model, the Bayesian model, and fixed-site $PM_{2.5}$ concentration as

ED_002220_00002287-00302

an exposure surrogate. Little difference was observed between the exposure simulator and Bayesian models, but the exposure simulator was less computationally intensive.

3.3.5 Exposure Assignment Methods in Epidemiologic Studies

Epidemiologic studies use a variety of methods to assign exposures or exposure concentrations to study participants. Study design, data availability, and research objectives are all important factors for epidemiologists when selecting an exposure or exposure concentration estimation method. Common methods for estimating exposure concentrations from monitoring data include using fixed-site ambient monitoring, averaging concentrations from multiple monitors, and selecting the closest monitor to represent population exposure concentration. Investigators may also use statistical adjustment methods, such as trimming extreme values, to prepare the exposure concentration data set. Alternatively, modeling approaches described in Section 3.2.2 (modeling) can be used to estimate more spatially or temporally resolved exposure concentrations when data and resources are available.

Comparison studies have illustrated differences among the methods for producing estimates of exposure concentrations. For example, Dionisio et al. (2013) simulated $PM_{2.5}$ mass concentration, $PM_{2.5-EC}$, and $PM_{2.5}$–SO_4^{2-} exposures or exposure concentrations using different methods including a fixed-site monitor, an AERMOD model, a hybrid model combining regional background estimates with local contributions by AERMOD, and the SHEDS exposure model. The methods differed more with respect to modeling spatial variability (as measured by coefficient of variation) compared with temporal variability, with spatial variability being greater for the AERMOD and hybrid approaches for all three pollutants. Temporal variability was similar across methods for $PM_{2.5}$ and SO_4^{2-} with some difference across methods for EC. Mannshardt et al. (2013) compared use of fixed-site monitor concentration data, exposure concentrations estimated by CMAQ output, and exposures calculated using SHEDS to study respiratory emergency department visits associated with $PM_{2.5}$ exposure in New York County, NY, Queens, NY, and Bronx, NY. They found that the use of the SHEDS model led to a very similar relative risk as using CMAQ but provided additional information that helped reduce uncertainty. The effect estimates associated with exposure modeled by SHEDS and exposure concentration modeled by CMAQ were both higher and more precise than the effect estimate obtained from using fixed-site data as an estimate for exposure concentration. However, Mcguinn et al. (2017) estimated $PM_{2.5}$ exposure concentration and risks of coronary artery disease and myocardial infarction using a fixed-site monitor, CMAQ run with a census tract-level downscaler and with data fusion at 12 km resolution, and a satellite at 1 km and 10 km resolution. They did not find a relationship of model resolution with exposure concentration or with the magnitude of the effect estimates or with precision of the effect estimate for either health outcome studied.

Additional studies have also explored the effect of using different spatial averaging techniques to handle exposure concentration estimates from fixed-site monitoring data. Goldman et al. (2012) and

ED_002220_00002287-00303